

NASA TECHNICAL NOTE



NASA TN D-4833

2.1

LOAN COPY: RETU-  
AFWL (WLIL-2  
KIRTLAND AFB, N

0131636



TECH LIBRARY KAFB, NM

NASA TN D-4833

# MECHANICAL PROPERTIES AND COLUMN BEHAVIOR OF THIN-WALL BERYLLIUM TUBING

*by Donald R. Rummler, H. Benson Dexter,  
George H. Harth III, and Raymond A. Buchanan*

*Langley Research Center  
Langley Station, Hampton, Va.*



0131636

✓  
MECHANICAL PROPERTIES AND COLUMN BEHAVIOR OF  
THIN-WALL BERYLLIUM TUBING

By Donald R. Rummler, H. Benson Dexter, George H. Harth III,  
and Raymond A. Buchanan

Langley Research Center  
Langley Station, Hampton, Va.

✓  
NATIONAL AERONAUTICS AND SPACE ADMINISTRATION

---

For sale by the Clearinghouse for Federal Scientific and Technical Information  
Springfield, Virginia 22151 - CFSTI price \$3.00

# MECHANICAL PROPERTIES AND COLUMN BEHAVIOR OF THIN-WALL BERYLLIUM TUBING

By Donald R. Rummler, H. Benson Dexter, George H. Harth III,  
and Raymond A. Buchanan  
Langley Research Center

## SUMMARY

The results of an experimental investigation to determine the mechanical properties and column behavior of commercially produced beryllium tubing at room temperature are presented. The investigation included three types of extruded tubing and one type of plasma-sprayed and sintered tubing. The diameters of the tubes ranged from 0.25 to 0.75 inch (6.35 to 19.05 mm). Wall thickness was either 0.020 or 0.040 inch (0.508 or 1.016 mm). Microhardness measurements and metallurgical studies were performed to characterize the tubing microstructure. On the basis of the results of mechanical-property determinations and column tests, the extruded tubing appeared to be suitable for use in truss-type structures. Column buckling loads could be predicted satisfactorily by using the tangent modulus, derived from compressive stress-strain curves, in the inelastic column-buckling equation. The results also indicated that the reproducibility of the dimensions and the mechanical properties of the extruded beryllium tubing were comparable to that of other aircraft structural materials.

## INTRODUCTION

The high stiffness and low density of beryllium make it attractive for structural applications. Despite these advantages, the structural application of beryllium is not widespread. This limited use is due, in part, to its brittle and anisotropic behavior under biaxial stresses. Most current applications use beryllium in sheet form (see, for example, refs. 1 to 4) and little attention has been given to the structural application of beryllium tubing. The use of beryllium tubing in truss-type structures appears promising since truss-type configurations offer the possibility of uniaxially loading the beryllium. Because of the interest in lightweight tubular spacecraft structures and because of the limited amount of information currently available on beryllium tubing, an investigation of thin-wall tubular beryllium for lightly loaded, truss-type structures has been initiated. The study reported herein includes the initial phase of this investigation.

The purposes of the present study were (1) to characterize both the microstructure and the room-temperature mechanical properties of commercially produced beryllium tubing and (2) to subject the tubing to column tests to verify predicted performance.

The investigation included three types of extruded tubing and one type of plasma-sprayed and sintered tubing. The tubing ranged in diameter from 0.25 to 0.75 inch (6.35 to 19.05 mm). The wall thickness of the tubes was either 0.020 or 0.040 inch (0.508 or 1.016 mm).

## SYMBOLS

The units used for physical quantities defined in this paper are given both in the U.S. Customary Units and in the International System of Units (SI). (See ref. 5.) Conversion factors pertinent to the present investigation are presented in appendix A.

A	area, inches <sup>2</sup> (meters <sup>2</sup> )
c	column-end-fixity coefficient
d	grain size, inches (meters)
D	outside diameter of tube, inches (meters)
e	total elongation in 2 inches (5 centimeters), in percent
e <sub>u</sub>	uniform elongation, in percent
E	Young's modulus in tension, pounds force/inch <sup>2</sup> (newtons/meter <sup>2</sup> )
E <sub>c</sub>	Young's modulus in compression, pounds force/inch <sup>2</sup> (newtons/meter <sup>2</sup> )
E <sub>t</sub>	tangent modulus, pounds force/inch <sup>2</sup> (newtons/meter <sup>2</sup> )
h	hardness
I	moment of inertia, inches <sup>4</sup> (meters <sup>4</sup> )
L	length, inches (meters)

N	number of samples
S	standard deviation
t	wall thickness, inches (meters)
$\bar{X}$	average value
$\epsilon$	strain
$\mu$	Poisson's ratio
$\rho$	radius of gyration, inches (meters)
$\sigma$	stress, pounds force/inch <sup>2</sup> (newtons/meter <sup>2</sup> )

Subscripts:

calc	calculated value
cp	compressive proportional limit
cr	buckling
cy	0.2-percent offset compressive yield
eff	effective
exp	experimental
max	maximum
n	nominal
tp	tensile proportional limit
tu	tensile ultimate
ty	0.2-percent offset tensile yield

1,2,3,4      directions defined with respect to longitudinal axis of tube

Notation and abbreviations:

CI              confidence interval for average value

hkl             Miller indices for crystallographic planes

KHN<sub>100</sub>      Knoop microhardness number determined by using a 100-gram mass

## EXPERIMENTAL PROCEDURE

### Materials

The beryllium tubing used in this investigation included three types of extruded tubing (types A, B, and BL) and one type of plasma-sprayed and sintered tubing (type PS). Tubing deliveries were completed in the fall of 1966. The supplier-furnished fabrication history for each type of tubing is presented in table I. The tubing diameters ranged from 0.25 to 0.75 inch (6.35 to 19.05 mm). The wall thickness was either 0.020 or 0.040 inch (0.508 or 1.016 mm). The specified diameter and wall thickness for each tubing type are listed in table II along with the supplier-furnished chemical composition and bulk density.

The specified dimensional tolerances on diameter, wall thickness, and straightness for each tubing type are presented in table III. These tolerances are comparable to those for the 5000 series of aluminum alloys (ASTM specification B 221-67).

### Metallurgical Examination

The need to determine the influence of fabrication history on microstructure and the interrelationships of factors such as grain size, orientation texture, and impurity level on the mechanical properties of beryllium products has been pointed out in reference 6. Therefore, the metallurgical examination of the beryllium tubing included (1) macroscopic and microscopic observations, (2) grain-size determinations, (3) microhardness measurements, and (4) X-ray diffraction studies.

Microscopic examination was accomplished by using standard metallographic specimen-preparation procedures (see, for example, ref. 7). Polished sections were prepared in both the longitudinal and transverse directions. Grain-size measurements were made by using the linear-intercept method on  $\times 500$  photomicrographs. A minimum of 150 grain-boundary intersections with 3.94-inch-long (10 cm) intercept lines was used to establish grain size.

Knoop microhardness determinations were made on polished sections by using a 100-gram mass and a 15-second indenter dwell time. Each average hardness number is based on a minimum of 10 microhardness determinations.

Standard X-ray diffraction patterns were made by exposing polished longitudinal sections of tubing to nickel-filtered copper  $K_{\alpha}$  radiation on a diffractometer. These patterns were used to estimate the type and amount of preferred orientation present in the tubing.

#### Bulk-Density Measurements

The bulk density of the plasma-sprayed and sintered tubes was determined by water-immersion techniques. Because of water penetration into open surface pores, reproducible density determinations could not be made by standard techniques. The specimens were, therefore, given a wash coat of cellulose nitrate to preclude water penetration. The calculated value for bulk density included a correction term for the volume of the wash coat (typically 2 percent of specimen volume) and the temperature of the water. The bulk density of a few extruded tubes was determined by standard water-immersion techniques.

#### Dimensional Measurements

The outside diameter, wall thickness, and straightness of the beryllium tubing were measured to verify conformance to the specified tolerances (table III) and to establish an estimate of the variability of diameter, wall thickness, area, and moment of inertia. Tubing which did not meet the specified dimensional tolerances was not included in this investigation. A minimum of six measurements of outside diameter and wall thickness was used to calculate an average wall thickness and diameter for each cross section of tubing measured. Typically, measurements were made at three equally spaced sections of the tubes which were from 1 to 10 inches (25 to 250 mm) long and at five equally spaced sections of the tubes longer than 10 inches (250 mm). The variability in diameter was calculated by using the average diameter determined at each measured section as a single observation. Wall-thickness variability was calculated in a similar manner. By assuming a circular cross section and a constant wall thickness, the area and moment of inertia of each measured section were calculated and used to determine the variability of these two section properties. Straightness measurements were made on tubes greater than 3 inches (76 mm) in length. Additional details of the equipment and procedures used for the dimensional measurements are presented in appendix B.

## Mechanical-Property Tests

Tensile and compressive mechanical-property tests were performed at room temperature in 120 000-lbf-capacity (534 kN) universal hydraulic testing machines.

The tensile specimens were prepared by adhesively bonding end fittings to the tubing. Most of the tensile specimens were chemically etched with a  $\text{Cr}_2\text{O}_3\text{-HF-H}_2\text{O}$  solution after bonding. The etching reduced the outside diameter of the specimen a minimum of 0.01 inch (0.25 mm). The length of the reduced section was at least 10 times the nominal outside diameter. To evaluate the effect of etching on mechanical properties some tensile specimens were etched with other solutions and some were tested in the unetched condition. Additional details of the equipment and procedures used to bond and etch the tensile specimens are presented in appendix C. Tensile tests were performed with precision-machined grip assemblies (fig. 1). Both the spherical bearing and the tapered socket of the split adapter were lubricated with molybdenum disulfide. The upper loading rod was attached to the testing machine with a lubricated spherical seated bearing. The lower loading rod was rigidly attached to the lower crosshead of the testing machine. The grips and loading rods were carefully aligned to minimize loading eccentricity.

Compressive specimens were tested in the as-received condition. The ends of these specimens had been ground plane, smooth, and perpendicular to within  $0.25^\circ$  of an axial line passing through the centroids of the specimen ends. The length-to-diameter ratio of the compression specimens was 4. Compressive specimens were supported on hardened-steel disks. Annealed-aluminum washers were inserted between the specimen ends and the steel disks. The plastic deformation of the aluminum washers helped to uniformly distribute the load on the specimen.

Both the tensile and the compressive specimens were enclosed in a protective cylindrical sleeve when tested. This sleeve was usually made from multiple layers of 0.008-inch (0.2 mm) latex sheet wound around either the steel support blocks of the compressive specimens or the aluminum end fittings of the tensile specimens. The sleeves were sealed with masking tape. After testing, the sleeves were removed while the assembly was immersed in acetone. This procedure eliminated contamination of the laboratory surrounding the testing machine by any beryllium dust which may have been generated during testing.

Strains for both tensile and compressive tests were measured with foil-type strain gages adhesively bonded to the specimens with a methyl 2-cyanoacrylate adhesive. Each strain-gage assembly included strain-sensing elements in both longitudinal and transverse directions. The gage assemblies were equally spaced about the circumference of each specimen. Two such assemblies were bonded to each 0.25 inch-diameter (6.35 mm)



specimen. Four gage assemblies were bonded to each specimen over 0.25 inch (6.35 mm) in diameter. The electrical outputs of the strain gages and a load-indicating deflectometer attached to the load dial of the testing machine were recorded on magnetic tape at a virtually continuous rate ( $\approx 2$  per second) up to yield and at  $\approx 0.5$  per second thereafter. The strain rate was manually controlled throughout each test. The instantaneous strain rate was monitored by comparing the output of a longitudinal strain gage on a strip-chart recorder with lines drawn on the recorder paper at the desired strain rate.

Preliminary experiments determined that an initial strain rate of 0.005 per minute could not be adequately maintained. Consequently, the nominal strain rate for the mechanical-property tests was 0.0015 per minute to yield and 0.015 per minute thereafter. Elongation measurements on tensile specimens were made by using finely scribed pencil lines at 0.40-inch (1 cm) intervals along the specimen. Both elongation in 2 inches (5 cm) and uniform elongation were measured. Uniform elongation is the amount of residual plastic strain in the unfractured portions of a tensile specimen (ref. 8). Uniform elongation does not include the region of the specimen near the fracture zone and was determined by averaging the residual plastic strain in each half of the fractured tensile specimens.

Data from the mechanical-property tests were reduced by means of a digital computer and associated automatic plotting equipment. To determine the tangent-modulus curves, short segments (seven consecutive data points) of the stress-strain curves were successively fitted to a second-order polynomial equation by the method of least squares. The first derivative of the fitted equation was used to calculate tangent modulus at the center of the fitted segment. To determine Poisson's ratio it was necessary to correct the indicated strains for transverse strain. By using the procedures presented in reference 9 for this type of correction, the following equations were developed in this study to account for the different transverse sensitivity coefficients in the longitudinal and transverse gages of the strain-gage assemblies:

$$\epsilon_1 = \frac{\epsilon_{c,1} (1 - \mu_o k_1) - k_1 \epsilon_{c,2} (1 - \mu_o k_2)}{1 - k_1 k_2}$$

$$\epsilon_2 = \frac{\epsilon_{c,2} (1 - \mu_o k_2) - k_2 \epsilon_{c,1} (1 - \mu_o k_1)}{1 - k_1 k_2}$$

where  $\epsilon_{c,1}$  and  $\epsilon_{c,2}$  are the apparent strains in the longitudinal and transverse gages,  $\mu_0$  is the Poisson's ratio of the isotropic bar on which the gages were calibrated, and  $k_1$  and  $k_2$  are the transverse sensitivity coefficients of the longitudinal and transverse gages. The reported Poisson's ratio for each specimen represents an average of the Poisson's ratios determined from each gage assembly on a specimen.

### Column Tests

Column tests were also made at room temperature in a 120 000-lbf capacity (534 kN) universal hydraulic testing machine. Column specimens ranged in length from 3 to 36 inches (76 to 914 mm). The columns were tested in the as-received condition. The ends of the columns were ground to the same tolerances as the compression specimens. The lower ends of the columns were supported on a hardened loading block (fig. 2). The top of the column was in contact with the crosshead loading platen. Figure 2 also shows the column alinement fixture used to aline the heads of the testing machine and to aline the column before testing. After alinement, a small preload was applied to the column. The alinement fixture was then removed and the latex-sheet protective sleeve was extended and secured to enclose the column before testing. The protective sleeve precluded contamination of the laboratory air should a column shatter during testing. Four foil-type strain gages were bonded to the center of each column (fig. 2). These gages were equally spaced about the circumference of the column and were used to establish an initial elastic modulus.

The end-fixity coefficient  $c$  for the column tests was established experimentally by using steel columns with stiffnesses comparable to the beryllium columns and the procedures outlined in reference 10. A graphical procedure which used the compressive tangent-modulus curve and the tangent-modulus column equation

$$\sigma_{cr} = \frac{\pi^2 E_t}{\left(\frac{L_{eff}}{\rho}\right)^2}$$

where

$$\left(\frac{L}{L_{eff}}\right)^2 = c = 3.94$$

was used to establish the column buckling stress over a range of effective slenderness ratios  $L_{\text{eff}}/\rho$  for each type of beryllium tubing. The experimental column buckling stress  $\sigma_{\text{cr,exp}}$  was taken as the average stress at maximum column load.

## RESULTS AND DISCUSSION

### Metallurgical Examinations

Macrostructure.- Typical macrostructures of the as-received tubing are shown in figure 3. The type A tubes were characterized by circumferential grinding marks and a bright surface. The other tubing types had dull matte surfaces. Surface defects in the types B and BL tubes included surface pits and, in some cases, shallow longitudinal grooves. The type PS specimens typically contained many surface pits. When the tubes were etched, additional defects were noted. These additional defects included shallow longitudinal grooves and some surface pits in the type A tubing and an increase in the number of surface pits for the other types of tubing, particularly the type PS tubing (fig. 4).

Microstructure.- The longitudinal and transverse microstructures of the four tubing types are shown in figures 5 to 8. Under bright-field illumination, the longitudinal microstructures of the extruded tubing (figs. 5(a), 6(a), and 7(a)) revealed evidence of inclusion stringers. These small inclusions, presumably beryllium oxide, were randomly distributed in the transverse direction (figs. 5(c), 6(c), and 7(c)). The larger angular inclusions visible in these microstructures are similar to those described as beryllium carbide in reference 11. The longitudinal bright-field microstructure of the type PS tubing (fig. 8(a)) contained randomly distributed inclusions and porosity. The transverse bright-field microstructure (fig. 8(c)) showed some orientation of the pores and inclusions. This circumferential orientation of pores and inclusions is consistent with the major direction of material flow during the fabrication of these tubes by plasma spraying.

Under polarized light, the longitudinal microstructures of the extruded tubes (figs. 5(b), 6(b), and 7(b)) exhibited a marked metallographic fibering. In contrast, the transverse microstructures of these tubes (figs. 5(d), 6(d), and 7(d)) were typically equiaxed. Under polarized light, the microstructures of the type PS tubes in both longitudinal and transverse directions were equiaxed (figs. 8(b) and (d)).

The results of the grain-size measurements on the extruded tubing are presented in table IV. With the exception of the type A tubing and the type BL tubing with an outside diameter of 0.50 inch (12.70 mm) and a nominal wall thickness of 0.020 inch (0.508 mm), the grain size of the extruded tubing was essentially the same. The grain size of the type A tubing was significantly smaller than the other extruded tubing. The

decreasing grain size as a function of orientation ( $d_1 > d_2 > d_4$ ) has also been observed in extruded beryllium bar stock (ref. 12). Although grain-size measurements were not made on the type PS tubes, the polarized-light photomicrographs (fig. 8(b)) indicated that the grain size of these tubes was comparable to the extruded tubing.

X-ray diffraction intensity measurements.- The results of the X-ray diffraction experiments are summarized in table V. The relative intensities of the diffraction lines were measured as peak heights above background and are expressed in percentages of the strongest line. The relative intensities from the ASTM standard powder diffraction pattern for beryllium have been included in this table as a random orientation reference. The extruded tubing characteristically indicated a preferred orientation of the (0002), (11 $\bar{2}$ 0), and (11 $\bar{2}$ 2) planes. In fact, these were the only planes which were detected on the extruded tubes. The relative intensities of the (11 $\bar{2}$ 2) planes were approximately 12 times the random value and those of the (0002) and (11 $\bar{2}$ 0) planes approximately 5 times the random value. A notable deviation from this trend was the comparatively low relative intensity of the (11 $\bar{2}$ 0) planes in the type A tubing. The orientation of the type PS specimens was essentially random with some indication of slight preferential orientation of the (0002), (11 $\bar{2}$ 0), and (11 $\bar{2}$ 2) planes.

The absence of a (10 $\bar{1}$ 0) diffraction peak in combination with the preferred orientation of the (0002), (11 $\bar{2}$ 2), and (11 $\bar{2}$ 0) planes is consistent with the textures of extruded tubing determined from pole figures (ref. 13) which show that the (10 $\bar{1}$ 0) planes in extruded tubing are at right angles to the extrusion direction and that the basal planes are parallel to the extrusion direction and randomly oriented to each other. It is of interest to note that the type A tubes which had the highest extrusion ratio (121.5:1) also exhibited the lowest relative intensity of the (11 $\bar{2}$ 0) planes. This low intensity may be due to the increased alignment of the basal planes in the radial direction which occurs at high extrusion ratios (ref. 13).

Microhardness.- The results of the microhardness measurements (fig. 9) on the extruded tubes are consistent with the hardness trends reported in the literature; that is, maximum hardness in the extrusion direction (ref. 14). In addition, both the microhardness results and the results of the X-ray intensity measurements are also in general agreement with hardness measurements made on beryllium single crystals (ref. 15) which indicate that beryllium is harder in the [0001] direction than perpendicular to the direction.

Further examination of figure 9 reveals another trend in the microhardness in the extruded tubing; that is,  $h_1 > h_2 > h_4 > h_3$ . A similar variation in microhardness can also be seen in the type PS specimens; that is,  $h_4 > h_3 > h_1 > h_2$ . When the major flow direction during fabrication in these two types of tubing (longitudinal for the extruded tubing and radial for the plasma-sprayed and sintered tubing is taken into consideration), the

observed average microhardness differences are probably due to crystallographic texture rather than to the effects of preferred inclusion orientation. The directionality of the inclusion stringers is, however, probably responsible for the greater variability of microhardness which was observed on the surface ( $h_1$  and  $h_2$  directions) of the extruded tubing (table VI). The microhardness measurements of type PS tubing lend further support to the suggestion that the major effect of inclusions was to increase the scatter between individual hardness measurements made in a given direction rather than to markedly increase the hardness. These specimens had a high inclusion content which was randomly distributed and exhibited a large variability of microhardness in all directions (table VI).

### Bulk-Density Measurements

The average bulk density and the corresponding 95-percent confidence interval of the type PS specimens was  $1.837 \pm 0.014 \text{ g/cm}^3$  ( $1.837 \pm 0.014 \text{ Mg/m}^3$ ) for the tubes with 0.020-inch-thick (0.508 mm) walls and  $1.814 \pm 0.007 \text{ g/cm}^3$  ( $1.814 \pm 0.007 \text{ Mg/m}^3$ ) for the tubes with 0.040-inch-thick (1.016 mm) walls. The densities are approximately 97.5 and 96.4 percent of the theoretical density of beryllium with 4.85 percent of BeO. The higher apparent bulk density of the tube with a wall thickness of 0.020 inch (0.508 mm) was probably due to a higher surface-area-to-volume ratio rather than to a real difference in the porosity of the type PS tubes. The wash coat would fill a larger number of pores per unit volume on the thinner walled tubes and, thus, they would have a higher apparent bulk density.

The apparent bulk densities of selected extruded tubes were found to be in agreement with supplier-furnished densities (table II).

### Dimensional Measurements

The results of the dimensional measurements are summarized in table VII. These data normalized with respect to their specified nominal values are presented in figure 10. As would be expected, the type A tubes which were machined to final dimensions exhibited the smallest variation in diameter and wall thickness. Typically the average diameter and wall thickness of the extruded tubes were somewhat above the specified nominal. This additional material produced average cross-sectional areas in excess of the nominal. Because of the small difference of the average diameter from the nominal, most of this additional area was due to the thicker-than-specified walls on the extruded tubes. The range of values about the nominal for both of the computed section properties (A and I) reflect the variation in wall thickness exhibited by the extruded tubing. It should be noted that the dimensional tolerances for all the beryllium tubing were comparable to those used for the 5000 series aluminum alloys. As a

consequence, the maximum deviation from any specified dimension observed in the beryllium tubing is comparable to that which would be expected in 5000 series aluminum tubing. The wall-thickness variance in the beryllium tubing is probably higher than that which would be expected in extruded aluminum tubing.

### Mechanical-Property Tests

The results of the mechanical-property tests are summarized in table VIII. The test results for individual specimens are presented in table IX for the tensile tests and in table X for the compressive tests. Typical tensile and compressive stress-strain curves for the four types of beryllium tubing are shown in figure 11. The proportional limit in tension is somewhat higher than that in compression for the extruded tubes (Bauschinger effect). This difference is probably due to the procedures used to straighten these tubes after extrusion. The increase in the tensile proportional limit was also reflected in the tensile yield strengths and was observed for tubing with other diameters and wall thicknesses (table VIII). The higher proportional limit of the type A tubing, compared with that of the other types of extruded tubing, was consistent with its finer grain size, higher hardness, and somewhat higher oxide content.

Effect of wall thickness and diameter.- Differences in wall thickness in the type BL specimens did not markedly affect either tensile strength or elastic modulus (table VIII). In the 0.50- and 0.75-inch-diameter (12.70 and 19.05 mm) tubes, the thinner walled tubes typically exhibited higher proportional limits and yield strengths (fig. 12(a)). In the type PS tubing, a marked difference in mechanical properties as a function of wall thickness was observed (table VIII). The specimens with the thicker walls had higher yield strengths and proportional limits. In addition, the type PS tubing with 0.040-inch-thick (1.016 mm) walls was the only tubing tested which exhibited a pronounced yield point in compression (fig. 12(b)). Figure 12(b) also illustrates the difference in properties due to the two sintering treatments used for the type PS tubing with a nominal diameter of 0.54 inch (13.72 mm) and a nominal wall thickness of 0.020 inch (0.508 mm). The single-sintered tubes exhibited slightly lower proportional limits, higher yield strengths, and lower elastic moduli (table X).

No significant differences in either the mechanical properties (table VIII) or in the shape of the typical stress-strain curves (fig. 13) were observed as a function of diameter in the type BL tubing.

Effect of surface treatment.- Most of the tensile specimens were etched with the  $\text{Cr}_2\text{O}_3$ -HF- $\text{H}_2\text{O}$  solution discussed in appendix C. In addition, some of the initial tensile tests were performed on specimens in the as-received condition and on specimens which had been etched with the  $\text{HNO}_3$ - $\text{H}_2\text{SO}_4$ - $\text{H}_2\text{O}$  solution recommended in reference 16. Although the type B specimens were etched prior to receipt, the results

of these tests (table IX) indicated that additional etching was desirable. These tests also suggested that the  $\text{Cr}_2\text{O}_3\text{-HF-H}_2\text{O}$  solution was superior to the  $\text{HNO}_3\text{-H}_2\text{SO}_4\text{-H}_2\text{O}$  solution. Specimens etched with the  $\text{Cr}_2\text{O}_3\text{-HF-H}_2\text{O}$  solution exhibited somewhat higher values of tensile strength and elongation. Similar tensile tests on type BL tubing also exhibited the highest values of tensile strength and elongation when  $\text{Cr}_2\text{O}_3\text{-HF-H}_2\text{O}$  etchant was used. However, a single tensile test on an unetched type A specimen indicated that no major change in either tensile strength or elongation occurred where these specimens were etched. This lack of change was probably due to the brittleness of these specimens even in the etched condition.

Elastic modulus and Poisson's ratio.- The average values of elastic modulus for the extruded tubing ranged from  $39.0$  to  $41.1 \times 10^6$  psi ( $269$  to  $283$  GN/m<sup>2</sup>) (table VIII). The elastic modulus of cross-rolled sheet ranges from  $42.0$  to  $44.0 \times 10^6$  psi ( $290$  to  $303$  GN/m<sup>2</sup>) (see, for example, refs. 17 and 18). The lower modulus of the extruded tubing is probably attributable to the elastic anisotropy of beryllium. The elastic modulus of beryllium single crystals is lower parallel to the basal planes than perpendicular to them (ref. 19). Since the extruded tubing has a more complete alignment of the basal planes parallel to the longitudinal axis than does cross-rolled sheet, a lower elastic modulus could be expected. The low elastic modulus exhibited by the type PS tubing is probably due to its porosity rather than to a high degree of basal plane alignment in the longitudinal direction of these tubes.

The stress dependence of compressive tangent modulus and Poisson's ratio are presented in figures 14 and 15, respectively, for typical specimens of each tubing type with a diameter of 0.50 inch (12.70 mm) and a wall thickness of 0.020 inch (0.508 mm). When compared to the types A and PS tubing, the types B and BL tubing exhibited significantly lower values of tangent modulus at stress levels above their rather low proportional limits. Above the proportional limit, all the tubing types exhibited the expected increase in Poisson's ratio. Although the initial increase in Poisson's ratio occurred more gradually in the types A and PS specimens, these specimens typically exhibited higher maximum values of Poisson's ratio than did the types B and BL specimens.

Reproducibility of mechanical properties.- The tensile test results for the type BL specimens were used to calculate an estimate  $S$  of the standard deviations for  $\sigma_{tu}$ ,  $\sigma_{ty}$ , and  $e$ . The results of these calculations are presented in table XI. This table also includes similar data, estimated from reference 20, for several typical aircraft structural materials. Although the variability  $S/\bar{X}$  of the tensile properties for the beryllium tubing is somewhat higher than the other materials, it is considered to compare favorably when the limited amount of fabrication experience with thin-wall tubular beryllium extrusions is taken into consideration.

Failure modes.- In tension, the trends in both elongation (table IX) and fracture surfaces (fig. 16) exhibited by the beryllium were consistent with those reported in reference 21 for beryllium tubing with different degrees of crystallographic texture. The double-extruded type A specimens (fig. 16(a)) characteristically failed at an angle of approximately  $25^{\circ}$  to the tube circumference. Although the single-extruded types B and BL specimens most often failed at the same characteristic angle, the fracture surfaces on these specimens (fig. 16(c)) usually had minor surface steps and changes in direction. In some cases, however, a large portion of the fracture was normal to the longitudinal axis of the tube (fig. 16(b)). The fracture surface of the type PS tubing was typically irregular and normal to the longitudinal axis of the tube. These fracture patterns are consistent with the crystallographic textures which were deduced from the X-ray diffraction studies; that is, the amount of preferred orientation of the tubes was highest in the type A tubes and lowest in the type PS tubes.

The anomalous low ductility of highly textured tubes has been attributed (ref. 21) to the generation of secondary stresses which activate a circumferential mode leading to low ductility failures. Greater elongation for tubing of lower texture (such as types B and BL tubing) and low elongation for tubes with little or no texture (such as type PS tubing) was also reported in reference 21.

The failure modes of the beryllium tubing in compression (fig. 17) were also consistent with the crystallographically induced anisotropy of mechanical properties. The extruded tubes (fig. 17(a)) developed longitudinal cracks after reaching a maximum compressive stress (table X). These longitudinal cracks were induced by the circumferential stresses which developed near the restrained ends of the short compression specimens and are the result of the low circumferential strength and elongation which would be expected in these textured tubes. The type PS specimens when subjected to approximately the same amount of circumferential strain did not split longitudinally; that is, they did not exhibit preferential properties in the longitudinal direction. It is of interest to note that even though the types A and PS tubes were, in the engineering sense, brittle (tensile elongation  $\leq 1$  percent), they were sufficiently ductile to develop a significant amount of plastic strain in compression. In fact, the maximum compressive stress (table X) which was developed by all the specimens was comparable to the maximum stresses which would be predicted for cylinder buckling by using extrapolated tangent-modulus curves. The cylinder buckling equation also predicts the higher maximum stresses which were developed by the tubes with 0.040-inch-thick (1.016 mm) walls. When the compressive specimens were strained beyond the maximum compressive stress, the extruded specimens continued to split. In one case (fig. 17(b)), a type B specimen developed considerable longitudinal strain while it continued to split longitudinally. The type PS specimens always failed by fracturing which produced no characteristic fracture pattern.



## Column Tests

The results of the column tests are presented in table XII. This table also presents the experimentally determined elastic modulus and the calculated buckling stress  $\sigma_{cr}$  for the columns. No corrections were made for the lack of column straightness. The elastic-modulus data from the column tests support the results of the mechanical-property tests; that is, the elastic modulus of the extruded tubing is less than that of cross-rolled sheet.

In figures 18 and 19 the results of the column tests are compared with the calculated buckling stresses. The elastic Euler equation and the Engesser tangent-modulus equation for both the average value of tangent modulus and the range in tangent modulus obtained from the compression tests were used in this calculation. For the extruded tubing (fig. 18), the agreement between the predicted and experimental column behavior is satisfactory. In addition, the range of predicted values is small and for type BL extruded tubing this range includes the variation in compressive properties which were observed for tubes with three different diameters in two wall thicknesses.

The consequences of the low proportional limit exhibited by the types B and BL tubing (fig. 18(b) and (c)) are well illustrated by comparing the tangent-modulus prediction band with the elastic Euler curve. Even for stresses as low as 15 ksi ( $103 \text{ MN/m}^2$ ) the use of the tangent modulus is necessary to predict the buckling stress of these beryllium columns.

The buckling strength of the type PS tubing with a diameter of 0.54 inch (13.72 mm) and a wall thickness of 0.020 inch (0.508 mm) (fig. 19(a) and (b)) in both the single- and double-sintered condition compared favorably with the average calculated value predicted from the mechanical-property tests. When compared to the extruded tubing, both the data scatter and the range of the prediction band reflected the lower reproducibility of mechanical properties which was exhibited by the type PS tubing with a diameter of 0.54 inch (13.72 mm) and a wall thickness of 0.020 inch (0.508 mm). The column behavior of the double-sintered type PS tubing with a diameter of 0.58 inch (14.73 mm) and a wall thickness of 0.040 inch (1.016 mm) (fig. 19(c)) was not within the prediction band established from mechanical-property tests. No completely adequate explanation could be found for the low buckling stresses exhibited by these columns.

Typical beryllium columns after testing are shown in figure 20. The straight lines next to the columns provide a reference for visualization of the curvature. It can be seen that even the plasma-sprayed and sintered type PS columns were ductile enough for a considerable amount of plastic deformation. In fact, on these specimens post-buckling deformation was large and the column inflection points can be seen.

## CONCLUDING REMARKS

This study was made to investigate the mechanical properties and column behavior of commercially produced thin-wall beryllium tubing at room temperature. On the basis of the results of the mechanical-property measurements and the column tests, the extruded tubing appeared to be suitable for use in truss-type structures. Column tests indicated that the buckling stress for the three types of extruded tubing studied could be satisfactorily predicted. They also demonstrated that the use of the tangent-modulus inelastic column-buckling equation was necessary at stresses as low as 15 ksi ( $103 \text{ MN/m}^2$ ) for some of the extruded tubing because of their low proportional limits. The predictability of the column buckling stress for the plasma-sprayed and sintered tubing was not completely satisfactory.

The mechanical properties and failure modes for all the tubing types investigated were found to be consistent with tubing fabrication history and microstructural characteristics. The mechanical-property tests also indicated that the elastic modulus of extruded tubing may be somewhat lower than that of cross-rolled sheet. This difference was attributed to a difference in crystallographic texture.

In view of the limited amount of fabrication experience with thin-wall tubular beryllium extrusions, the reproducibility of mechanical properties of the extruded beryllium tubing was considered comparable to that of other aircraft structural materials.

Langley Research Center,  
National Aeronautics and Space Administration,  
Langley Station, Hampton, Va., May 21, 1968,  
124-08-01-05-23.

## APPENDIX A

### CONVERSION OF U.S. CUSTOMARY UNITS TO SI UNITS

The International System of Units (SI) was adopted by the Eleventh General Conference on Weights and Measures in 1960 (ref. 5). Conversion factors for the units used herein are given in the following table:

Physical quantity	U.S. Customary Unit	Conversion factor (*)	SI Unit (**)
Length . . . . .	in.	0.0254	meters (m)
Load . . . . .	lbf	4.448	newtons (N)
Mass . . . . .	ozm	0.0283	kilograms (kg)
Modulus or stress . .	{ psi = lbf/in <sup>2</sup>	$6.895 \times 10^3$	newtons per square meter (N/m <sup>2</sup> )
	{ ksi = kips/in <sup>2</sup>	$6.895 \times 10^6$	newtons per square meter (N/m <sup>2</sup> )
Pressure . . . . .	torr	133	newtons per square meter (N/m <sup>2</sup> )
Temperature . . . . .	(°F + 460)	5/9	degrees Kelvin (°K)
Volume . . . . .	{ gal	$3.8 \times 10^{-3}$	cubic meters (m <sup>3</sup> )
	{ liter	$1 \times 10^{-3}$	cubic meters (m <sup>3</sup> )

\*Multiply value given in U.S. Customary Units by conversion factor to obtain equivalent value in SI Unit.

\*\*Prefixes to indicate multiple of units are as follows:

Prefix	Multiple
micro (μ)	10 <sup>-6</sup>
milli (m)	10 <sup>-3</sup>
centi (c)	10 <sup>-2</sup>
deci (d)	10 <sup>-1</sup>
kilo (k)	10 <sup>3</sup>
mega (M)	10 <sup>6</sup>
giga (G)	10 <sup>9</sup>

## APPENDIX B

### EQUIPMENT AND PROCEDURES FOR TUBING DIMENSIONAL INSPECTION

This appendix describes the pertinent features of the equipment and procedures used to measure the beryllium tubing. The basic components of the dimensional-measurement equipment are shown in figure 21. This configuration was used to determine wall thickness. The tubing was supported on a small anvil (fig. 22) attached to the support rod. This anvil established the indicator zero point and assured a point contact for determination of wall thickness at any point of the tube. For long tubes of small diameter, it was necessary to use a smaller support rod which was prestressed in axial tension to minimize deflection of the anvil during measurement. After each measurement, the indicator plunger was retracted from the tube surface to preclude plunger wear and surface damage to the beryllium tubes.

The basic configuration of the measurement equipment was modified as shown in figure 23 to determine the outside diameter of the tubing. The tube was supported, at the point of measurement, between two precision roller bearings. One of these bearings was attached to the indicator plunger. The indicator was zeroed with precision gage blocks. This type of double-roller assembly permitted rapid determination of several tubing outside diameters at the same longitudinal cross section without damage to the tubing or appreciable abrasion of the support rollers.

Tubing-straightness measurements were made with the assembly attachments shown in figure 24. The tube was supported against two alinement plates by spring clips and was prevented from rotating by alinement pins. To measure straightness, the whole indicator assembly was traversed on the measurement bench the length of the tube. The roller plunger tip was used on the indicator. For small-diameter long tubes, the indicator plunger was retracted and an adjustable vee-groove support was placed under the tube. The vee block was adjusted to support the tube under the plunger load and yet not change the straightness characteristics of the tube being measured.

The bench attachments shown in figure 25 were utilized to determine the angle that a tube end made with an axial line passing through the centroids of the tube ends. These attachments included a spring-loaded conical end support, an adjustable vee-groove support, and a pivoted rotation indicator. To accomplish the measurement, the vee-groove support was adjusted to aline the centroid of the tube end being measured with the pivot of the rotation indicator. The spring-loaded conical end support on the other end of the tube assured contact with the tube end and the rotation indicator. When deviations from perpendicular occurred, the indicator rotated about its pivot point and displaced the indicator pointer on a calibrated scale.

## APPENDIX C

### EQUIPMENT AND PROCEDURES FOR TENSILE SPECIMEN PREPARATION

A variety of methods for gripping the beryllium tubes for tensile testing was investigated in order to minimize misalignment of the specimen with respect to the end fittings and to assure fracture of the specimen in the center section of the tube. The most suitable method investigated and the one which was used for the majority of tensile tests is presented in this appendix. This method consisted of adhesively bonding aluminum end fittings to the beryllium tubes. The center section of the tube was then chemically etched.

#### Adhesive Bonding

Before bonding, both the beryllium tubes and the aluminum end fittings and split collars were chemically cleaned by using the following procedure:

1. Vapor degrease in trichloroethylene for at least 1 minute.
2. Within 30 minutes after step 1, alkaline clean. Soak parts in cleaner at least 5 minutes.
3. Rinse thoroughly with water (spray and soak rinse preferred). Check for water breaks; if breaks are present, repeat steps 1 and 2.
4. Within 30 minutes, immerse parts in chromic-sulfuric solution. Agitation of solution should be stopped prior to immersion of parts. Solution temperature should be maintained between 70° and 80° F (294° and 300° K). The beryllium should be immersed for 30 seconds after the first evolution of bubbles and the aluminum should be immersed for 10 to 15 minutes. The solution should remove less than 0.0003 in./side (7.6  $\mu\text{m}$ /side). Chromic-sulfuric acid is made by combining the following:

Chromic acid

(Federal O-C-303) . . . . . 5 ounces mass (141.5 grams)

Sulfuric acid

(Federal O-A-115; class A; grade 2). . 23 ounces mass (651 grams)

Water . . . . . to make 1 gallon (3.8 dm<sup>3</sup>)

5. Immediately on removal of parts from the chromic-sulfuric solution, spray rinse parts thoroughly with cold water for 3 to 5 minutes and immersion rinse for 4 to 6 minutes in cold water. ("Cold" water is water at or below 75° F (297° K).)
6. Spray rinse parts for 3 to 5 minutes again in cold water and check for water break; if breaks are present, repeat steps 1, 2, 3, 4, and 5.

## APPENDIX C

7. Within 30 minutes of the last rinse, the parts should be dried in a vented oven at a temperature not to exceed  $150^{\circ}\text{ F}$  ( $339^{\circ}\text{ K}$ ).

Typical beryllium tubes before and after bonding are shown in figure 26. The bonding fixture used to align the beryllium tubes and the aluminum end fittings is shown in figure 27. The epoxy-based film adhesive was wrapped around the joint sections to a thickness of at least 0.010 inch (0.25 mm) to assure complete bonding of the split collars to the tube and end fittings. The cured bond-line thickness was approximately 0.005 inch (0.13 mm). The maximum average shear stress on the bonded area of the beryllium tubes ( $3000\text{ psi}$  ( $20.7\text{ MN/m}^2$ )) was based on a tube strength of 100 ksi ( $690\text{ MN/m}^2$ ).

### Chemical Etching

The need to chemically remove damaged surface layers in machined beryllium tensile specimens is well recognized (ref. 16). The ideal etchant would produce a smooth pit-free surface. It would also produce smooth radii with no undercutting (radius grooving) at the intersections of etched and unetched surfaces. The effect of different surface treatments on the tensile properties of the beryllium tubing has been previously discussed. The purpose of this section is to (1) describe the most satisfactory procedure developed to etch the tensile specimens, (2) to characterize the surfaces produced on extruded tubing with four different etching solutions, and (3) to characterize the etching behavior of the  $\text{Cr}_2\text{O}_3\text{-HF-H}_2\text{O}$  etching solution used to etch most of the tensile specimens.

The  $\text{HNO}_3\text{-H}_2\text{SO}_4\text{-H}_2\text{O}$  etchant recommended in reference 16 was used to develop the etching procedures for the tensile specimens. This etchant often produced surface defects such as pitting, increased surface roughness and/or waviness, and uncontrolled etching rates adjacent to the marked edges (radius grooving and/or feathering). A variety of etching procedures were evaluated in an attempt to minimize the defects produced by this etchant. The most satisfactory procedure developed included the following:

1. The end fittings were masked with two layers of thin plastic tape.
2. The specimen was rotated about its longitudinal axis ( $\approx 10\text{ rpm}$ ) at a  $45^{\circ}$  angle to the vertical during etching.
3. The etchant was slowly circulated and the etchant temperature was controlled to within  $\pm 2^{\circ}\text{ F}$  ( $\pm 1^{\circ}\text{ K}$ ).
4. The section to be etched was immersed a minimum of 2 inches (5 cm) below the surface of the etchant.

## APPENDIX C

By using these procedures the three etchants recommended in reference 16 were evaluated on a single length of the type B tubing. The tube was etched to remove 0.006 to 0.012 inch (0.15 to 0.30 mm) from the wall thickness. In figures 28 to 30, the overall appearance of the etched section, a selected area of the intersection of the etched and unetched surfaces, and a view of the radius produced at this intersection are shown for each of the etchants investigated. Only the  $\text{Cr}_2\text{O}_3\text{-H}_2\text{SO}_4\text{-H}_3\text{PO}_4$  etchant produced a polished surface with no surface pitting (fig. 28(a)). This etchant, however, produced severe radius grooving and some feathering at the masking-tape interface (figs. 28(a) and (b)). All the etchants characteristically produced the more severe radius grooving on the masking-tape interface which was deeper in the etching solution (see, for example, fig. 28(a)).

The surfaces produced with the  $\text{HNO}_3\text{-H}_2\text{SO}_4\text{-H}_2\text{O}$  etchant are shown in figure 29. This etchant produced a matte surface with some pitting (fig. 29(a)), an increase in surface roughness and minor feathering (fig. 29(b)), and some radius grooving (figs. 29(a) and (c)). The most satisfactory etchant suggested in reference 16 was the  $\text{HNO}_3\text{-HF-H}_2\text{O}$  solution. This etchant produced a light matte surface (figs. 30(a) and (b)) with less surface roughness and fewer pits than the surfaces etched with the  $\text{HNO}_3\text{-H}_2\text{SO}_4\text{-H}_2\text{O}$  solution. The  $\text{HNO}_3\text{-HF-H}_2\text{O}$  etchant also produced some radius grooving at the lower masking-tape interface (fig. 30(a)). No grooving was evident on the upper masking-tape interface.

The development of a large pit was observed during the etching experiments with the  $\text{HNO}_3\text{-H}_2\text{SO}_4\text{-H}_2\text{O}$  solution. An inclusion was first observed after a light etch (fig. 31(a)). The inclusion, presumably beryllium oxide, was not visibly attacked by this etchant. The pit (fig. 31(b)), which remained after additional etching, allowed the inclusion to fall out. Because of this large difference in dissolution rate between the pit-producing inclusions and the beryllium, an etchant containing chromic acid ( $\text{Cr}_2\text{O}_3$ ) and hydrofluoric acid (HF) was investigated in an attempt to reduce surface pitting and, at the same time, eliminate radius grooving. A 4:1 volume ratio of 48-percent HF to a  $\text{Cr}_2\text{O}_3\text{-H}_2\text{O}$  solution was selected. The  $\text{Cr}_2\text{O}_3\text{-H}_2\text{O}$  solution was prepared by dissolving 1 gram of  $\text{Cr}_2\text{O}_3$  in 10 millimeters ( $0.01 \text{ dm}^3$ ) of distilled water. With this  $\text{Cr}_2\text{O}_3\text{-HF-H}_2\text{O}$  concentrate, the effects of additional dilution with distilled water on the surface characteristics and etching rates were evaluated on a single beryllium tube. All the solutions investigated were circulated and maintained at  $80^\circ \pm 1^\circ \text{ F}$  ( $300^\circ \pm 0.5^\circ \text{ K}$ ). The etching rates varied in a logarithmic manner from  $1 \times 10^{-4} \text{ in./min/side}$  ( $0.04 \text{ }\mu\text{m/s/side}$ ) at a dilution of 250:1 of the concentrate to  $1.5 \times 10^{-3} \text{ in./min/side}$  ( $0.6 \text{ }\mu\text{m/s/side}$ ) at a dilution of 10:1. The slower etching rates produced surfaces which were comparable to those produced with the

## APPENDIX C

$\text{Cr}_2\text{O}_3\text{-H}_2\text{SO}_4\text{-H}_3\text{PO}_4$  etchant; that is, a polished surface with severe radius grooving. The faster etching solutions produced rougher surfaces with little or no pitting or radius grooving. The solution which was selected to etch the tensile specimens was the slowest which would produce no radius grooving and a minimum of surface pits. The solution ingredients were as follows:

- 4 parts by volume of 48-percent HF
- 1 part by volume of  $\text{Cr}_2\text{O}_3\text{-H}_2\text{O}$  concentrate solution
- 20 parts by volume of distilled water

The surfaces produced by the selected etchant are shown in figure 32. Although this etchant did not completely eliminate surface pits (fig. 32(a)) and did increase surface roughness (fig. 32(b)), it did not produce radius grooving (fig. 32(c)).

The tensile specimens were etched one at a time in a tank containing approximately 41 liters ( $41\text{ dm}^3$ ) of etchant. Solution temperatures ranged from  $72^\circ$  to  $92^\circ\text{ F}$  ( $296$  to  $307^\circ\text{ K}$ ). The temperature dependence of the etching rate for some of the tensile specimens is shown in figure 33. The etching rates on the extruded tubing (types A, B, and BL) were essentially the same and varied in a linear manner (fig. 33(a)). The etching rate on the type PS specimens was much higher (fig. 33(b)) and was not reproducible from specimen to specimen. This etchant also produced severe pitting in the type PS tubes (see fig. 4). The tensile specimens were etched to remove a minimum of 0.010 inch (0.25 mm) from the original diameter. The area of the reduced section was calculated by using the original diameter and wall thickness and the difference in diameter on a single cross section in the center of the specimen before and after etching.



## REFERENCES

1. Finn, J. M.; Koch, L. C.; and Muehlberger, D. E.: Design, Fabrication, and Ground Testing of the F-4 Beryllium Rudder. AFFDL-TR-67-68, U. S. Air Force, Apr. 1967.
2. Finn, J. M.; Koch, L. C.; and Muehlberger, D. E.: Design, Fabrication, and Test of an Aerospace Plane Beryllium Wing-Box. AFFDL-TR-67-38, U. S. Air Force, Mar. 1967.
3. Oken, S.; and Dilks, B. H.: Structural Evaluation of Beryllium Solar Panel Spars. AFFDL-TR-65-45, U. S. Air Force, Aug. 1966.
4. King, Bryce: A Review of Advances in Beryllium Applications Since the 1961 International Conference on the Metallurgy of Beryllium. Beryllium Technology, Vol. 2. Vol. 33 of Metallurgical Society Conferences, L. McDonald Schetky and Henry A. Johnson, eds., Gordon and Breach, Sci. Publ., Inc., c.1966, pp. 963-990.
5. Comm. on Metric Pract.: ASTM Metric Practice Guide. NBS Handbook 102, U. S. Dep. Comm., Mar. 10, 1967.
6. Comm. on Beryllium Met.: Fifth Progress Report. Publ. MAB-199-M(5), Nat. Acad. Sci. - Nat. Res. Council, Feb. 1966.
7. Danforth, Arthur L.; and Krashes, David: Polishing Beryllium by Vibration. Metal Progr., vol. 91, no. 2, Feb. 1967, p. 115.
8. Heimerl, George J.; Baucom, Robert M.; Manning, Charles R., Jr.; and Braski, David N.: Stability of Four Titanium-Alloy and Four Stainless-Steel Sheet Materials After Exposures Up to 22 000 Hours at 550° F (561° K). NASA TN D-2607, 1965.
9. Baumberger, R.; and Hines, F.: Practical Reduction Formulas for Use on Bonded Wire Strain Gages in Two-Dimensional Stress Fields. Proc. Soc. Exp. Stress Analysis, vol. II, no. 1, 1944, pp. 113-127.
10. Lundquist, Eugene E.; Rossman, Carl A.; and Houbolt, John C.: A Method for Determining the Column Curve From Tests of Columns With Equal Restraints Against Rotation on the Ends. NACA TN 903, 1943.
11. Udy, Murray C.: Metallography of Beryllium and Beryllium-Rich Alloys. The Metal Beryllium, D. W. White, Jr., and J. E. Burke, eds., Amer. Soc. Metals, 1955, pp. 505-529.
12. Jacobson, M. I.: Beryllium Research and Development Program - Metallurgical Factors Affecting the Ductile-Brittle Transition in Beryllium. ASD-TDR-62-509, Vol. V, U.S. Air Force, July 1964.

13. Hill, N. A.; and Williams, J.: Textures in Beryllium Rods and Tubes Extruded From Consolidated Powder. Powder Met., no. 5, 1960, pp. 116-129.
14. Hill, N. A.; and Jones, J. W. S.: The Crystallographic Dependence of Low Load Indentation Hardness in Beryllium. J. Nucl. Mater., vol. 3, no. 2, Feb. 1961, pp. 138-155.
15. Kaufmann, Albert R.; Gordon, Paul; and Lillie, D. W.: The Metallurgy of Beryllium. Trans. Amer. Soc. Metals, vol. 42, 1950, pp. 785-844.
16. Subcom. on Test Methods: Evaluation Test Methods for Beryllium. Publ. MAB-205-M. (ARPA Contract SD-118), Nat. Acad. Sci. - Nat. Res. Council, Mar. 1966.
17. Anon.: Beryllium Properties & Products. Bull. 2100, Beryllium Corp., [1965].
18. Fenn, Raymond W., Jr.; Glass, Richard A.; Needham, Robert A., and Steinberg, Morris A.: Beryllium-Aluminum Alloys. J. Spacecraft Rockets, vol. 2, no. 1, Jan.-Feb. 1965, pp. 87-93.
19. Smith, J. F.; and Arbogast, C. L.: Elastic Constants of Single Crystal Beryllium. J. Appl. Phys., vol. 31, no. 1, Jan. 1960, pp. 99-102.
20. Lyman, Taylor, ed.: Metals Handbook. Volume 1.- Properties and Selection of Metals. 8th ed., Amer. Soc. Metals, c.1961.
21. Sumner, G.: Brittle Behavior in Extruded Beryllium Tubes. Int. J. Fracture Mech., vol. 2, no. 2, June 1966, pp. 448-459.

TABLE I.- FABRICATION HISTORY FOR BERYLLIUM TUBING

Type	Fabrication history <sup>a</sup>
A	Extruded from hot-pressed block. First extrusion at 1750° F (1228° K) at a reduction ratio of 9:1. Second extrusion at 1750° F (1228° K) at a reduction ratio of 13.5:1. Tubes were ground to final dimensions.
B	Hot-pressed billet extruded at 1850° F (1283° K) at a reduction ratio of 28:1. Straightened at 1400° F (1033° K) by using skew-roll techniques. Steel jacket and core removed and tubing machined to length. Tubes chemically etched to final dimensions.
BL	Hot-pressed and machined extrusion billets canned in mild steel containers by using a core-type mandrel. Billets extruded in the temperature range from 1700° to 1900° F (1200° to 1311° K) by employing reduction ratios of greater than 10:1. After extrusion, tubes were cut to length and hot straightened. The steel jacket was then removed and the tubing was honed and chemically etched to final dimensions.
PS	S-200 grade powder plasma-sprayed on tubular copper mandrel in argon atmosphere. Tubes machined and mandrel leached out. Vacuum sintered at $2.5 \times 10^{-5}$ torr (3.3 mN/m <sup>2</sup> ) for 4 hours at 700° F (644° K). Cooled in vacuum to 700° F (644° K). Tubing with bulk density less than 1.80 g/cm <sup>3</sup> (1.80 Mg/m <sup>3</sup> ) resintered for 4 hours at 2150° F (1450° K).

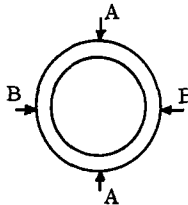
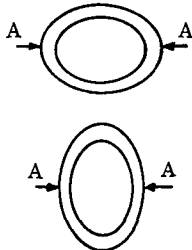
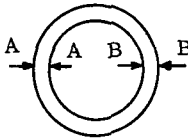
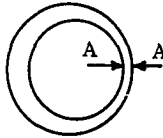
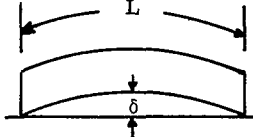
<sup>a</sup>Information furnished by supplier.

TABLE II.- NOMINAL DIAMETER, NOMINAL WALL THICKNESS, CHEMICAL COMPOSITION,  
AND BULK DENSITY OF BERYLLIUM TUBING<sup>a</sup>

Type	Nominal diameter, D <sub>n</sub>		Nominal wall thickness, t <sub>n</sub>		Chemical composition								All other metallic impurities, percent	Bulk density, g/cm <sup>3</sup> (Mg/m <sup>3</sup> )
					Beryllium assay, percent	Beryllium oxide, percent	Carbon, percent	Iron, percent	Aluminum, percent	Silicon, percent	Magnesium, percent	Copper, percent		
	in.	mm	in.	mm										
A	0.50	12.70	0.020	0.508	98.88	1.50	0.033	0.042	0.029	0.010	0.001	---	0.04	1.84
B	0.50	12.70	0.020	0.508	98.95	1.09	0.083	0.070	0.048	0.046	0.006	---	0.04	1.856
BL	.025	6.35	0.020	0.508	99.02	0.92	0.069	0.075	0.030	0.041	0.010	---	0.04	----
	.25	6.35	.040	1.016	99.02	.92	.069	.075	.030	.041	.010	---	.04	----
	.50	12.70	.020	.508	98.92	1.04	.077	.077	.084	.065	.016	---	.04	1.850
	.50	12.70	.040	1.016	98.73	1.20	.094	.085	.057	.066	.080	---	.04	1.851
	.75	19.05	.020	.508	98.93	1.02	.078	.074	.061	.063	.028	---	.04	1.853
	.75	19.05	.040	1.016	98.91	1.13	.099	.053	.059	.043	.005	---	.04	1.851
PS	0.54	13.72	0.020	0.508	96.00	4.85	0.100	0.140	0.077	0.050	0.004	0.40	---	----
	.58	14.73	.040	1.016	96.00	4.85	.100	.140	.077	.050	.004	.40	---	----

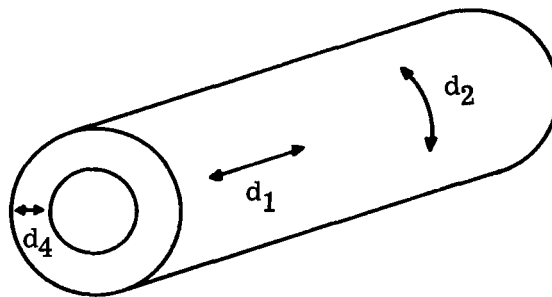
<sup>a</sup>Information furnished by supplier.

TABLE III.- DIMENSIONAL TOLERANCES FOR BERYLLIUM TUBING

Diameter variations			Wall-thickness variations			Straightness variations		
Size	Ovalness		Wall thickness	Eccentricity				
Maximum deviation of mean diameter <sup>a</sup> from specified diameter: difference between $\frac{1}{2}(AA + BB)$ and specified diameter	Maximum deviation of diameter at any point from specified diameter: difference between AA and specified diameter		Maximum deviation of mean wall thickness from specified wall thickness: difference between $\frac{1}{2}(AA + BB)$ and specified wall thickness	Maximum deviation of wall thickness at any point from mean wall thickness: difference between AA and mean wall thickness		Maximum deviation from straight: $\frac{\delta}{L} \times 100$ at point of maximum $\delta$ obtained by rotating finished tube through 360° while resting on a plane surface		
								
Tolerance, plus and minus				Tolerance, plus and minus				
Type	in.	mm	in.	mm	in.	mm	percent of mean wall thickness	Tolerance, percent
A	0.010	0.254	0.020	0.508	0.006	0.152	20	0.83
B	.010	.254	.020	.508	.006	.152	10	1.66
BL	.015	.381	.030	.762	.009	.223	15	.83
PS	.010	.254	.020	.508	.006	.152	10	.83

<sup>a</sup>Mean diameter is the average of two diameter measurements taken at right angles to each other at any point along the length.

TABLE IV.- GRAIN SIZE OF BERYLLIUM TUBING



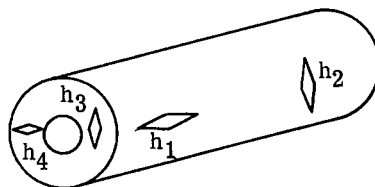
Type	$D_n$		$t_n$		Grain size, $\mu\text{m}$ , for -		
	in.	mm	in.	mm	$d_1$	$d_2$	$d_4$
A	0.50	12.70	0.020	0.508	11.0	4.6	4.1
B	0.50	12.70	0.020	0.508	13.6	8.4	7.5
BL	0.25	6.35	0.020	0.508	13.0	11.7	9.9
	.25	6.35	.040	1.016	13.0	10.1	8.1
	.50	12.70	.020	.508	13.7	9.8	7.0
	.50	12.70	.040	1.016	17.2	14.0	11.5
	.75	19.05	.020	.508	13.2	10.0	9.8
	.75	19.05	.040	1.016	12.9	10.6	9.8

TABLE V.- X-RAY DIFFRACTION INTENSITY RATIOS FOR BERYLLIUM TUBING

Type	D <sub>n</sub>		t <sub>n</sub>		Diffracting planes (hkl)							
	in.	mm	in.	mm	10 $\bar{1}$ 0	0002	10 $\bar{1}$ 1	10 $\bar{1}$ 2	11 $\bar{2}$ 0	10 $\bar{1}$ 3	20 $\bar{2}$ 0	11 $\bar{2}$ 2
Random <sup>a</sup>	---	----	----	----	20	14	100	12	12	12	2	8
A	0.50	12.70	0.020	0.508	--	80	---	--	19	--	-	100
B	0.50	12.70	0.020	0.508	--	45	---	--	78	--	-	100
BL	0.25	6.35	0.020	0.508	--	69	---	--	77	--	-	100
	.25	6.35	.040	1.016	--	67	---	--	69	--	-	100
	.50	12.70	.020	.508	--	77	---	--	98	--	-	100
	.50	12.70	.040	1.016	--	70	---	--	66	--	-	100
	.75	19.05	.020	.508	--	94	---	--	56	--	-	100
	.75	19.05	.040	1.016	--	69	---	--	69	--	-	100
PS	0.54	13.72	0.020	0.508	38	29	100	10	18	16	-	22
	.58	14.73	.040	1.016	34	26	100	15	21	19	-	26

<sup>a</sup>From ASTM standard powder diffraction pattern.

TABLE VI.- MICROHARDNESS OF BERYLLIUM TUBING



Type	D <sub>n</sub>		t <sub>n</sub>		h <sub>1</sub>		h <sub>2</sub>		h <sub>3</sub>		h <sub>4</sub>	
	in.	mm	in.	mm	KHN <sub>100</sub>	95-percent CI <sup>a</sup>	KHN <sub>100</sub>	95-percent CI <sup>a</sup>	KHN <sub>100</sub>	95-percent CI <sup>a</sup>	KHN <sub>100</sub>	95-percent CI <sup>a</sup>
A	0.50	12.70	0.020	0.508	272.6	13.9	239.6	6.9	233.9	4.6	247.6	4.9
B	0.50	12.70	0.020	0.508	237.3	18.5	198.6	10.1	185.1	6.0	197.8	3.0
BL	0.25	6.35	0.020	0.508	241.7	15.6	214.8	8.9	198.6	10.1	199.5	2.7
	.25	6.35	.040	1.016	235.6	10.3	211.4	7.9	191.1	4.3	204.9	3.8
	.50	12.70	.020	.508	246.9	20.1	205.2	7.6	190.5	4.3	209.2	3.3
	.50	12.70	.040	1.016	202.5	16.0	203.9	16.2	176.5	4.1	177.6	4.1
	.75	19.05	.020	.508	221.6	19.8	206.0	10.0	192.1	4.4	204.1	2.6
	.75	19.05	.020	.508	224.3	14.9	191.8	14.0	183.7	3.8	190.4	3.7
PS	0.54	13.72	0.020	0.508	258.4	17.1	234.1	16.4	255.5	10.9	267.7	13.6
	.58	14.73	.040	1.016	249.8	23.4	244.3	22.3	249.5	25.3	280.1	17.6

<sup>a</sup>95-percent confidence interval based on 10 determinations of microhardness.



TABLE VII.- SUMMARY OF DIMENSIONAL INSPECTION OF BERYLLIUM TUBING

(a) U.S. Customary Units

Material	A				B				BL				PS	
Number of observations	86	85	109	91	109	118	117	141	74	87				
Number of tubes	27	27	35	30	34	32	31	36	23	29				
Outside diameter, in.:														
Nominal	0.5000	0.5000	0.2500	0.2500	0.5000	0.5000	0.7500	0.7500	0.5400	0.5800				
Average	.5029	.4981	.2589	.2563	.5055	.5077	.7556	.7536	.5394	.5756				
Maximum	.5046	.5043	.2646	.2639	.5137	.5141	.7648	.7632	.5469	.5938				
Minimum	.5005	.4935	.2498	.2499	.4998	.4992	.7447	.7408	.5307	.5674				
Standard deviation	.0010	.0024	.0031	.0039	.0037	.0036	.0045	.0056	.0042	.0036				
Wall thickness, in.:														
Nominal	0.0200	0.0200	0.0200	0.0400	0.0200	0.0400	0.0200	0.0400	0.0200	0.0400				
Average	.0224	.0204	.0226	.0422	.0214	.0433	.0214	.0409	.0191	.0374				
Maximum	.0247	.0238	.0262	.0486	.0262	.0469	.0272	.0471	.0224	.0398				
Minimum	.0194	.0168	.0176	.0343	.0170	.0332	.0134	.0319	.0154	.0332				
Standard deviation	.0011	.0016	.0021	.0038	.0024	.0030	.0027	.0031	.0027	.0012				
Area, in <sup>2</sup> :														
Nominal	$3.016 \times 10^{-2}$	$3.016 \times 10^{-2}$	$1.445 \times 10^{-2}$	$2.639 \times 10^{-2}$	$3.016 \times 10^{-2}$	$5.781 \times 10^{-2}$	$4.587 \times 10^{-2}$	$8.922 \times 10^{-2}$	$3.267 \times 10^{-2}$	$6.786 \times 10^{-2}$				
Average	3.381	3.057	1.680	2.838	3.254	6.322	4.939	9.157	3.116	6.327				
Maximum	3.704	3.549	1.920	3.250	3.984	6.465	6.270	10.546	3.687	6.797				
Minimum	2.934	2.518	1.303	2.347	2.585	4.868	3.085	7.184	2.523	5.631				
Standard deviation	.160	.228	.143	.230	.359	.431	.615	.671	.444	.218				
Moment of inertia, in <sup>4</sup> :														
Nominal	$8.700 \times 10^{-4}$	$8.700 \times 10^{-4}$	$0.963 \times 10^{-4}$	$1.507 \times 10^{-4}$	$8.700 \times 10^{-4}$	$1.541 \times 10^{-3}$	$3.058 \times 10^{-3}$	$5.640 \times 10^{-3}$	$1.060 \times 10^{-3}$	$2.487 \times 10^{-3}$				
Average	9.779	8.734	1.182	1.689	9.552	1.719	3.330	5.833	1.056	2.302				
Maximum	10.582	10.275	1.338	1.989	11.700	1.759	4.226	6.725	1.267	2.628				
Minimum	8.513	7.174	.893	1.426	7.578	1.329	2.072	4.623	.846	2.058				
Standard deviation	.442	.622	.093	.140	1.038	.117	.410	.420	.152	.095				

TABLE VII.- SUMMARY OF DIMENSIONAL INSPECTION OF BERYLLIUM TUBING - Concluded

(b) SI Units

Material	A	B	BL						PS	
Number of observations	86	85	109	91	109	118	117	141	74	87
Number of tubes	27	27	35	30	34	32	31	36	23	29
Outside diameter, mm:										
Nominal	12.700	12.700	6.350	6.350	12.700	12.700	19.050	19.050	13.716	14.732
Average	12.774	12.652	6.577	6.510	12.841	12.900	19.193	19.142	13.700	14.619
Maximum	12.817	12.809	6.721	6.703	13.048	13.058	19.426	19.385	13.891	15.082
Minimum	12.713	12.535	6.345	6.348	12.695	12.680	18.943	18.816	13.480	14.412
Standard deviation	.026	.061	.078	.098	.093	.092	.114	.143	.107	.091
Wall thickness, mm:										
Nominal	0.508	0.508	0.508	1.016	0.508	1.016	0.508	1.016	0.508	1.016
Average	.569	.517	.575	1.086	.544	1.101	.544	1.039	.484	.950
Maximum	.627	.604	.666	1.242	.666	1.191	.691	1.196	.569	1.011
Minimum	.493	.427	.447	.871	.432	.843	.340	.810	.391	.843
Standard deviation	.028	.040	.054	.096	.061	.077	.068	.078	.069	.031
Area, mm <sup>2</sup> :										
Nominal	19.46	19.46	9.32	17.03	19.46	37.29	29.59	57.56	21.08	43.78
Average	21.81	19.72	10.84	18.31	21.00	40.79	31.86	59.08	20.10	40.82
Maximum	23.90	22.90	12.39	20.97	25.70	45.20	40.45	68.04	23.78	43.86
Minimum	18.93	16.25	8.41	15.14	16.68	31.40	19.91	46.34	16.28	36.33
Standard deviation	1.03	1.47	.92	1.48	2.31	2.78	3.97	4.33	2.86	1.41
Moment of inertia, mm <sup>4</sup> :										
Nominal	362.2	362.2	40.08	62.75	362.2	641.2	1272.7	2347.5	460.3	1035.2
Average	407.0	363.5	49.21	70.32	397.6	715.4	1386.2	2427.9	439.5	958.1
Maximum	440.5	427.7	55.70	82.78	487.0	785.5	1759.1	2799.2	527.4	1094.0
Minimum	354.3	298.6	37.17	59.36	315.4	553.3	862.5	1924.1	352.1	856.7
Standard deviation	18.4	25.9	3.85	5.81	43.2	48.7	170.5	174.7	63.3	39.3

TABLE VIII.- SUMMARY OF ROOM-TEMPERATURE MECHANICAL PROPERTIES FOR BERYLLIUM TUBING

Type	D <sub>n</sub>		t <sub>n</sub>		σ <sub>tu</sub>		σ <sub>ty</sub>		σ <sub>cy</sub>		σ <sub>tp</sub>		σ <sub>cp</sub>		E		E <sub>c</sub>		μ <sub>tp</sub>	μ <sub>cp</sub>	e	e <sub>u</sub>
	in.	mm	in.	mm	ksi	MN/m <sup>2</sup>	ksi	MN/m <sup>2</sup>	ksi	MN/m <sup>2</sup>	ksi	MN/m <sup>2</sup>	ksi	MN/m <sup>2</sup>	psi	GN/m <sup>2</sup>	psi	GN/m <sup>2</sup>				
A	0.50	12.70	0.020	0.508	67.5	465	64.5	445	65.3	450	44	307	31	211	40.7 × 10 <sup>6</sup>	278	40.2 × 10 <sup>6</sup>	277	0.071	0.078	<1	<1
B	0.50	12.70	0.020	0.508	<sup>a</sup> 57.3	<sup>a</sup> 395	<sup>a</sup> 42.4	<sup>a</sup> 293	41.6	287	<sup>a</sup> 21	<sup>a</sup> 145	19	128	<sup>a</sup> 41.0 × 10 <sup>6</sup>	<sup>a</sup> 283	39.0 × 10 <sup>6</sup>	269	<sup>a</sup> 0.058	0.091	<sup>a</sup> <1	<sup>a</sup> <1
BL	0.25	6.35	0.020	0.508	89.4	617	53.1	366	43.8	302	22	155	19	134	40.0 × 10 <sup>6</sup>	276	39.1 × 10 <sup>6</sup>	270	.070	.163	5	---
	.25	6.35	.040	1.016	84.7	584	46.0	317	44.5	307	23	159	22	149	40.2	277	40.2	277	.76	.100	5	5
	.50	12.70	.020	.508	85.8	592	42.4	292	42.6	294	24	166	19	134	41.1	283	39.6	273	.070	.085	7	6
	.50	12.70	.040	1.016	83.3	574	40.7	281	38.3	264	19	130	17	116	40.8	281	39.4	272	.076	.090	9	7
	.75	19.05	.020	.508	78.1	538	43.8	302	41.7	288	23	159	18	122	41.0	283	39.2	270	.078	.085	5	4
	.75	19.05	.020	1.016	85.0	586	42.3	291	39.6	273	17	117	19	129	40.1	277	39.4	272	.067	.088	7	7
PS	0.54	13.72	0.020	0.508	46.4	320	----	----	56.6	390	29	203	35	250	39.4 × 10 <sup>6</sup>	272	40.6 × 10 <sup>6</sup>	280	0.081	0.086	<1	<1
	.58	14.73	.040	1.016	72.8	502	----	----	79.0	544	50	346	50	346	40.5	279	40.1	276	.071	.070	<1	<1

<sup>a</sup>Tested in as-received condition.

TABLE IX.- RESULTS OF ROOM-TEMPERATURE TENSILE TESTS ON BERYLLIUM TUBING<sup>a</sup>

Type	Specimen	D <sub>n</sub>		t <sub>n</sub>		$\sigma_{cp}$		$\sigma_{ty}$		$\sigma_{tu}$		E		$\mu_{tp}$	e <sub>u</sub>	e
		in.	mm	in.	mm	ksi	MN/m <sup>2</sup>	ksi	MN/m <sup>2</sup>	ksi	MN/m <sup>2</sup>	psi	GN/m <sup>2</sup>			
A	b <sub>1</sub>	0.50	12.70	0.020	0.508	40	276	65.8	454	66.2	457	40.0 × 10 <sup>6</sup>	276	0.068	<1	<1
	2	↓	↓	↓	↓	29	201	62.8	433	69.2	477	42.3	292	.070	1	1
	3	↓	↓	↓	↓	46	314	65.0	448	69.7	481	41.1	283	.070	--	<1
	4	↓	↓	↓	↓	65	448	---	---	71.8	495	40.0	276	.075	<1	<1
	5	↓	↓	↓	↓	42	290	---	---	64.9	447	39.8	274	.077	<1	<1
	6	↓	↓	↓	↓	45	314	---	---	63.1	435	38.3	264	.068	<1	<1
B	Average	↓	↓	↓	↓	44	307	64.5	445	67.5	465	40.7 × 10 <sup>6</sup>	278	0.071	<1	<1
	b <sub>7</sub>	0.50	12.70	0.020	0.508	22	152	42.5	293	55.5	383	40.8 × 10 <sup>6</sup>	281	---	<1	--
	b <sub>8</sub>	↓	↓	↓	↓	21	145	42.2	291	59.6	411	41.7	288	0.055	1	--
	b <sub>9</sub>	↓	↓	↓	↓	14	97	42.3	292	56.4	389	40.6	280	.059	<1	--
	b <sub>10</sub>	↓	↓	↓	↓	27	186	42.7	294	57.7	398	41.0	283	.061	1	--
	Average	↓	↓	↓	↓	21	145	42.4	293	57.3	395	41.0 × 10 <sup>6</sup>	283	0.058	<1	--
C	c <sub>11</sub>	0.50	12.70	0.020	0.508	25	172	41.0	283	62.0	427	41.0 × 10 <sup>6</sup>	283	0.065	2	--
	c <sub>12</sub>	↓	↓	↓	↓	27	183	41.0	283	69.0	476	41.3	285	.064	3	--
	Average	↓	↓	↓	↓	26	178	41.0	283	65.5	452	41.2 × 10 <sup>6</sup>	284	0.064	2.5	--
	13	0.50	12.70	0.020	0.508	13	90	41.0	283	53.3	368	41.1 × 10 <sup>6</sup>	283	0.064	2	1
	14	↓	↓	↓	↓	36	248	52.8	364	93.7	646	41.0	283	.072	7	--
	Average	↓	↓	↓	↓	25	169	46.9	323	73.5	507	41.1 × 10 <sup>6</sup>	283	0.068	4.5	1
D	15	0.25	6.35	0.020	0.508	16	109	45.6	314	73.1	504	39.7 × 10 <sup>6</sup>	274	0.079	--	3
	16	↓	↓	↓	↓	22	155	46.1	318	82.6	570	39.3	271	.069	--	5
	17	↓	↓	↓	↓	40	275	58.4	402	97.5	672	39.6	274	.075	--	5
	18	↓	↓	↓	↓	23	160	58.6	404	95.2	656	40.4	279	.063	--	5
	19	↓	↓	↓	↓	11	77	56.8	392	98.6	682	40.8	281	.062	--	6
	Average	↓	↓	↓	↓	22	155	53.1	366	89.4	617	40.0 × 10 <sup>6</sup>	276	0.070	--	5
E	20	0.25	6.35	0.040	1.016	24	164	48.0	331	83.5	575	40.0 × 10 <sup>6</sup>	276	0.065	--	4
	21	↓	↓	↓	↓	25	172	47.6	328	86.4	592	39.5	272	.068	4	--
	22	↓	↓	↓	↓	25	170	47.4	327	78.0	538	40.2	277	.100	3	--
	23	↓	↓	↓	↓	19	128	41.0	283	89.9	620	41.1	283	.072	9	--
	24	↓	↓	↓	↓	23	159	46.0	317	84.7	584	40.2 × 10 <sup>6</sup>	277	0.076	5	4
	Average	↓	↓	↓	↓	23	159	46.0	317	84.7	584	40.2 × 10 <sup>6</sup>	277	0.076	5	4
F	b <sub>25</sub>	0.50	12.70	0.020	0.508	12	83	41.0	283	58.7	405	41.0 × 10 <sup>6</sup>	283	0.061	2	--
	c <sub>26</sub>	↓	↓	↓	↓	18	124	48.0	331	80.2	553	41.0	283	.064	<1	--
	27	0.50	12.70	0.020	0.508	26	177	42.8	295	89.7	619	40.7 × 10 <sup>6</sup>	281	0.074	8	10
	28	↓	↓	↓	↓	20	141	43.8	302	87.1	601	40.5	279	.061	6	8
	29	↓	↓	↓	↓	27	186	44.0	303	87.7	604	42.8	295	.069	5	5
	30	↓	↓	↓	↓	23	161	41.3	285	82.2	567	41.0	283	.070	6	8
G	31	↓	↓	↓	↓	26	180	41.2	284	82.3	567	40.6	280	.075	6	6
	Average	↓	↓	↓	↓	24	169	42.6	294	85.8	592	41.1 × 10 <sup>6</sup>	284	0.070	6	7
	32	0.50	12.70	0.040	1.016	16	110	37.2	256	82.3	567	39.8 × 10 <sup>6</sup>	274	---	8	10
	33	↓	↓	↓	↓	17	117	45.0	310	84.4	582	40.6	280	---	4	7
	34	↓	↓	↓	↓	18	124	38.6	266	85.3	588	40.3	278	---	10	10
	35	↓	↓	↓	↓	23	161	42.8	295	79.4	547	41.2	284	.062	4	6
H	36	↓	↓	↓	↓	20	138	40.0	276	85.0	586	42.0	290	.091	10	10
	Average	↓	↓	↓	↓	19	130	40.7	281	83.3	574	40.8 × 10 <sup>6</sup>	281	0.076	7	9
	b <sub>37</sub>	0.75	19.05	0.020	0.508	21	145	46.0	317	54.4	375	40.3 × 10 <sup>6</sup>	278	0.060	<1	<1
	b <sub>38</sub>	↓	↓	↓	↓	25	172	40.6	280	63.5	438	40.0	276	.080	<1	<1
	Average	↓	↓	↓	↓	23	159	43.3	299	59.0	406	40.2 × 10 <sup>6</sup>	277	0.070	<1	<1
	39	0.75	19.05	0.020	0.508	30	207	42.5	293	79.9	551	39.1 × 10 <sup>6</sup>	270	0.090	5	5
I	40	↓	↓	↓	↓	31	214	44.0	303	75.3	519	41.5	286	.076	3	4
	41	↓	↓	↓	↓	29	200	44.0	303	88.8	612	41.5	286	.075	7	7
	42	↓	↓	↓	↓	25	172	45.2	312	86.3	595	41.2	284	.062	5	5
	43	↓	↓	↓	↓	25	172	45.0	310	61.6	425	42.6	294	.084	1	--
	44	↓	↓	↓	↓	19	131	42.0	290	76.4	526	40.0	276	.078	4	4
	Average	↓	↓	↓	↓	26	183	43.8	302	78.0	538	41.0 × 10 <sup>6</sup>	283	0.078	4	5
J	45	0.75	19.05	0.040	1.016	25	172	42.0	290	86.7	598	39.8 × 10 <sup>6</sup>	274	0.073	8	8
	46	↓	↓	↓	↓	12	83	41.0	283	79.2	546	39.5	273	.066	5	5
	47	↓	↓	↓	↓	15	103	41.0	283	82.8	571	40.0	276	.070	7	8
	48	↓	↓	↓	↓	16	110	45.0	310	91.3	630	41.1	283	.060	6	--
	Average	↓	↓	↓	↓	17	117	42.2	291	85.0	586	40.1 × 10 <sup>6</sup>	277	0.067	6	7
	49	0.54	13.72	0.020	0.508	21	143	---	---	49.0	338	35.4 × 10 <sup>6</sup>	244	0.082	<1	<1
K	50	0.54	13.72	0.020	0.508	---	---	---	---	33.2	229	39.2 × 10 <sup>6</sup>	270	---	<1	--
	51	↓	↓	↓	↓	16	110	---	---	39.2	270	41.0	283	0.085	<1	<1
	52	↓	↓	↓	↓	51	354	---	---	64.0	442	42.0	290	.077	<1	<1
	Average	↓	↓	↓	↓	34	232	---	---	45.5	314	40.7 × 10 <sup>6</sup>	281	0.081	<1	<1
	53	0.58	14.73	0.020	0.508	54.0	372	---	---	73.8	509	40.8 × 10 <sup>6</sup>	281	0.065	<1	<1
	54	↓	↓	↓	↓	53.0	365	---	---	72.5	500	41.2	284	.067	<1	<1
L	55	↓	↓	↓	↓	43.6	301	---	---	71.9	496	39.6	273	.083	<1	<1
	Average	↓	↓	↓	↓	50.2	346	---	---	72.8	502	40.5 × 10 <sup>6</sup>	279	0.071	<1	<1

<sup>a</sup>Specimens etched with Cr<sub>2</sub>O<sub>3</sub>-HF-H<sub>2</sub>O solution unless otherwise noted.<sup>b</sup>Specimen not etched.<sup>c</sup>Specimen etched with HNO<sub>3</sub>-H<sub>2</sub>SO<sub>4</sub>-H<sub>2</sub>O solution.<sup>d</sup>Specimen exposed to single-sintering cycle.

TABLE X.- RESULTS OF ROOM-TEMPERATURE COMPRESSIVE TESTS ON BERYLLIUM TUBING

Type	Specimen	D <sub>n</sub>		t <sub>n</sub>		$\sigma_{cp}$		$\sigma_{cy}$		$\sigma_{max}$		E <sub>c</sub>		$\mu_{cp}$
		in.	mm	in.	mm	ksi	MN/m <sup>2</sup>	ksi	MN/m <sup>2</sup>	ksi	MN/m <sup>2</sup>	psi	GN/m <sup>2</sup>	
A	1	0.50	12.70	0.020	0.508	39	269	66.4	458	114.5	790	40.2 × 10 <sup>6</sup>	277	0.070
	2	↓	↓	↓	↓	33	228	62.5	431	108.8	750	39.6	273	----
	3	↓	↓	↓	↓	33	228	64.0	441	112.0	772	38.6	266	.080
	4	↓	↓	↓	↓	26	179	59.6	411	106.1	732	40.0	276	.080
	5	↓	↓	↓	↓	22	152	74.0	510	113.6	783	42.4	292	.080
	Average . . . . .					31	211	65.3	450	111.0	765	40.2 × 10 <sup>6</sup>	277	0.078
B	6	0.50	12.70	0.020	0.508	21	145	41.3	285	72.6	501	39.0 × 10 <sup>6</sup>	269	0.085
	7	↓	↓	↓	↓	20	138	41.4	285	79.5	548	39.0	269	----
	8	↓	↓	↓	↓	15	103	40.8	281	74.9	516	40.0	276	.090
	9	↓	↓	↓	↓	20	138	43.7	301	64.8	447	38.6	266	.099
	10	↓	↓	↓	↓	17	117	40.9	282	79.5	548	38.5	265	----
	Average . . . . .					19	128	41.6	287	74.3	512	39.0 × 10 <sup>6</sup>	269	0.091
	11	0.25	6.35	0.020	0.508	18	124	40.3	278	106.4	734	39.3 × 10 <sup>6</sup>	271	0.200
	12	↓	↓	↓	↓	22	152	41.1	283	103.2	712	39.8	274	.127
	13	↓	↓	↓	↓	19	131	42.7	294	101.9	703	38.6	266	----
	14	↓	↓	↓	↓	20	138	44.6	308	98.5	679	38.0	262	----
	15	↓	↓	↓	↓	18	124	50.2	346	123.6	852	39.9	275	----
	Average . . . . .					19	134	43.8	302	106.7	736	39.1 × 10 <sup>6</sup>	270	0.163
	16	0.25	6.35	0.040	1.016	16	110	41.9	289	114.5	790	40.5 × 10 <sup>6</sup>	279	0.085
	17	↓	↓	↓	↓	23	159	43.5	300	109.5	755	38.7	267	.115
	18	↓	↓	↓	↓	22	152	44.3	305	125.5	865	39.9	275	----
	19	↓	↓	↓	↓	24	165	47.1	325	150.0	1035	41.7	288	----
	20	↓	↓	↓	↓	23	159	45.5	314	116.9	806	40.3	278	----
	Average . . . . .					22	149	44.5	307	123.3	850	40.2 × 10 <sup>6</sup>	277	0.100
	21	0.50	12.70	0.020	0.508	19	131	41.7	288	84.4	582	38.9 × 10 <sup>6</sup>	268	----
	22	↓	↓	↓	↓	18	124	37.5	259	71.2	491	38.8	267	0.085
	23	↓	↓	↓	↓	19	131	46.3	319	82.3	567	38.6	266	----
	24	↓	↓	↓	↓	22	152	43.0	296	80.9	558	40.8	281	----
	25	↓	↓	↓	↓	19	131	42.4	292	77.3	533	40.9	282	----
	Average . . . . .					19	134	42.2	291	79.2	546	39.6 × 10 <sup>6</sup>	273	0.085
BL	26	0.50	12.70	0.040	1.016	13	90	37.5	259	91.4	630	40.6 × 10 <sup>6</sup>	280	----
	27	↓	↓	↓	↓	19	131	38.0	262	80.5	555	38.0	262	----
	28	↓	↓	↓	↓	15	103	35.8	247	101.0	696	39.8	274	0.100
	29	↓	↓	↓	↓	20	138	42.0	290	113.0	779	39.3	271	.080
	Average . . . . .					17	116	38.3	264	96.5	665	39.4 × 10 <sup>6</sup>	272	0.090
	30	0.75	19.05	0.020	0.508	17	117	39.9	275	73.7	508	39.5 × 10 <sup>6</sup>	272	----
	31	↓	↓	↓	↓	20	138	40.7	281	75.5	521	38.0	262	----
	32	↓	↓	↓	↓	17	117	40.0	276	72.3	499	39.2	270	0.080
	33	↓	↓	↓	↓	17	117	41.0	283	60.5	417	38.8	268	.090
	34	↓	↓	↓	↓	12	83	40.9	282	72.4	499	40.0	276	----
	35	↓	↓	↓	↓	18	124	40.3	278	59.9	413	39.5	272	----
	36	↓	↓	↓	↓	23	159	49.2	339	64.6	445	39.3	271	----
	Average . . . . .					18	122	41.7	288	68.4	472	39.2 × 10 <sup>6</sup>	270	0.085
	37	0.75	19.05	0.040	1.016	17	117	39.3	271	93.5	645	39.0 × 10 <sup>6</sup>	269	0.080
	38	↓	↓	↓	↓	15	103	39.8	274	87.2	601	41.2	284	.050
	39	↓	↓	↓	↓	19	131	39.2	270	84.9	585	39.2	270	.090
	40	↓	↓	↓	↓	20	138	39.4	272	83.9	579	40.5	279	.130
	41	↓	↓	↓	↓	23	159	41.0	283	85.3	588	38.0	262	.090
	42	↓	↓	↓	↓	18	124	39.6	273	83.7	523	38.4	265	----
	Average . . . . .					19	129	39.7	274	86.4	587	39.4 × 10 <sup>6</sup>	272	0.088
	<sup>a</sup> 43	0.54	13.72	0.020	0.508	45	310	84.5	583	97.0	669	35.8 × 10 <sup>6</sup>	246	----
	44	↓	↓	↓	↓	27	193	61.5	424	87.4	603	36.8	254	0.080
	45	↓	↓	↓	↓	25	172	52.6	363	75.5	521	33.0	228	.100
	46	↓	↓	↓	↓	27	186	60.4	416	84.8	585	33.4	230	.090
	Average . . . . .					31	215	64.8	447	86.1	594	34.8 × 10 <sup>6</sup>	240	0.090
	47	0.54	13.72	0.020	0.508	22	200	52.0	359	60.6	418	40.2 × 10 <sup>6</sup>	277	----
	48	↓	↓	↓	↓	46	317	61.0	421	67.7	467	41.0	283	----
	49	↓	↓	↓	↓	39	269	59.1	407	76.5	528	40.5	279	0.080
	50	↓	↓	↓	↓	31	214	54.1	373	77.5	534	40.5	279	.080
	Average . . . . .					35	250	56.6	390	70.6	487	40.6 × 10 <sup>6</sup>	280	0.080
PS	51	0.58	14.73	0.040	1.016	54	372	77.9	537	122.0	841	39.0 × 10 <sup>6</sup>	269	0.070
	52	↓	↓	↓	↓	58	400	85.2	587	136.0	938	40.6	280	.070
	53	↓	↓	↓	↓	58	400	82.5	569	127.0	876	39.0	269	.070
	54	↓	↓	↓	↓	48	331	80.1	552	120.0	827	38.7	267	----
	55	↓	↓	↓	↓	53	365	81.0	558	118.8	819	40.2	277	----
	56	↓	↓	↓	↓	38	262	74.0	510	119.4	823	41.8	288	----
	57	↓	↓	↓	↓	53	365	76.5	527	114.8	792	40.7	281	----
	58	↓	↓	↓	↓	40	276	74.8	516	121.8	840	40.5	279	----
	Average . . . . .					50	346	79.0	544	122.5	845	40.1 × 10 <sup>6</sup>	276	0.070

<sup>a</sup>Single-sintered specimen.

TABLE XI. - MECHANICAL PROPERTIES FOR SELECTED MATERIALS

Material	$\sigma_{tu}$						$\sigma_{ty}$						e			
	N	$\bar{X}$		S		$\frac{S}{\bar{X}} \times 100$ , percent	N	$\bar{X}$		S		$\frac{S}{\bar{X}} \times 100$ , percent	N	$\bar{X}$ , percent	S, percent	$\frac{S}{\bar{X}} \times 100$ , percent
		ksi	MN/m <sup>2</sup>	ksi	MN/m <sup>2</sup>			ksi	MN/m <sup>2</sup>	ksi	MN/m <sup>2</sup>					
Beryllium, (type BL extruded tube)	30	84.1	580	7.8	54	9.3	29	44.7	308	5.4	37	12.1	30	5.9	2.3	39
Magnesium (AZ31B-F extrusion) <sup>a</sup>	395	38.0	262	1.7	12	4.4	395	29.0	200	2.5	17	8.6	395	15.0	3.0	20
Aluminum (6061-T6 sheet) <sup>a</sup>	1648	45.0	310	2.3	16	5.2	1648	40.0	276	5.3	36	13.3	1641	12.0	2.8	23.6
Titanium (Ti-6Al-4V annealed sheet and bar) <sup>a</sup>	2619	135.5	934	6.7	46	4.7	2619	130.7	901	7.3	50	5.6	2619	12.4	2.5	20.2
Aluminum (7075-T6 clad sheet) <sup>a</sup>	250	76.0	524	3.6	25	4.7	250	67.0	462	3.6	25	5.4	250	11.0	2.3	21.0

<sup>a</sup>Estimated from reference 20.

TABLE XII.- RESULTS OF COLUMN TESTS ON BERYLLIUM TUBING

Type	Specimen	Length		$D_n$		$t_n$		$L_{eff}$ $\rho$	$E_c$		$\sigma_{cr,exp}$		$\sigma_{cr,calc}$		$\frac{\sigma_{cr,exp}}{\sigma_{cr,calc}}$
		in.	mm	in.	mm	in.	mm		psi	GN/m <sup>2</sup>	ksi	MN/m <sup>2</sup>	ksi	MN/m <sup>2</sup>	
A	1	3.0	76	0.50	12.70	0.020	0.508	8.8	$39.7 \times 10^{-6}$	274	107.5	741	---	---	---
	2	3.0	76	---	---	---	---	8.8	39.8	274	105.3	726	---	---	---
	3	10.0	254	---	---	---	---	29.4	39.2	270	62.9	434	61.0	421	1.03
	4	10.0	254	---	---	---	---	29.4	39.9	275	67.0	462	61.0	421	1.10
	5	13.5	343	---	---	---	---	39.7	39.2	270	57.9	399	58.0	400	1.00
	6	13.5	343	---	---	---	---	39.5	39.0	269	59.3	409	58.0	400	1.02
	7	13.5	343	---	---	---	---	39.7	40.1	276	60.3	416	58.0	400	1.04
	8	13.5	343	---	---	---	---	39.7	38.8	268	55.6	383	58.0	400	.96
	9	34.0	864	---	---	---	---	99.8	43.7	301	33.7	232	35.6	246	.95
	10	34.0	864	---	---	---	---	100.0	41.6	287	31.1	214	35.5	245	.88
B	11	3.0	76	0.50	12.70	0.020	0.508	8.9	$40.8 \times 10^{-6}$	281	76.3	526	---	---	---
	12	3.0	76	---	---	---	---	8.8	37.9	261	76.9	530	---	---	---
	13	10.0	254	---	---	---	---	29.8	40.5	279	44.3	305	39.5	272	1.12
	14	10.0	254	---	---	---	---	29.5	40.1	276	46.6	321	39.6	273	1.18
	15	13.5	343	---	---	---	---	40.1	38.8	268	36.9	255	35.2	243	1.05
	16	13.5	343	---	---	---	---	40.0	39.3	271	38.3	264	35.4	244	1.08
	17	13.5	343	---	---	---	---	40.2	38.8	268	36.8	254	35.3	243	1.04
	18	13.5	343	---	---	---	---	40.0	40.0	276	36.2	250	35.4	244	1.02
	19	34.0	864	---	---	---	---	101.0	39.4	272	21.3	147	24.1	166	.88
	20	34.0	864	---	---	---	---	100.0	41.8	288	27.4	189	24.3	168	1.13
BL	21	34.0	864	---	---	---	---	101.4	40.0	276	25.3	173	24.2	167	1.04
	22	3.0	76	0.25	6.35	0.020	0.508	17.8	$40.6 \times 10^{-6}$	280	60.7	418	---	---	---
	23	3.0	76	---	---	---	---	17.9	40.0	276	60.3	415	---	---	---
	24	6.0	152	---	---	---	---	35.7	41.0	283	38.1	263	37.7	260	1.01
	25	6.0	152	---	---	---	---	35.9	39.5	272	39.4	272	37.6	259	1.05
	26	24.0	610	---	---	---	---	145.0	40.0	276	13.2	91	17.0	117	.78
	27	24.0	610	---	---	---	---	144.8	40.8	281	14.4	100	17.1	118	.84
	28	24.0	610	---	---	---	---	140.2	41.2	284	17.5	121	17.5	121	1.00
	29	30.0	762	---	---	---	---	177.9	40.8	281	11.5	80	12.5	86	.92
	30	30.0	762	---	---	---	---	186.6	41.1	283	12.9	89	11.5	79	1.12
PS	31	30.0	762	---	---	---	---	175.6	41.0	283	11.4	79	12.7	88	.90
	32	6.0	152	0.25	6.35	0.040	1.016	38.4	$38.8 \times 10^{-6}$	278	40.5	279	37.8	261	1.07
	33	6.0	152	---	---	---	---	39.2	40.0	276	42.0	290	37.5	259	1.12
	34	13.5	343	0.50	12.70	0.020	0.508	39.7	$38.8 \times 10^{-6}$	268	41.5	286	36.7	253	1.13
	35	13.5	343	---	---	---	---	39.7	39.1	270	41.2	284	36.7	253	1.12
	36	34.0	864	---	---	---	---	100.0	40.3	278	24.7	170	23.5	162	1.05
	37	13.5	343	0.50	12.70	0.040	1.016	40.6	$39.0 \times 10^{-6}$	269	32.2	222	33.8	233	0.95
	38	34.0	864	---	---	---	---	104.0	37.9	261	17.8	123	21.5	148	.83
	39	34.0	864	---	---	---	---	102.1	39.7	274	21.6	149	21.7	149	1.00
	40	20.0	508	0.75	19.05	0.020	0.508	38.7	$39.7 \times 10^{-6}$	274	36.1	249	36.2	250	1.00
PS	41	20.0	508	---	---	---	---	38.6	41.4	285	36.4	251	36.2	250	1.00
	42	36.0	914	---	---	---	---	70.2	39.3	271	25.6	176	29.0	200	.88
	43	36.0	914	---	---	---	---	69.7	42.3	292	31.7	218	29.1	201	1.09
	44	36.0	914	---	---	---	---	69.2	40.4	278	29.9	206	29.3	202	1.02
	45	20.0	508	0.75	19.05	0.040	1.016	39.7	$38.7 \times 10^{-6}$	267	36.3	250	34.7	239	1.05
	46	20.0	508	---	---	---	---	39.3	39.5	272	37.0	255	34.9	241	1.06
	47	36.0	914	---	---	---	---	70.4	40.9	282	25.8	178	27.0	168	.99
	48	36.0	914	---	---	---	---	70.9	43.8	302	27.6	191	26.9	186	1.03
	49	10.0	254	0.54	13.72	0.020	0.508	27.0	$36.2 \times 10^{-6}$	250	58.5	403	61.8	426	0.95
	50	13.5	343	---	---	---	---	36.7	31.6	218	59.0	407	58.5	403	1.01
PS	51	13.5	343	---	---	---	---	37.0	35.4	244	55.6	383	58.4	403	.95
	52	13.5	343	---	---	---	---	37.1	39.5	272	78.8	543	58.3	402	1.35
	53	10.0	254	0.54	13.72	0.020	0.508	27.4	-----	---	56.6	390	57.8	398	0.98
	54	13.5	343	---	---	---	---	36.6	-----	---	44.7	308	53.5	369	.84
	55	13.5	343	---	---	---	---	36.0	-----	---	49.1	338	53.8	371	.91
	56	10.0	254	0.58	14.73	0.040	1.016	26.4	$40.7 \times 10^{-6}$	281	70.3	485	78.7	543	0.89
	57	10.0	254	---	---	---	---	26.3	40.9	282	55.2	381	78.6	542	.70
	58	10.0	254	---	---	---	---	26.4	41.6	287	72.6	501	78.7	543	.92
	59	13.5	343	---	---	---	---	35.7	41.1	283	58.6	404	77.2	532	.76
	60	13.5	343	---	---	---	---	35.8	41.3	285	65.3	450	77.3	533	.84
	61	13.5	343	---	---	---	---	35.8	40.7	281	69.8	481	77.3	533	.90

<sup>a</sup>Single-sintered specimen.

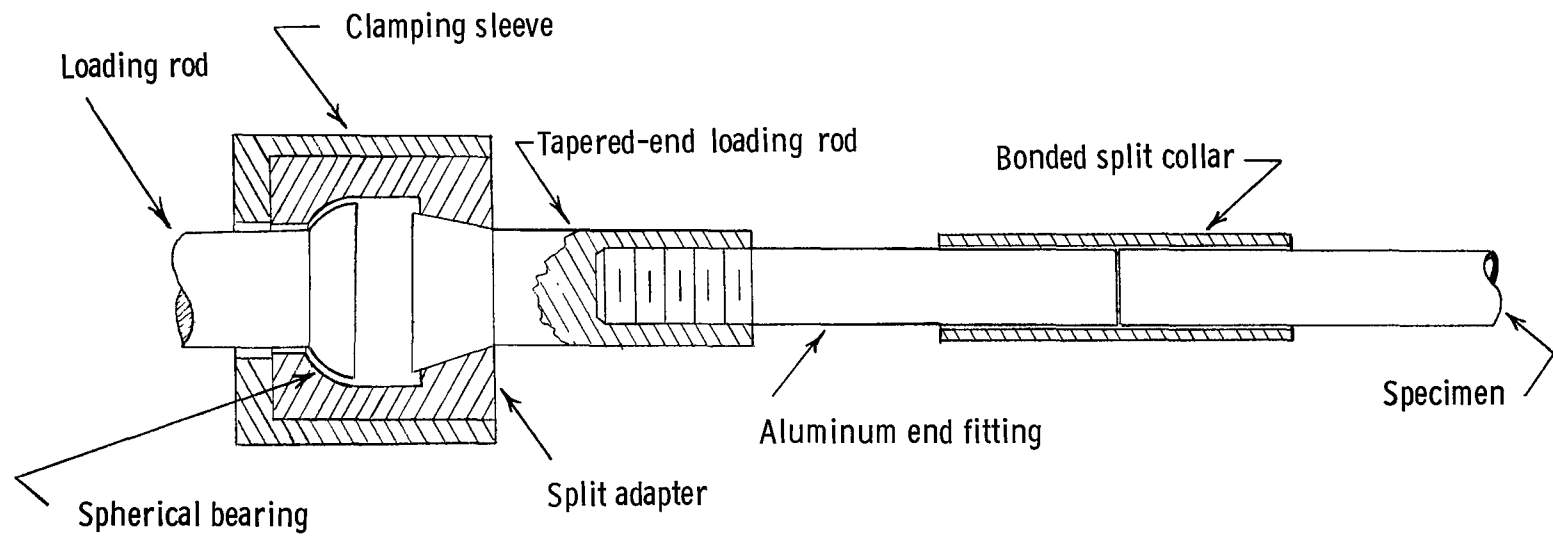


Figure 1.- Grip assembly for tubular beryllium tensile specimens.



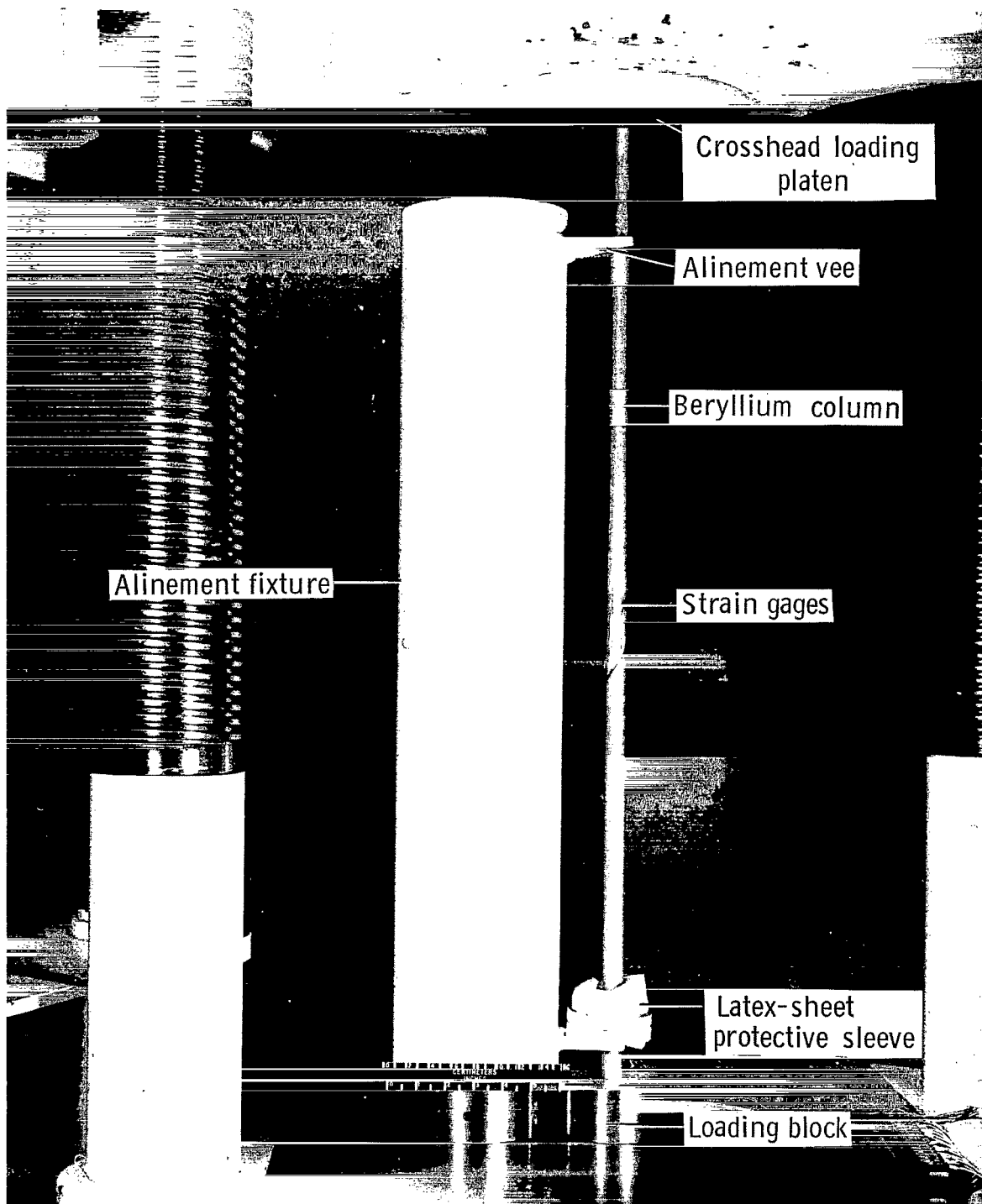
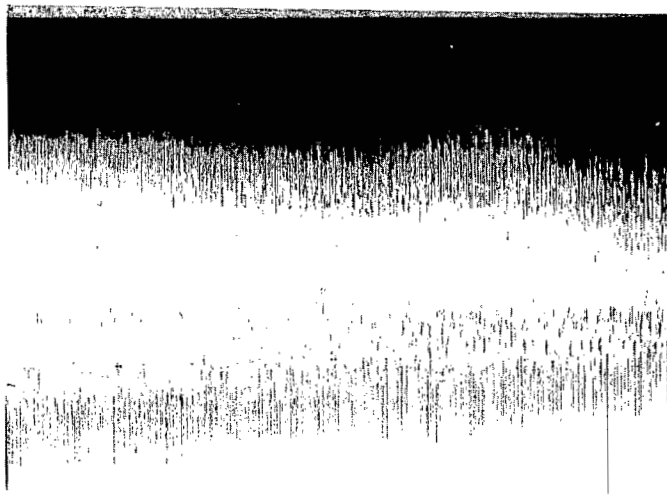
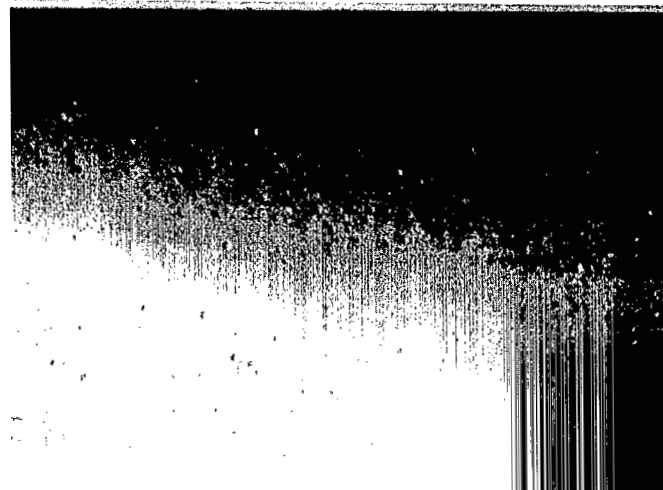


Figure 2.- Column test apparatus.

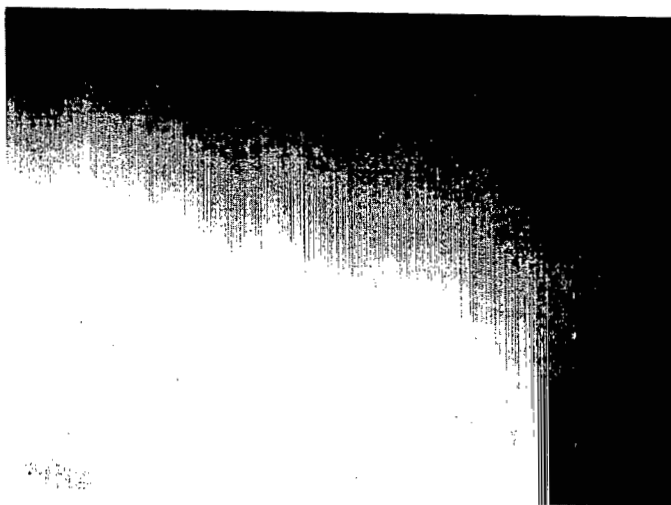
L-66-5878.1



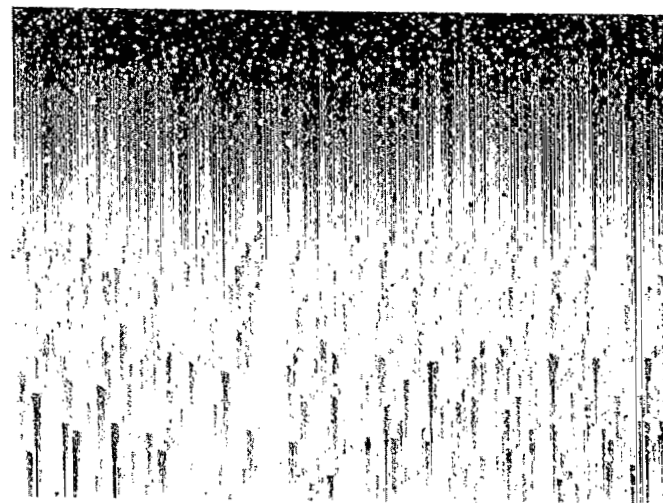
(a) Type A.



(b) Type B.

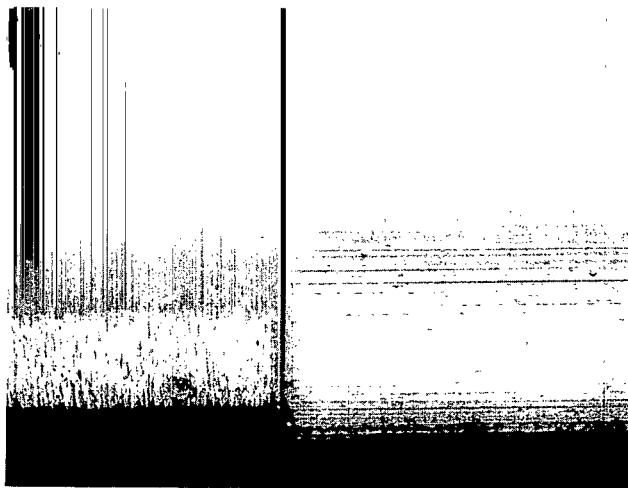


(c) Type BL.

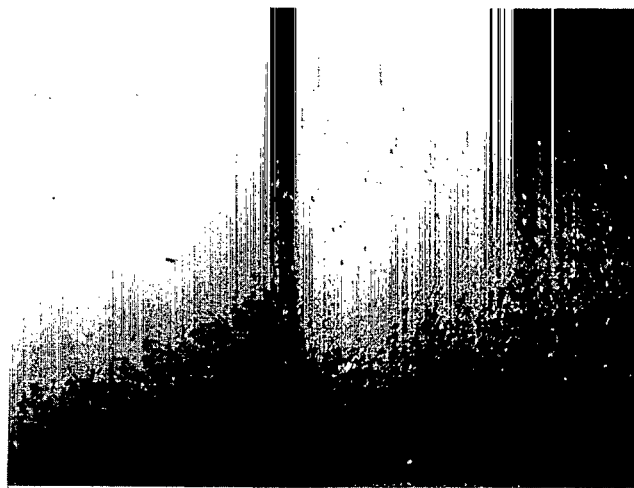


(d) Type PS.

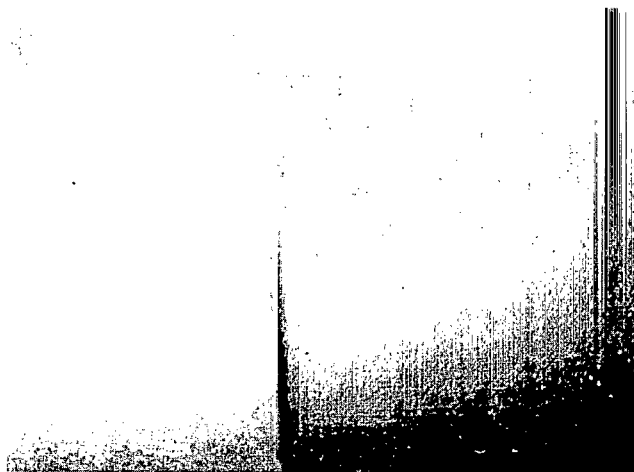
Figure 3.- Typical macrostructure of 0.50-inch-diameter (12.70 mm) beryllium tubing. X5.



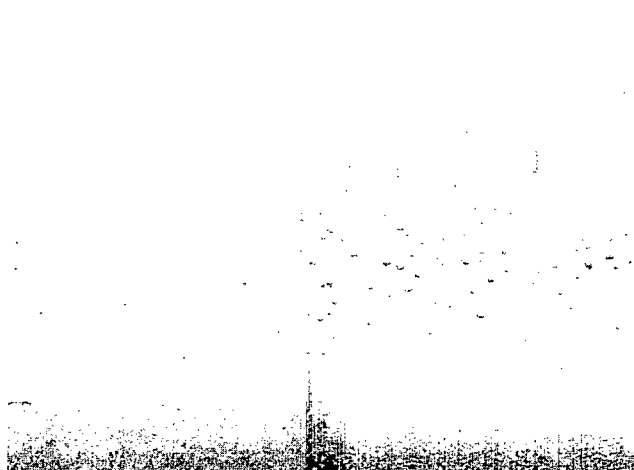
(a) Type A.



(b) Type B.



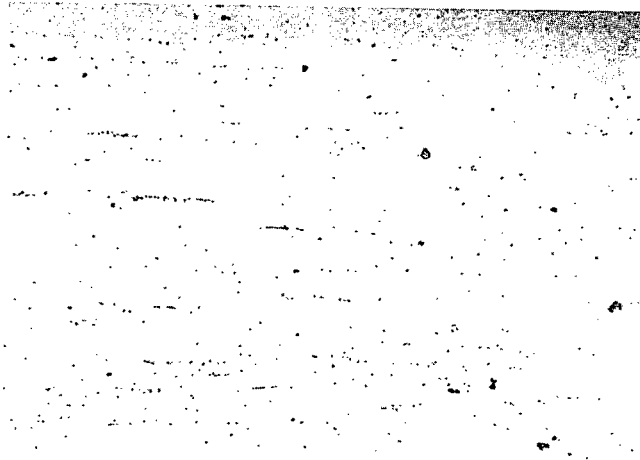
(c) Type BL.



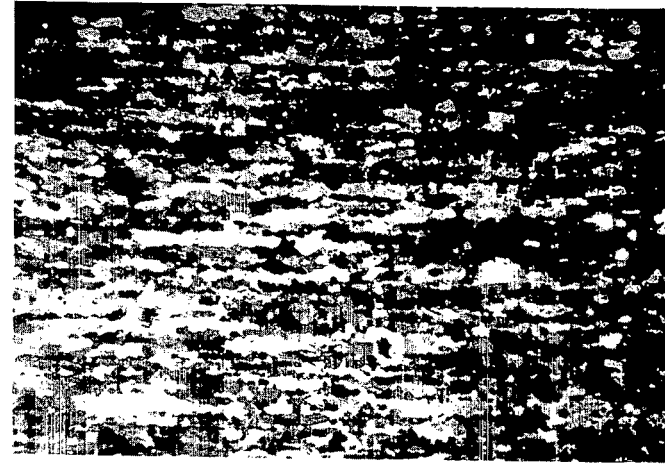
(d) Type PS.

Figure 4.- Surfaces of 0.50-inch-diameter (12.70 mm) beryllium tubing before and after etching with  $\text{Cr}_2\text{O}_3\text{-HF-H}_2\text{O}$ . X5.

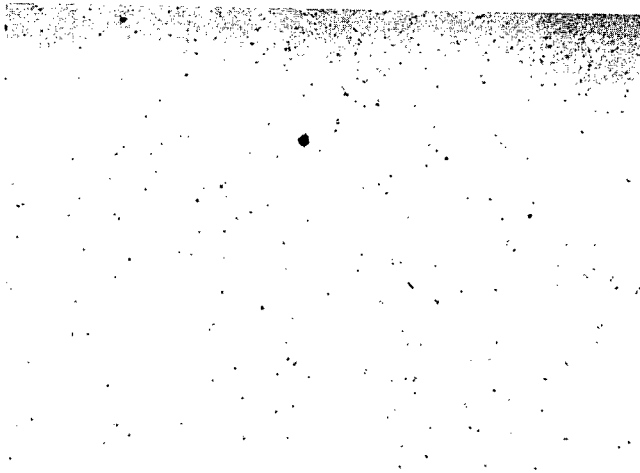
L-68-5648



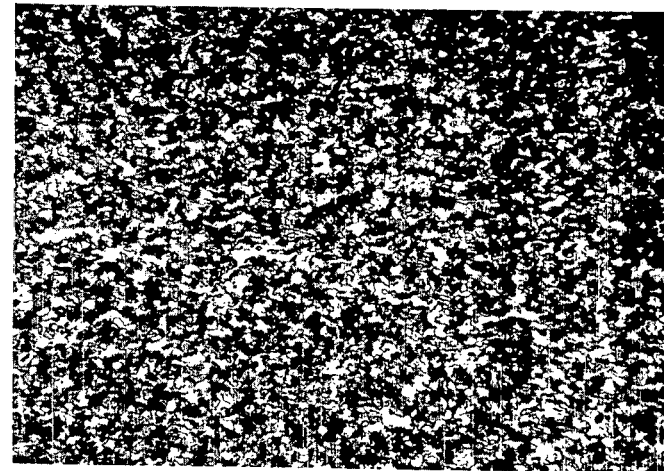
(a) Longitudinal; bright-field illumination.



(b) Longitudinal; polarized light.



(c) Transverse; bright-field illumination.



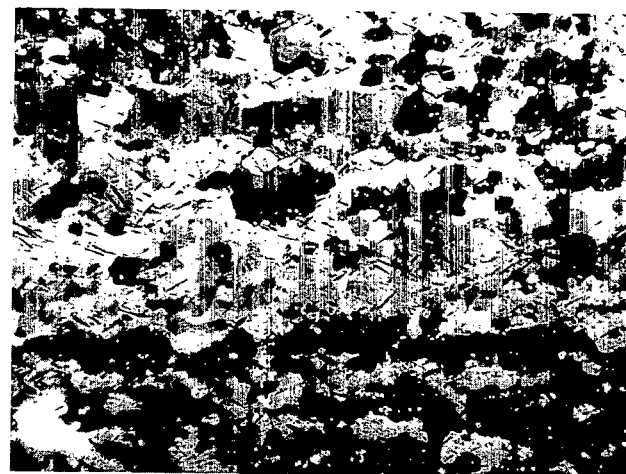
(d) Transverse; polarized light.

Figure 5.- Microstructure of type A extruded tubing. Unetched; X250.

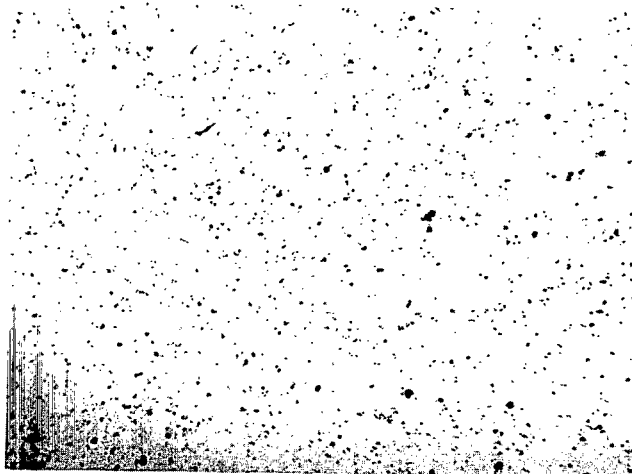
L-68-5649



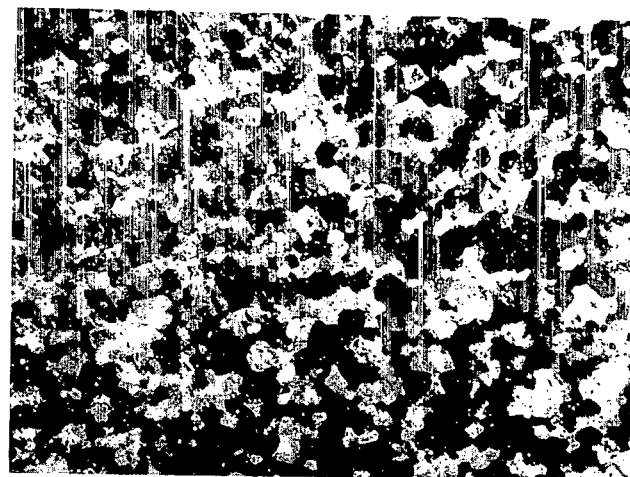
(a) Longitudinal; bright-field illumination.



(b) Longitudinal; polarized light.



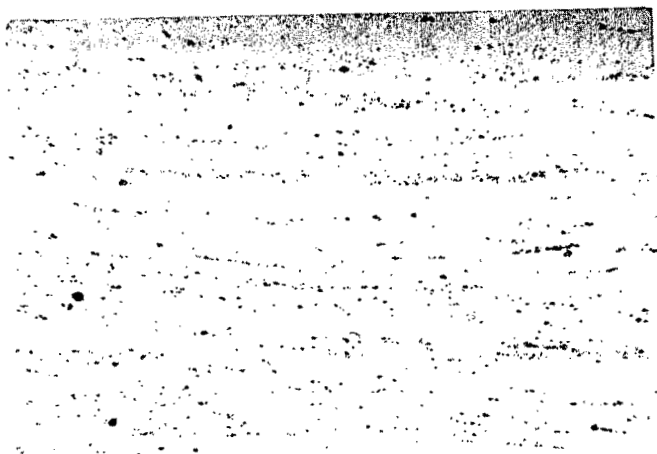
(c) Transverse; bright-field illumination.



(d) Transverse; polarized light.

Figure 6.- Microstructure of type B extruded tubing. Unetched; X250.

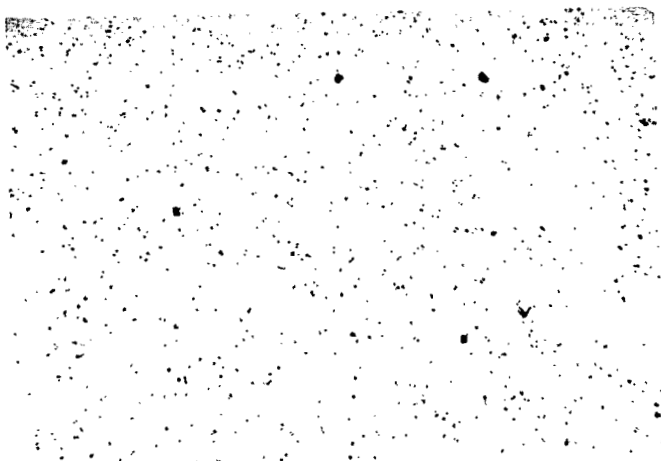
L-68-5650



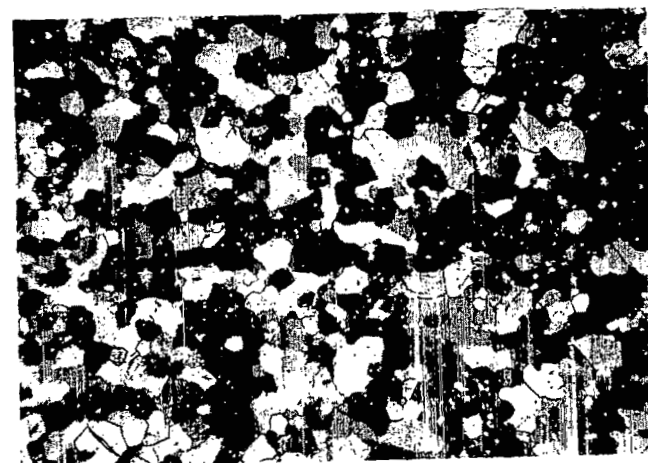
(a) Longitudinal; bright-field illumination.



(b) Longitudinal; polarized light.



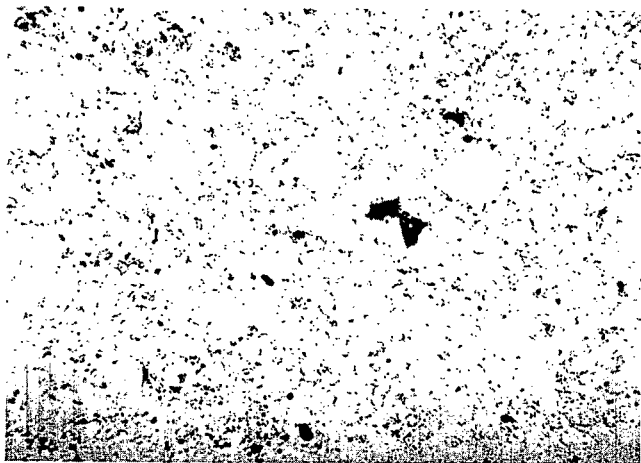
(c) Transverse; bright-field illumination.



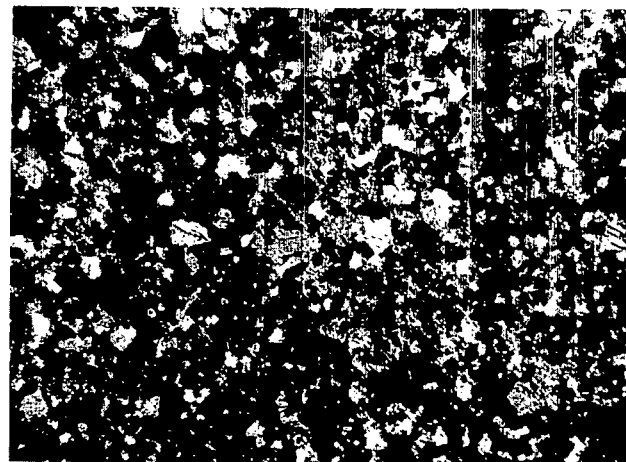
(d) Transverse; polarized light.

Figure 7.- Microstructure of type BL extruded tubing. Unetched; X250.

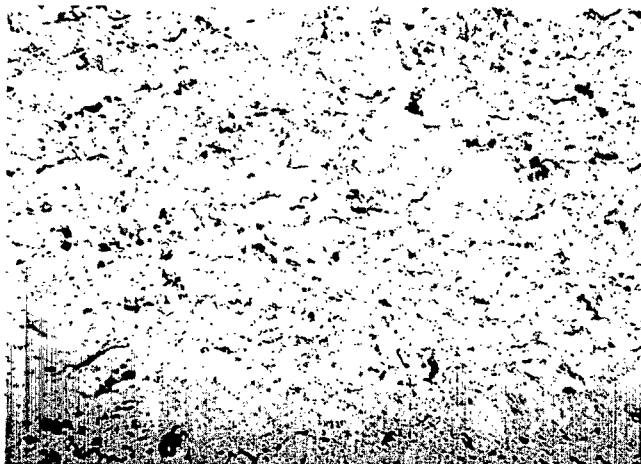
L-68-5651



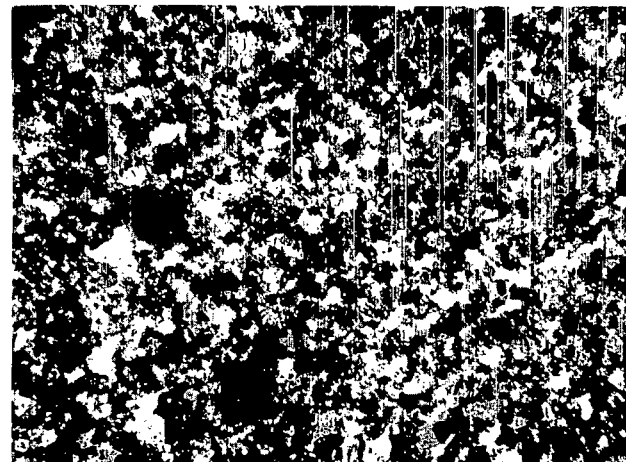
(a) Longitudinal; bright-field illumination.



(b) Longitudinal; polarized light.



(c) Transverse; bright-field illumination.



(d) Transverse; polarized light.

Figure 8.- Microstructure of type PS plasma-sprayed and sintered tubing. Unetched; X250.

L-68-5652

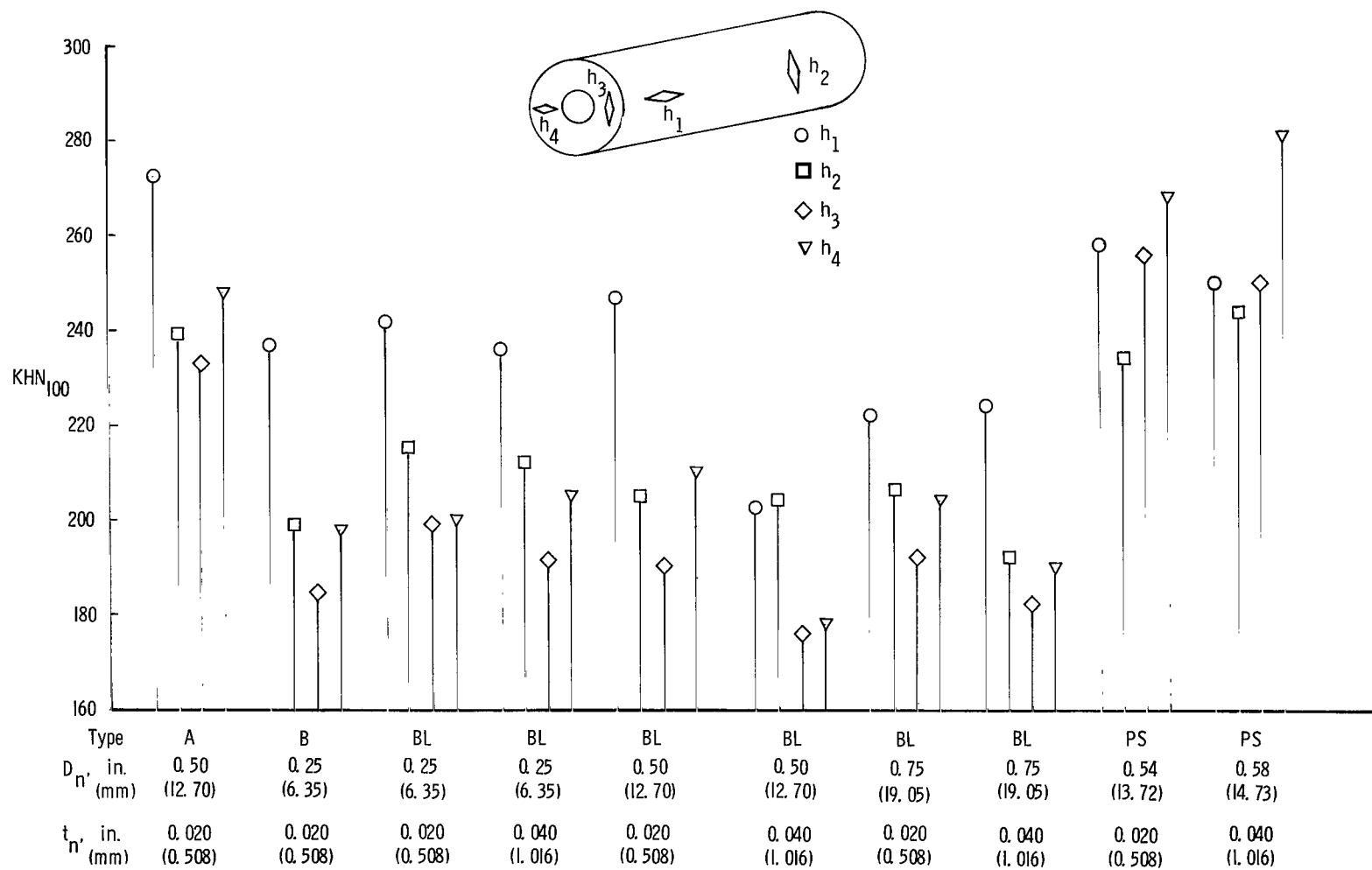


Figure 9.- Microhardness of beryllium tubing.



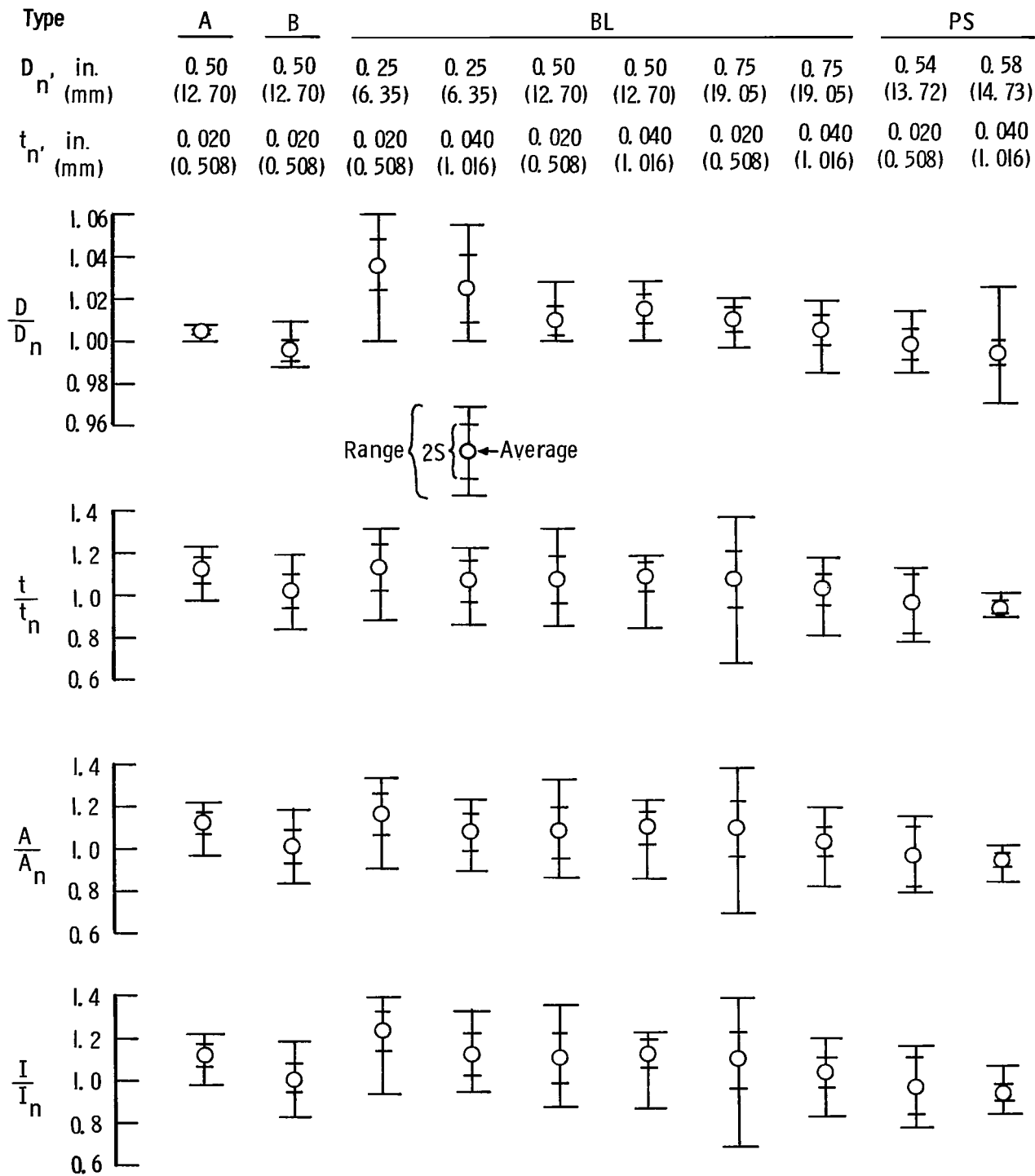


Figure 10.- Normalized dimensional variation of beryllium tubing.

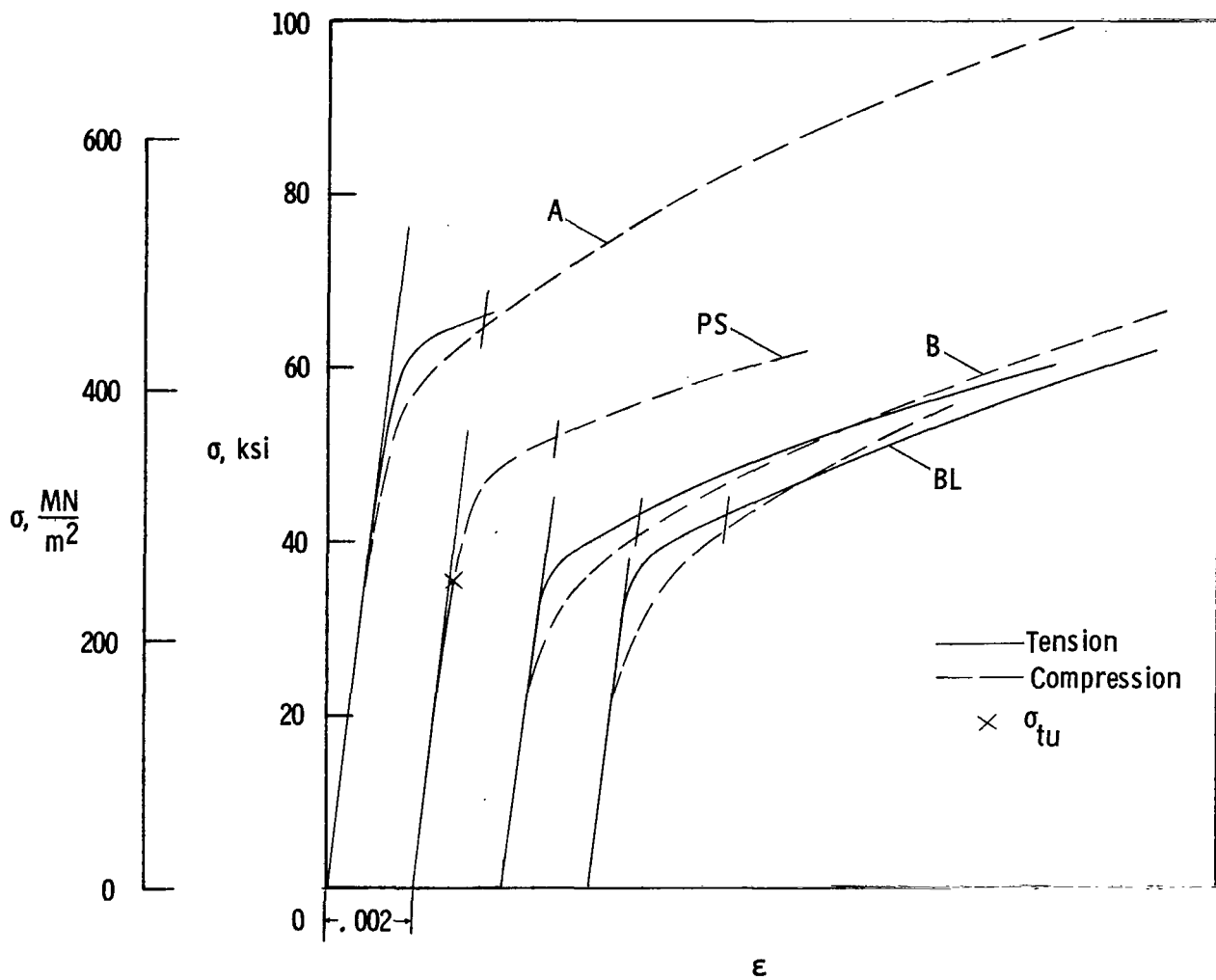
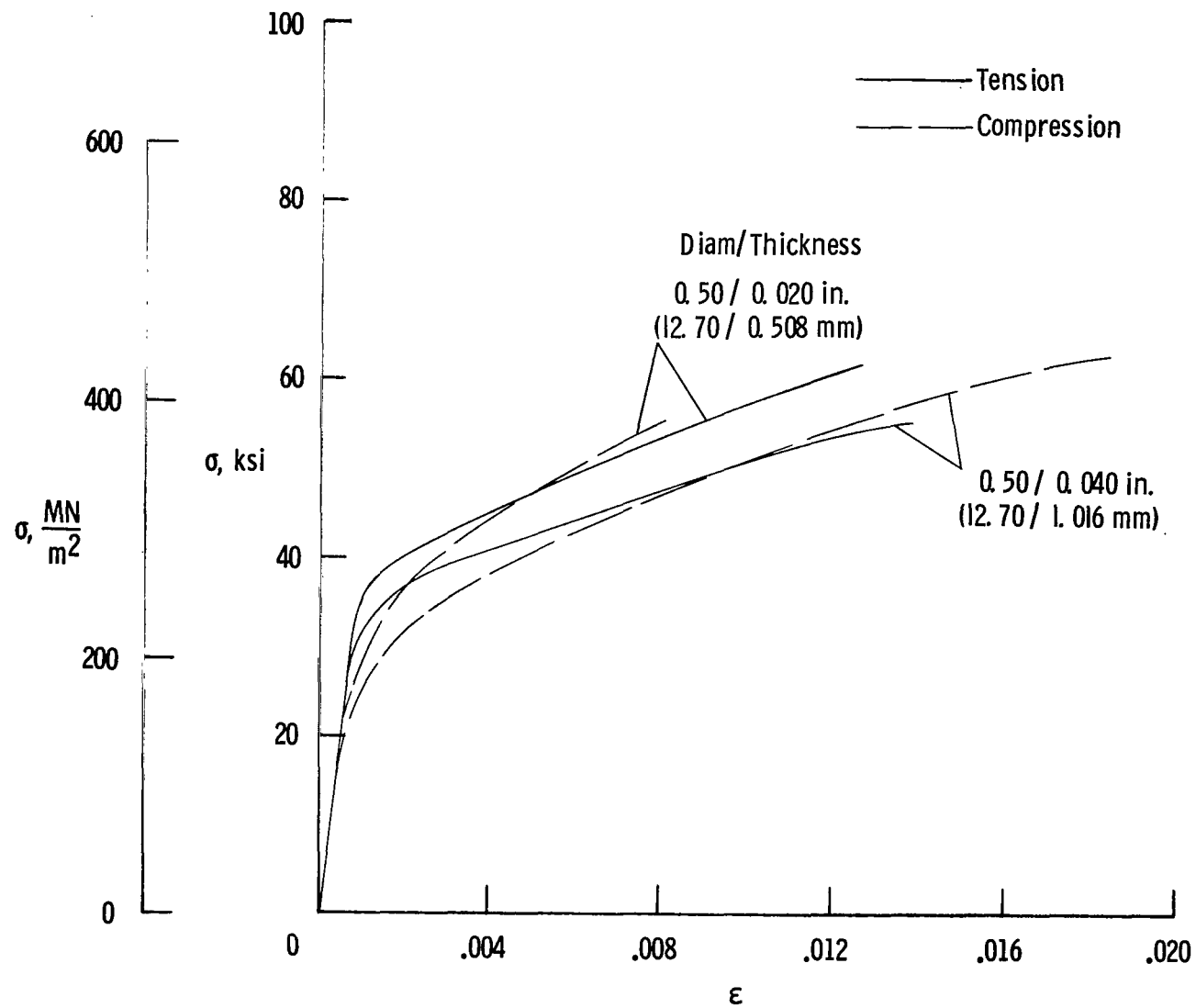
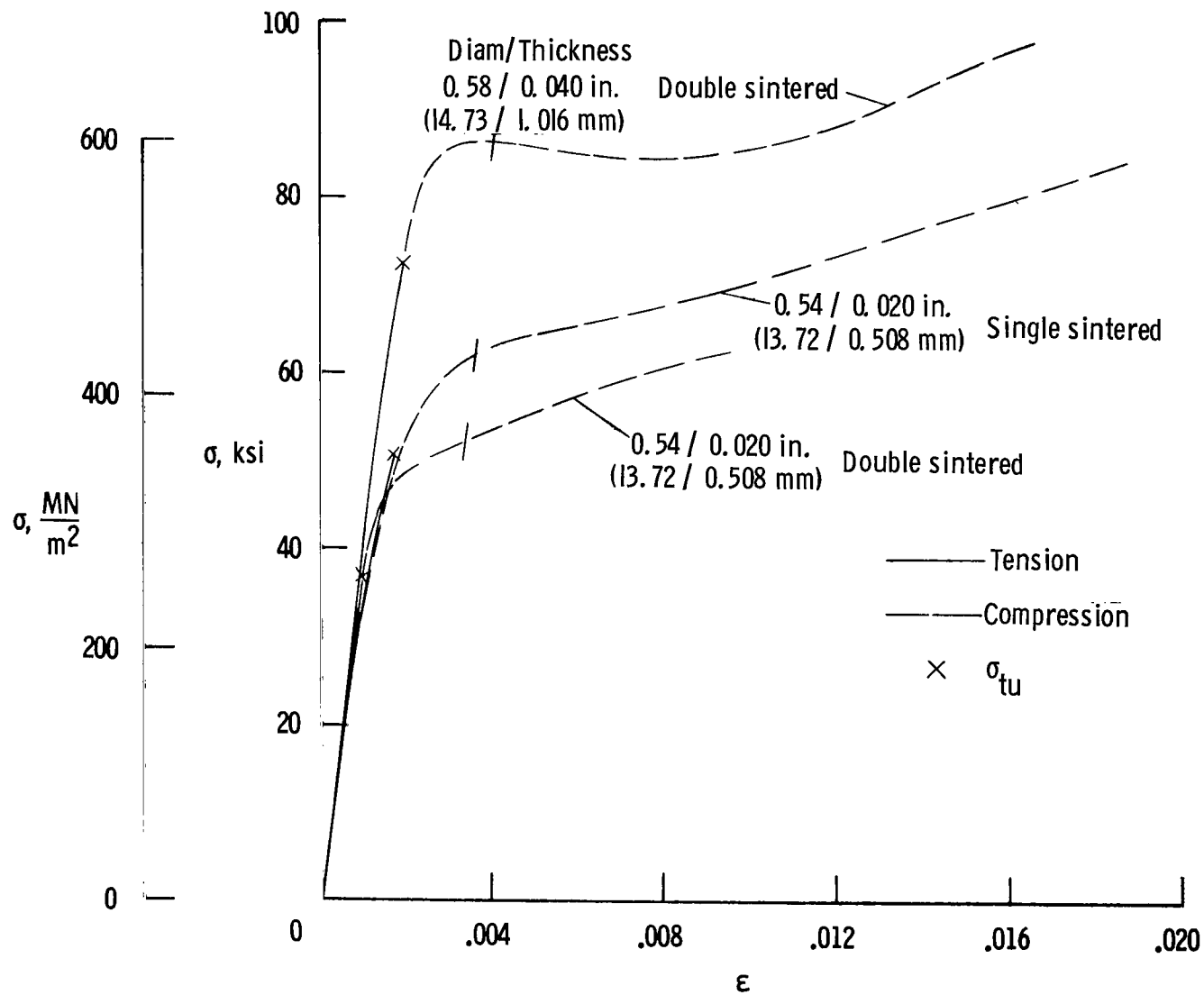


Figure 11.- Typical stress-strain curves for beryllium tubing with diameter of 0.50 inch (12.70 mm) and wall thickness of 0.020 inch (0.508 mm).



(a) Type BL.

Figure 12.- Effect of wall thickness on typical stress-strain curves for beryllium tubing.



(b) Type PS.

Figure 12.- Concluded.

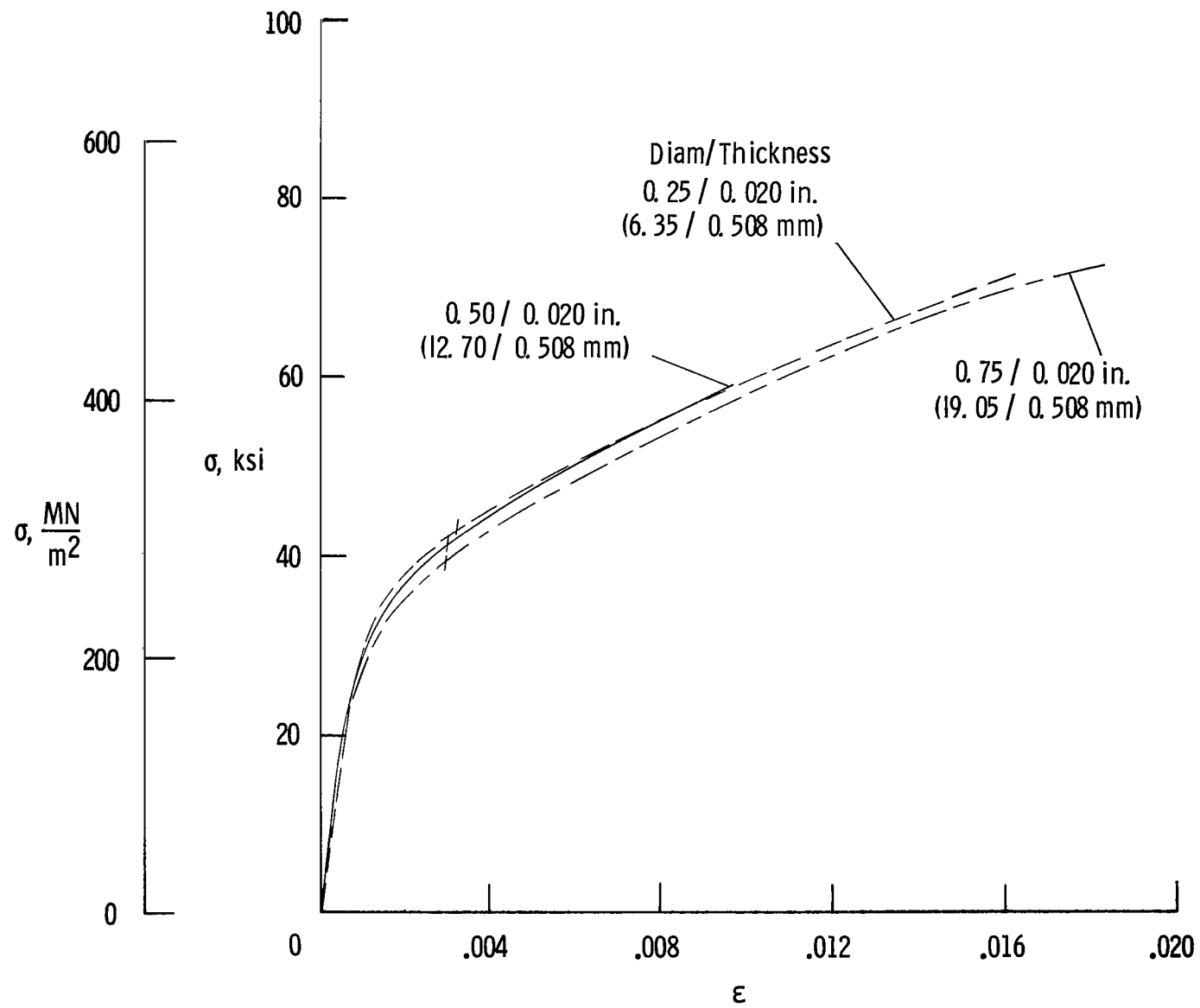


Figure 13.- Effect of diameter on typical compressive stress-strain curves for type BL beryllium tubing.

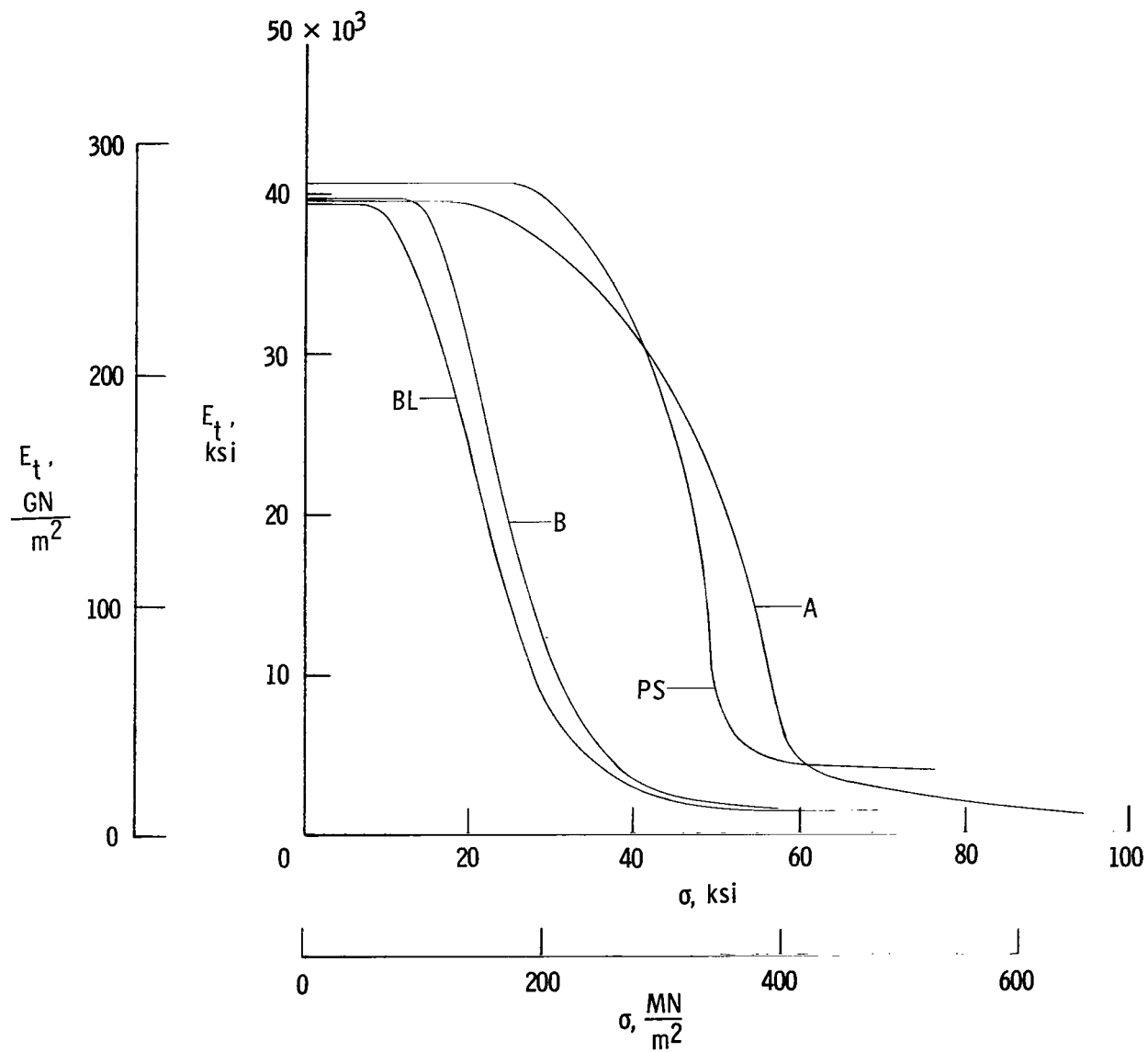


Figure 14.- Variation of compressive tangent modulus as a function of stress for typical beryllium tubing with diameter of 0.50 inch (12.70 mm) and wall thickness of 0.020 inch (0.508 mm).

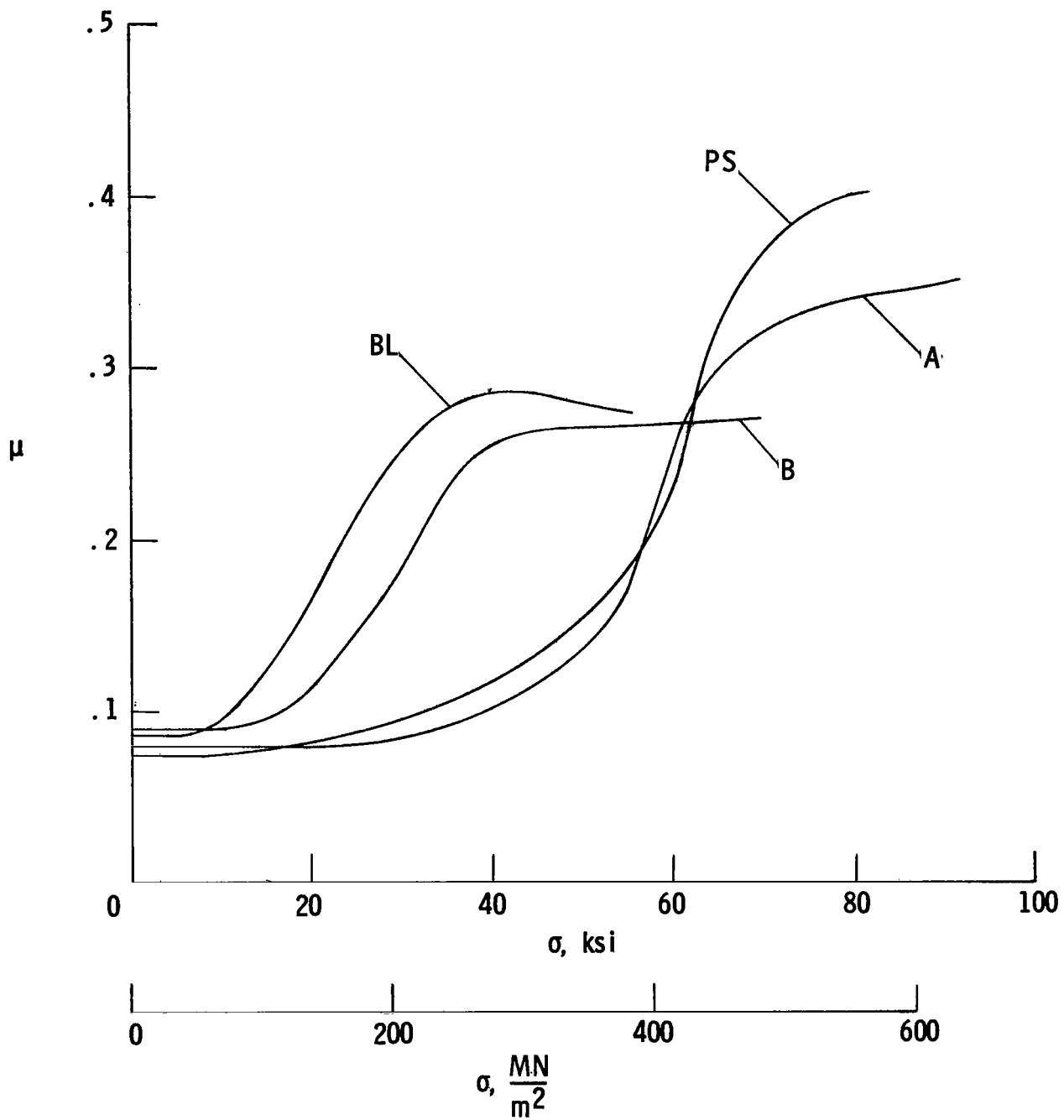
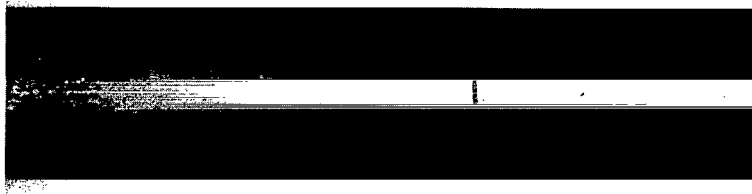


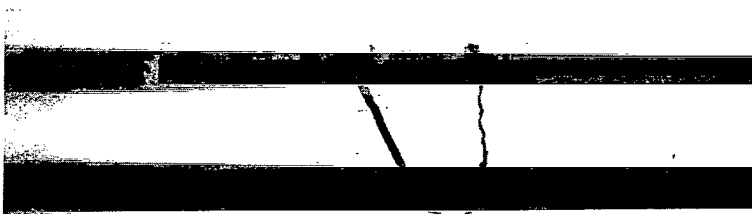
Figure 15.- Variation of Poisson's ratio as a function of stress for typical beryllium tubing with diameter of 0.50 inch (12.70 mm) and wall thickness of 0.020 inch (0.508 mm).



(a) Type A.



(b) Type B.



(c) Type BL.



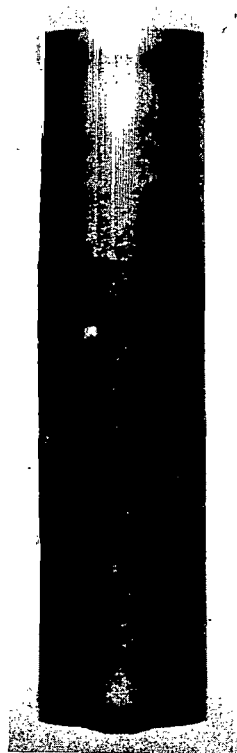
1 in. (25 mm)

(d) Type PS.

Figure 16.- Typical fracture modes of beryllium tubing.

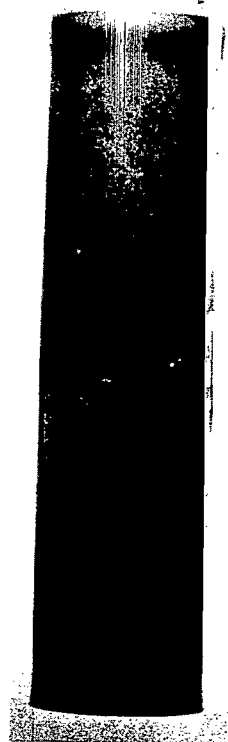
L-68-5653





Type

A



BL



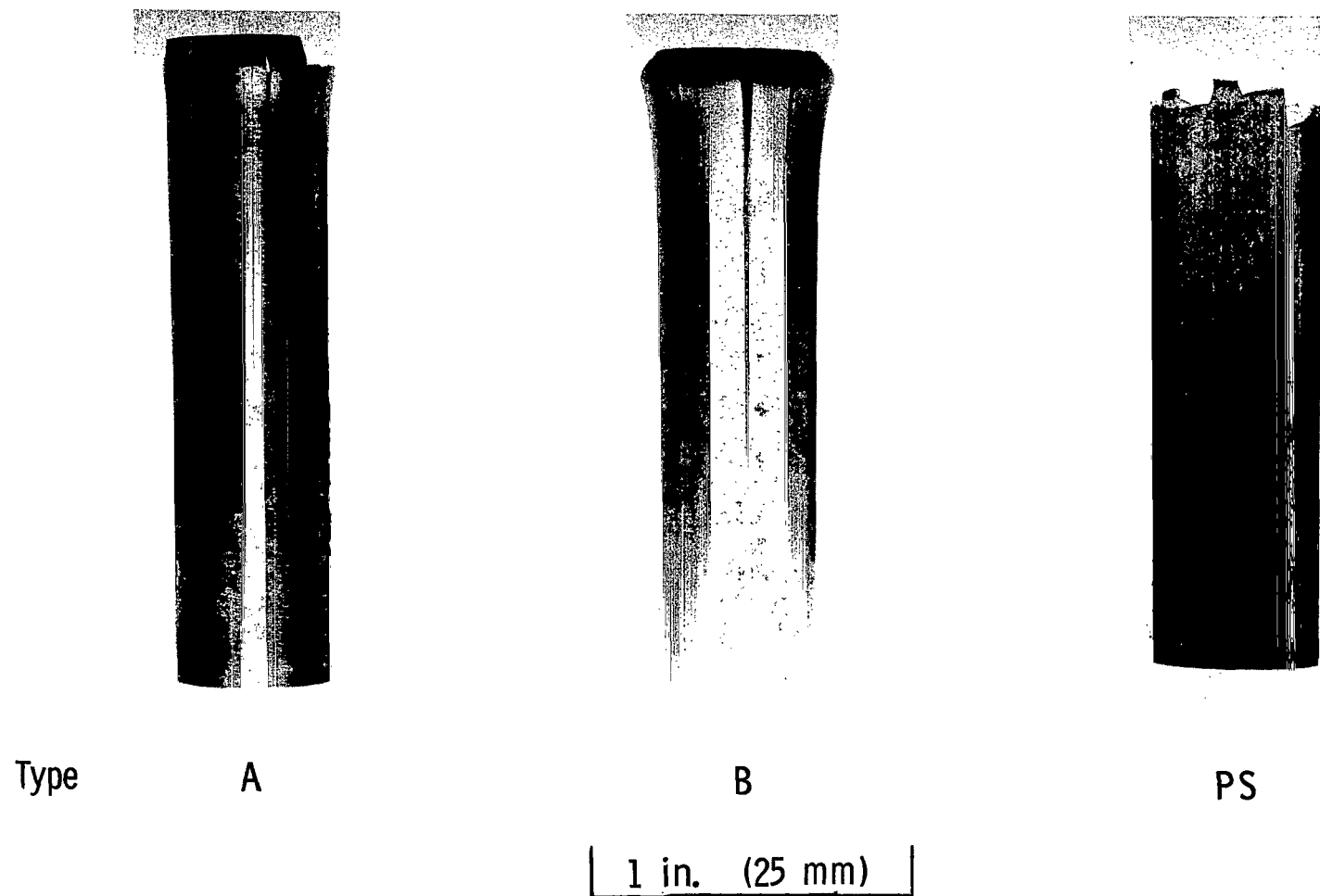
PS

1 in. (25 mm)

(a) Initial failure.

Figure 17.- Typical compressive failure modes for beryllium tubing.

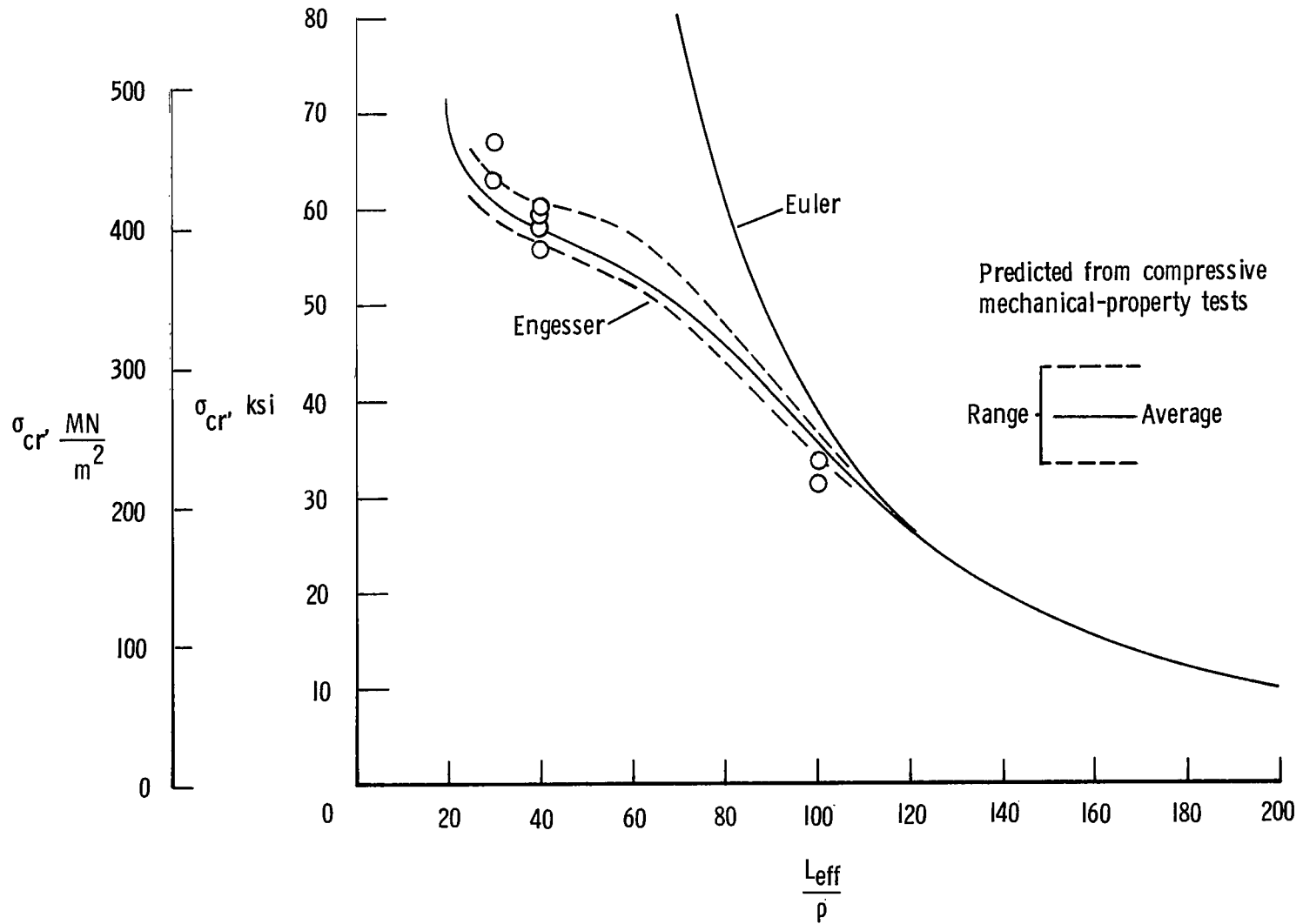
L-68-5654



(b) Final failure.

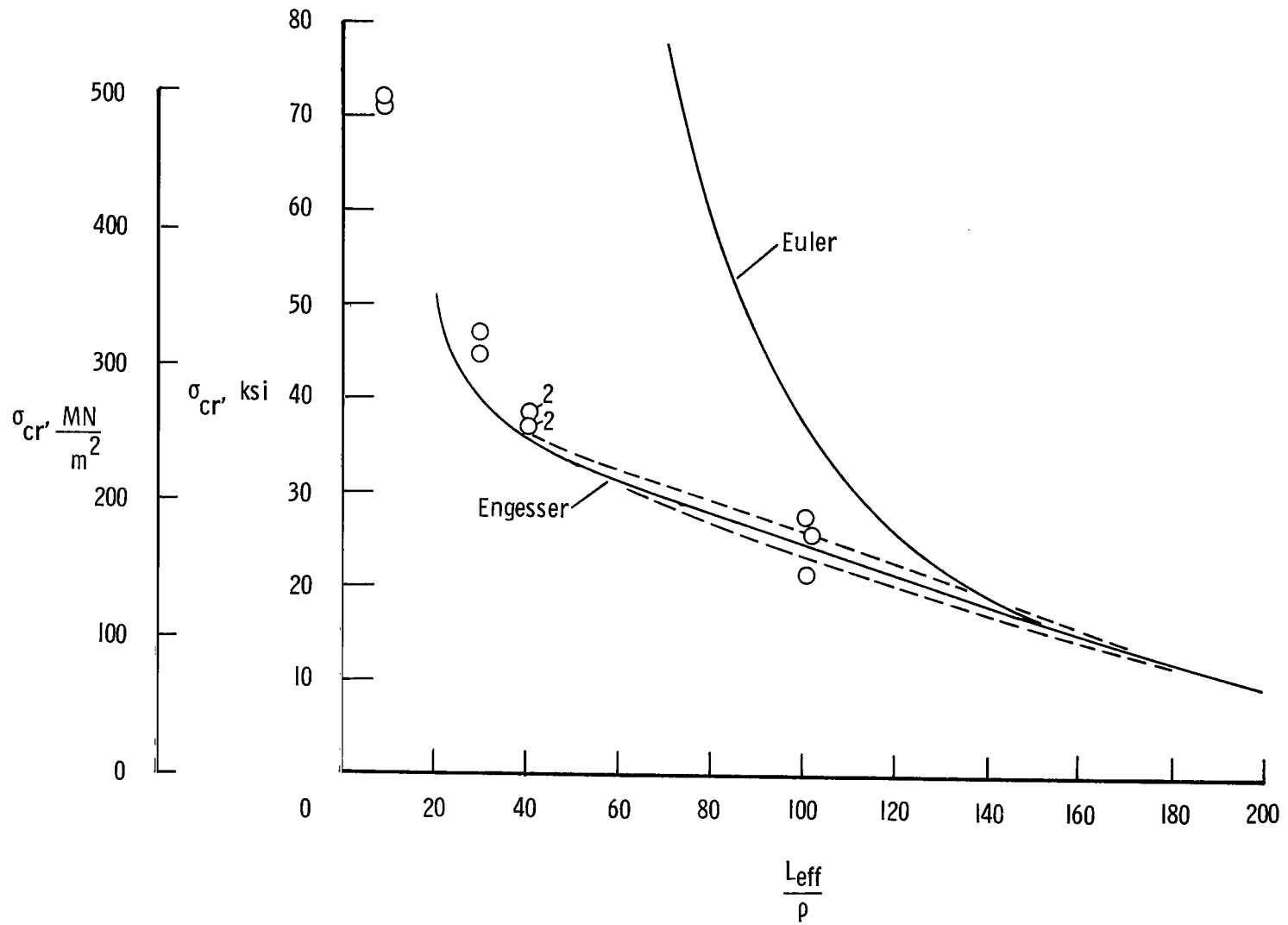
Figure 17.- Concluded.

L-68-5655



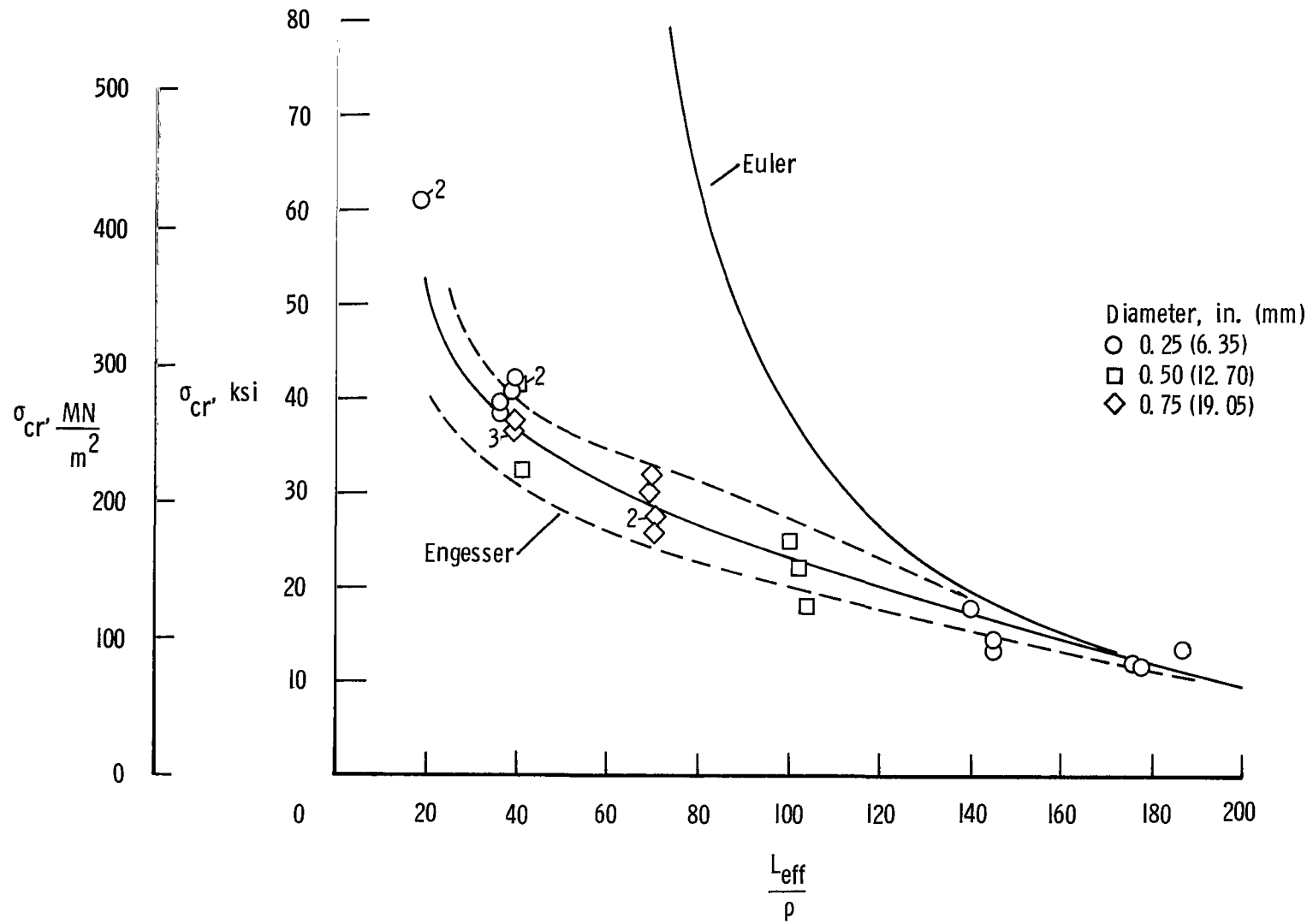
(a) Type A columns with diameter of 0.50 inch (12.70 mm) and wall thickness of 0.020 inch (0.508 mm).

Figure 18.- Column behavior of extruded beryllium tube columns.



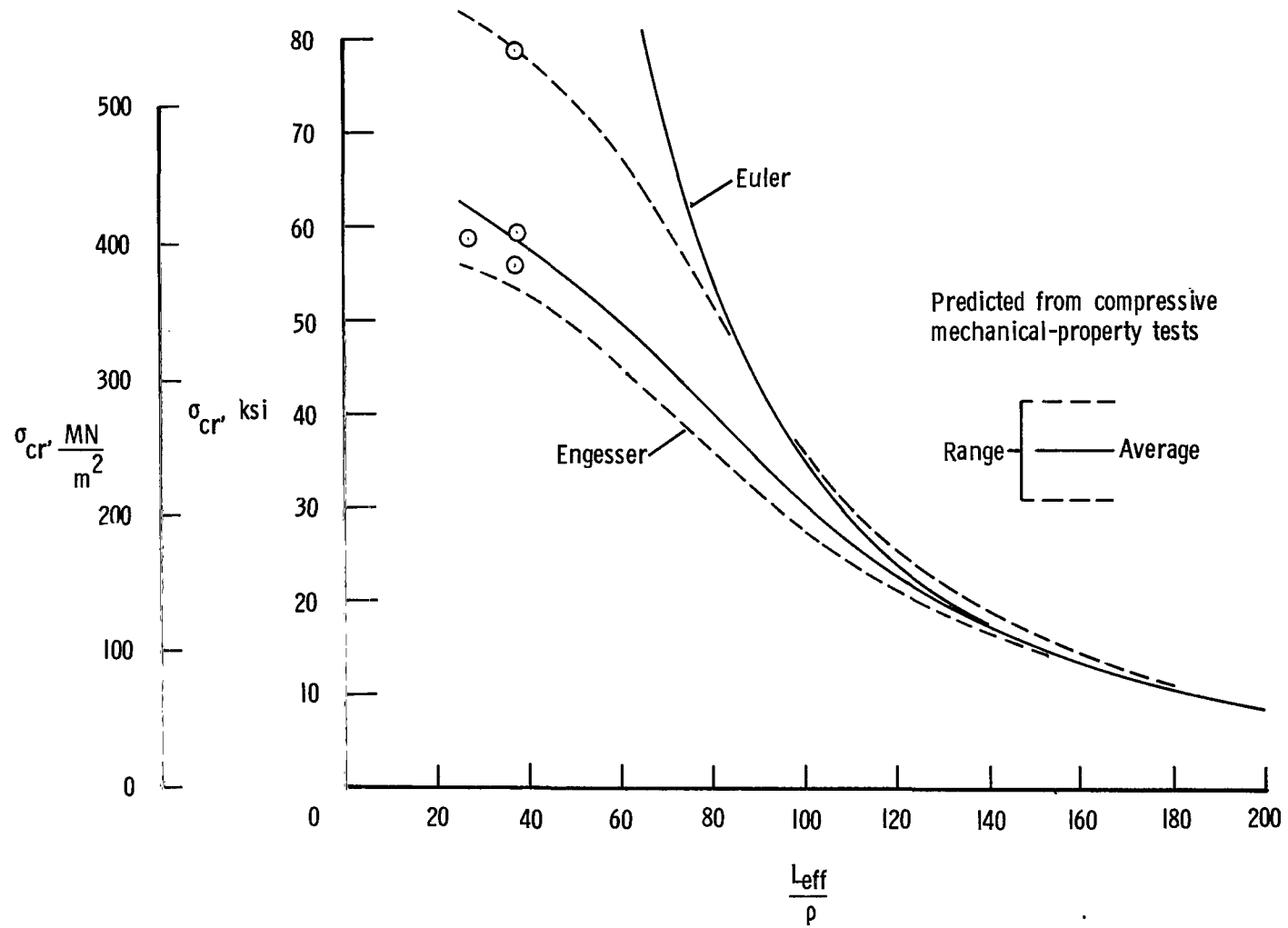
(b) Type B columns with diameter of 0.50 inch (12.70 mm) and wall thickness of 0.020 inch (0.508 mm).

Figure 18.- Continued.



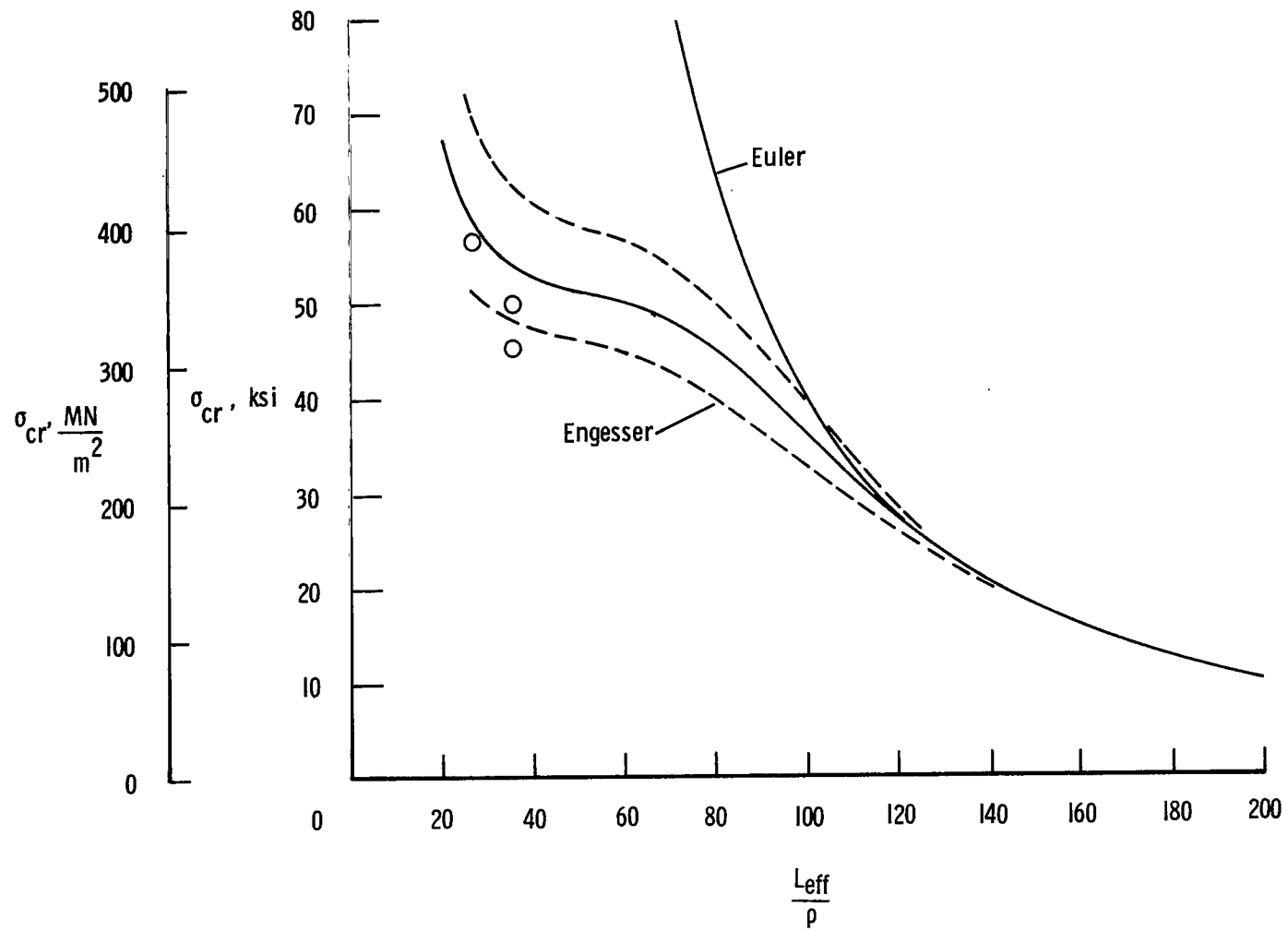
(c) Type BL columns.

Figure 18.- Concluded.



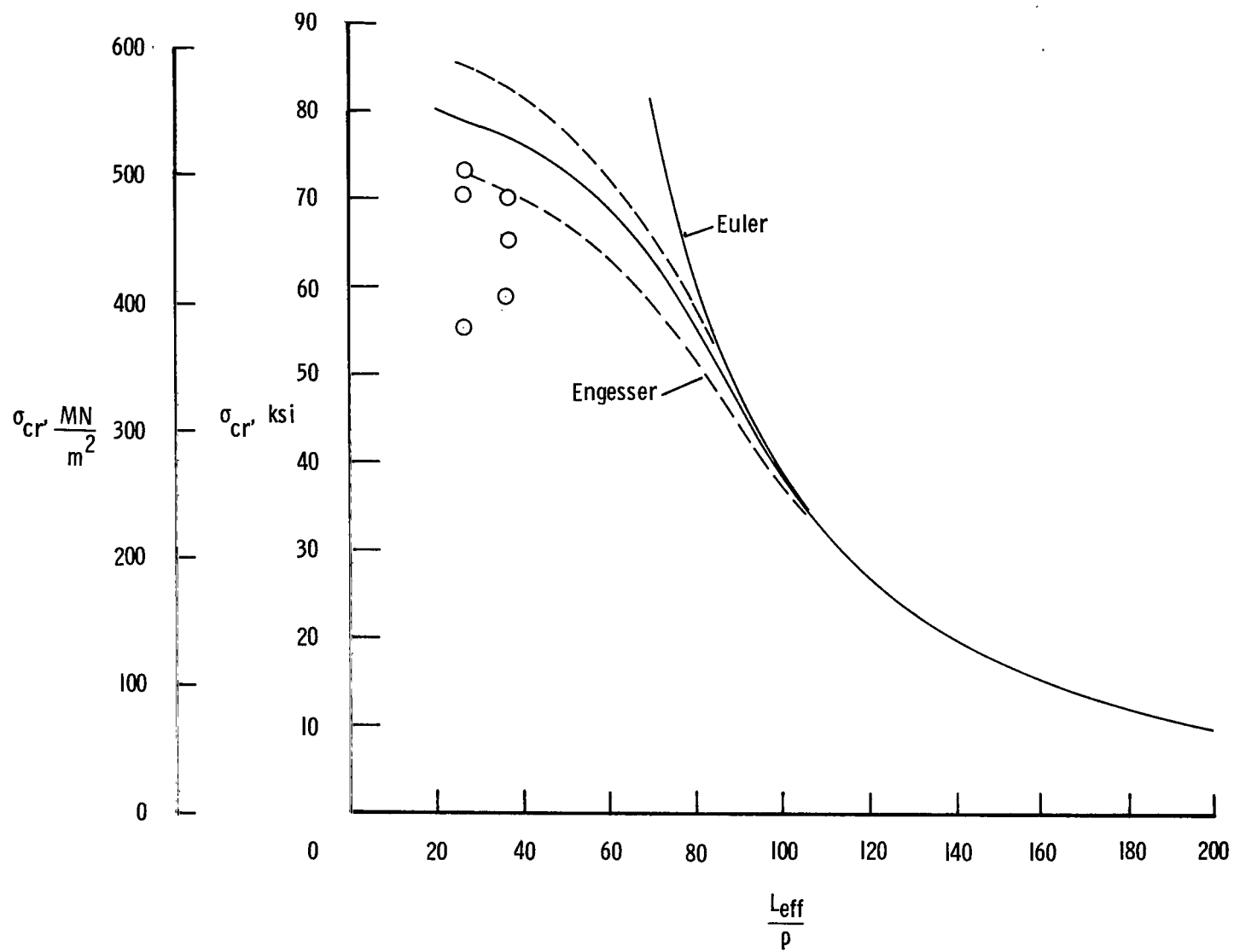
(a) Single-sintered type PS columns with diameter of 0.54 inch (13.72 mm) and wall thickness of 0.020 inch (0.508 mm).

Figure 19.- Column behavior of type PS tubing.



(b) Double-sintered type PS columns with diameter of 0.54 inch (13.72 mm) and wall thickness of 0.020 inch (0.508 mm).

Figure 19.- Continued.



(c) Double-sintered columns with diameter of 0.58 inch (14.73 mm) and wall thickness of 0.040 inch (1.016 mm).

Figure 19.- Concluded.



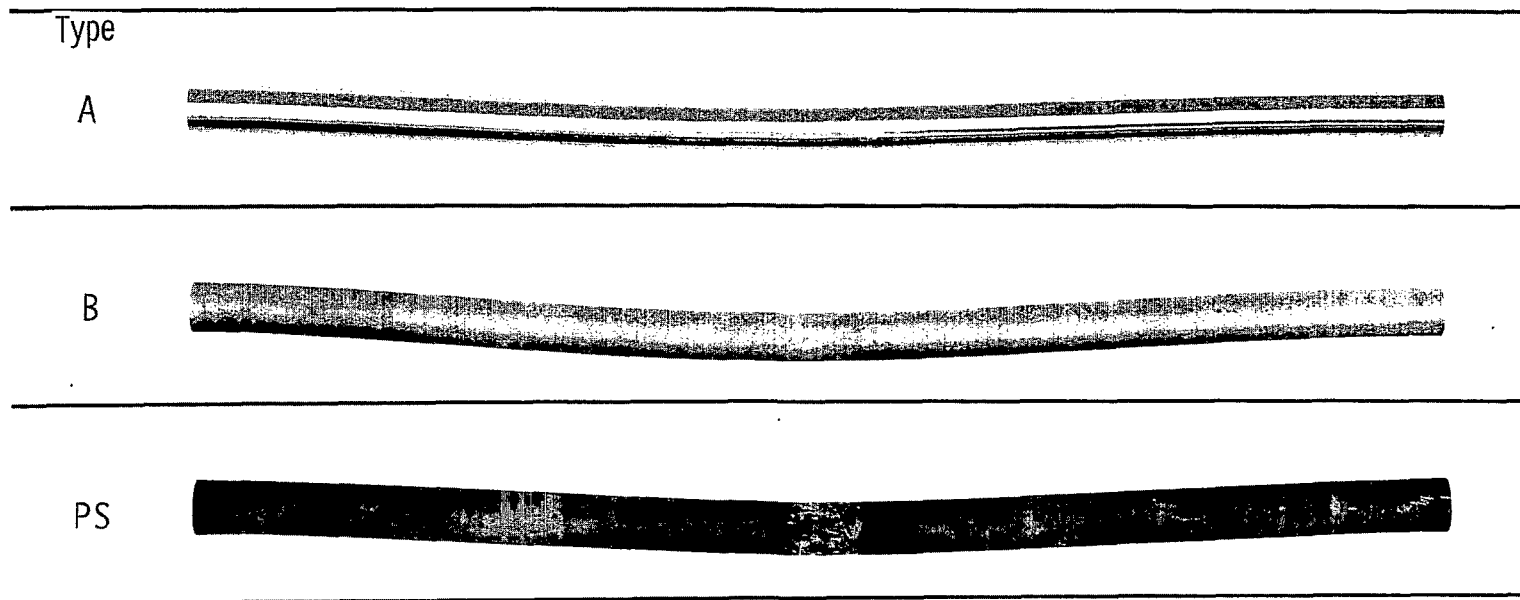


Figure 20.- Typical beryllium columns after testing.

L-66-7318.1

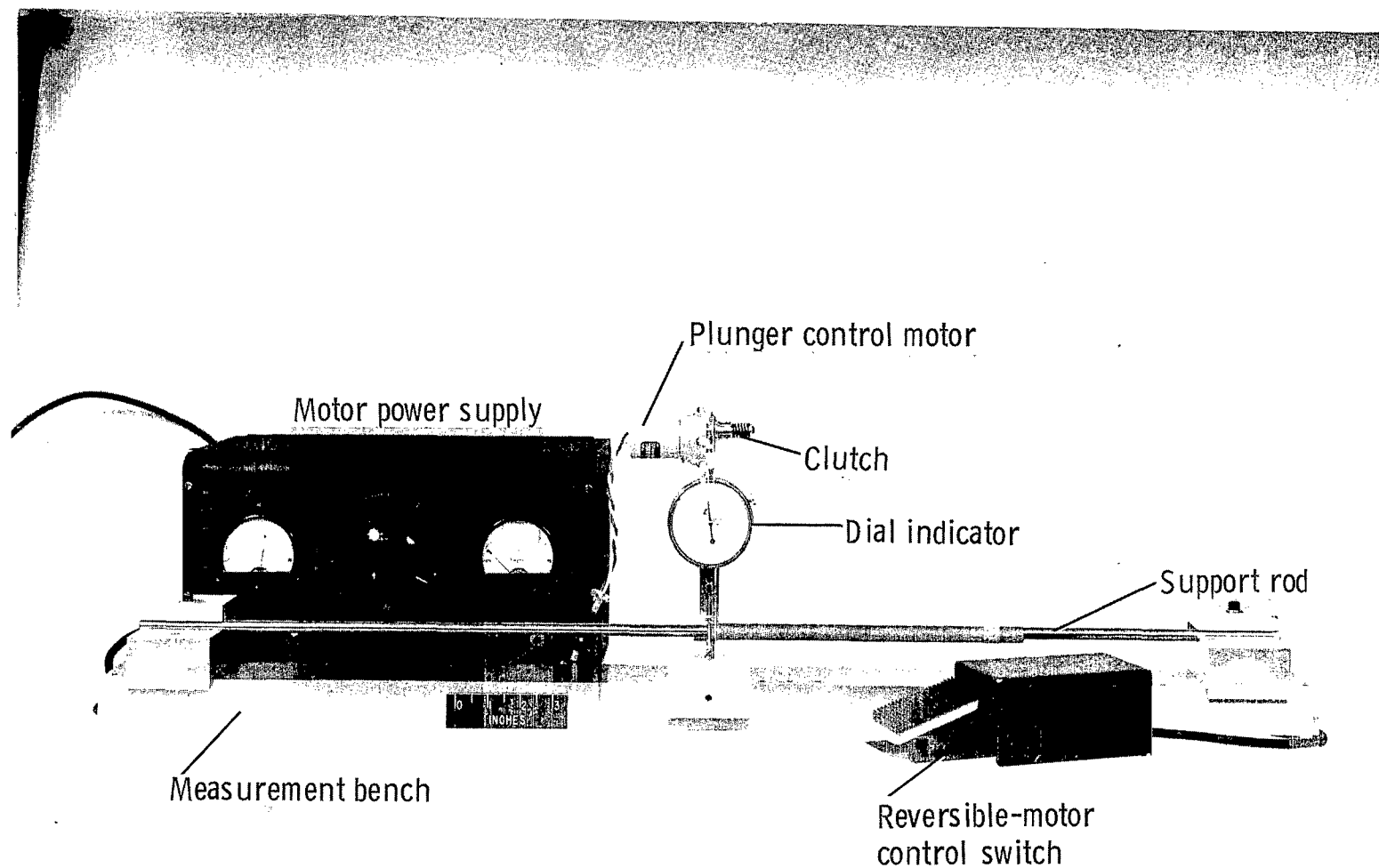


Figure 21.- Basic components of dimensional-measurement equipment.

L-65-2831.1

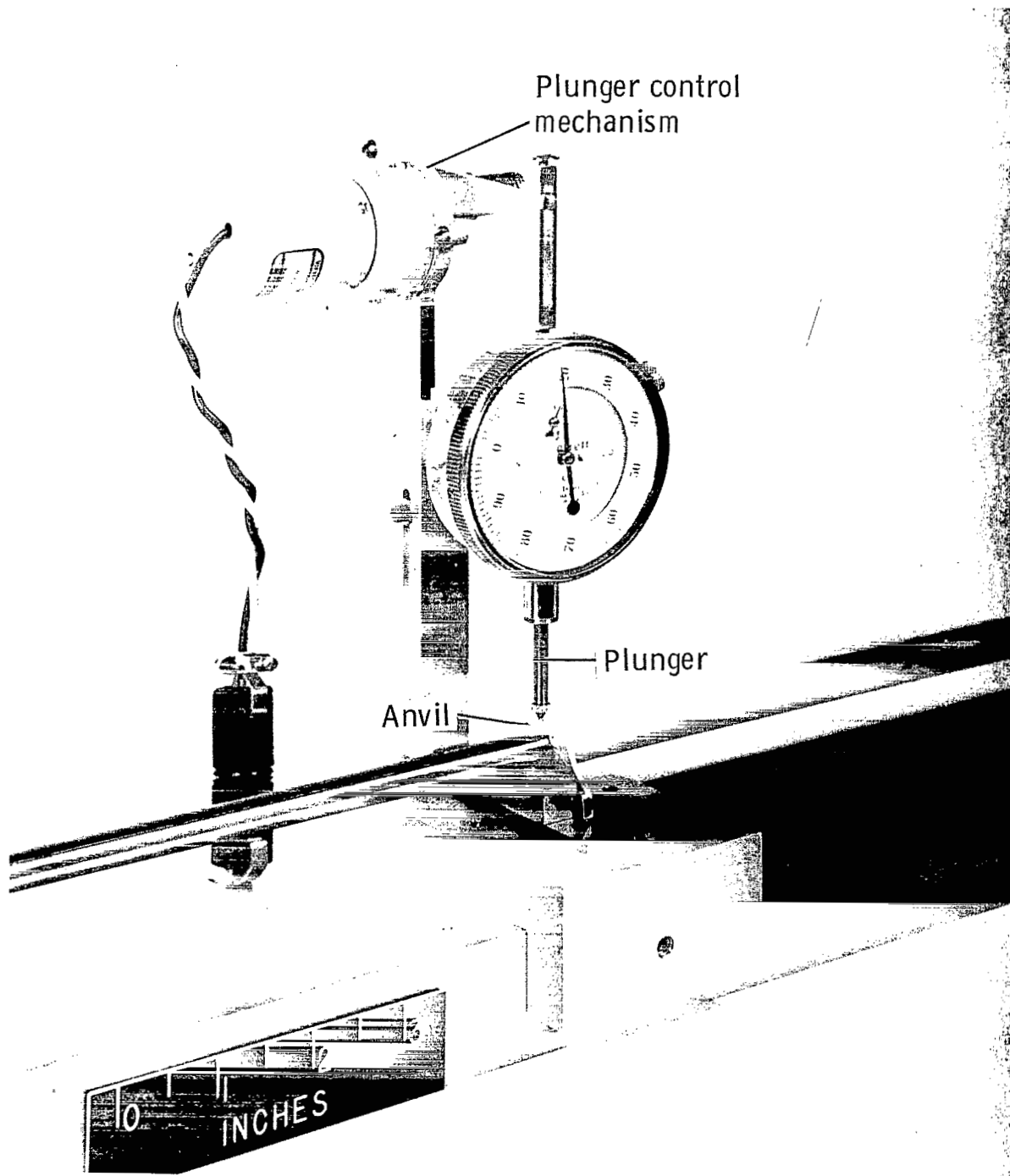


Figure 22.- Details of wall-thickness-measurement apparatus.

L-65-2829.1

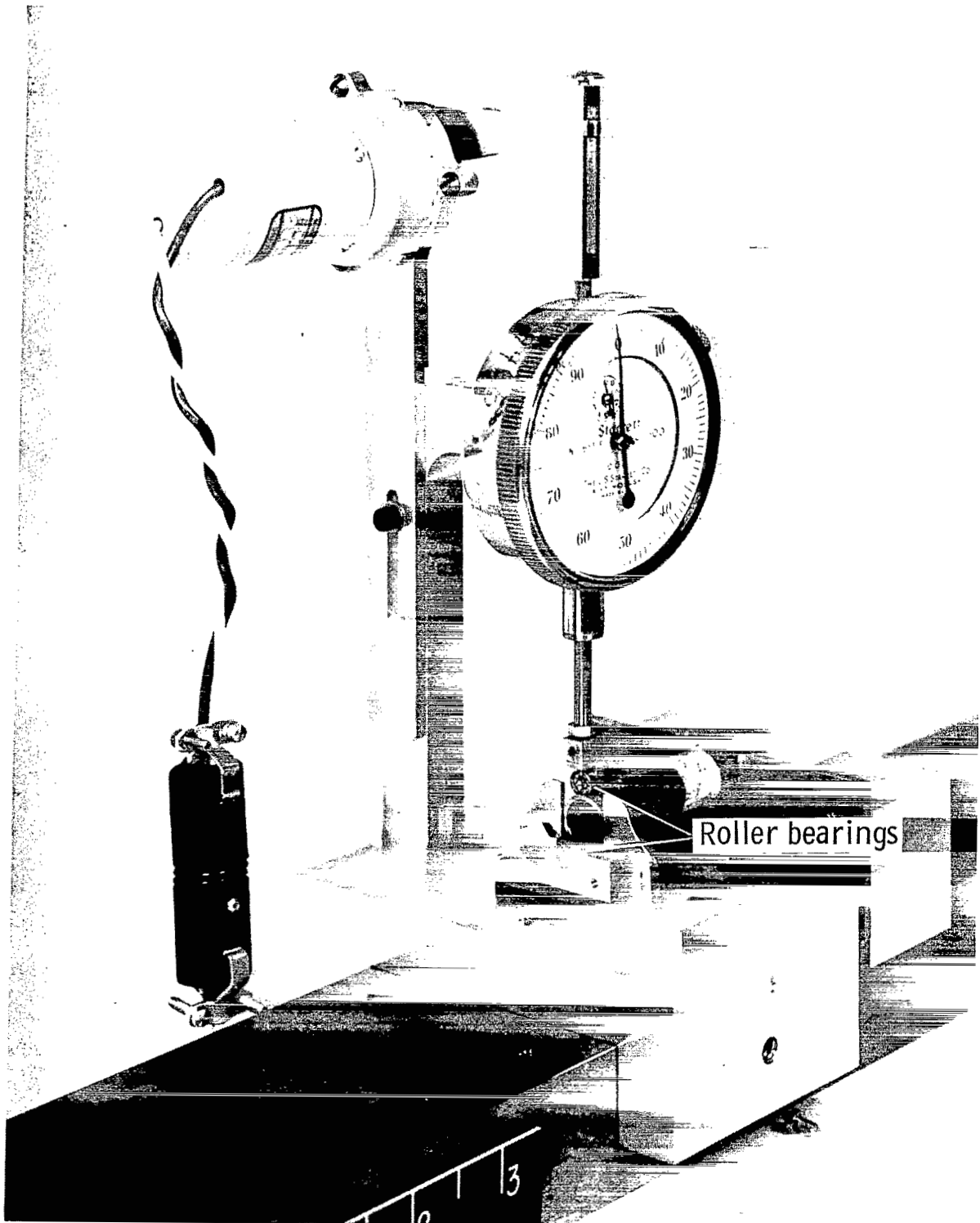


Figure 23.- Apparatus for diameter measurement.

L-65-2828.1

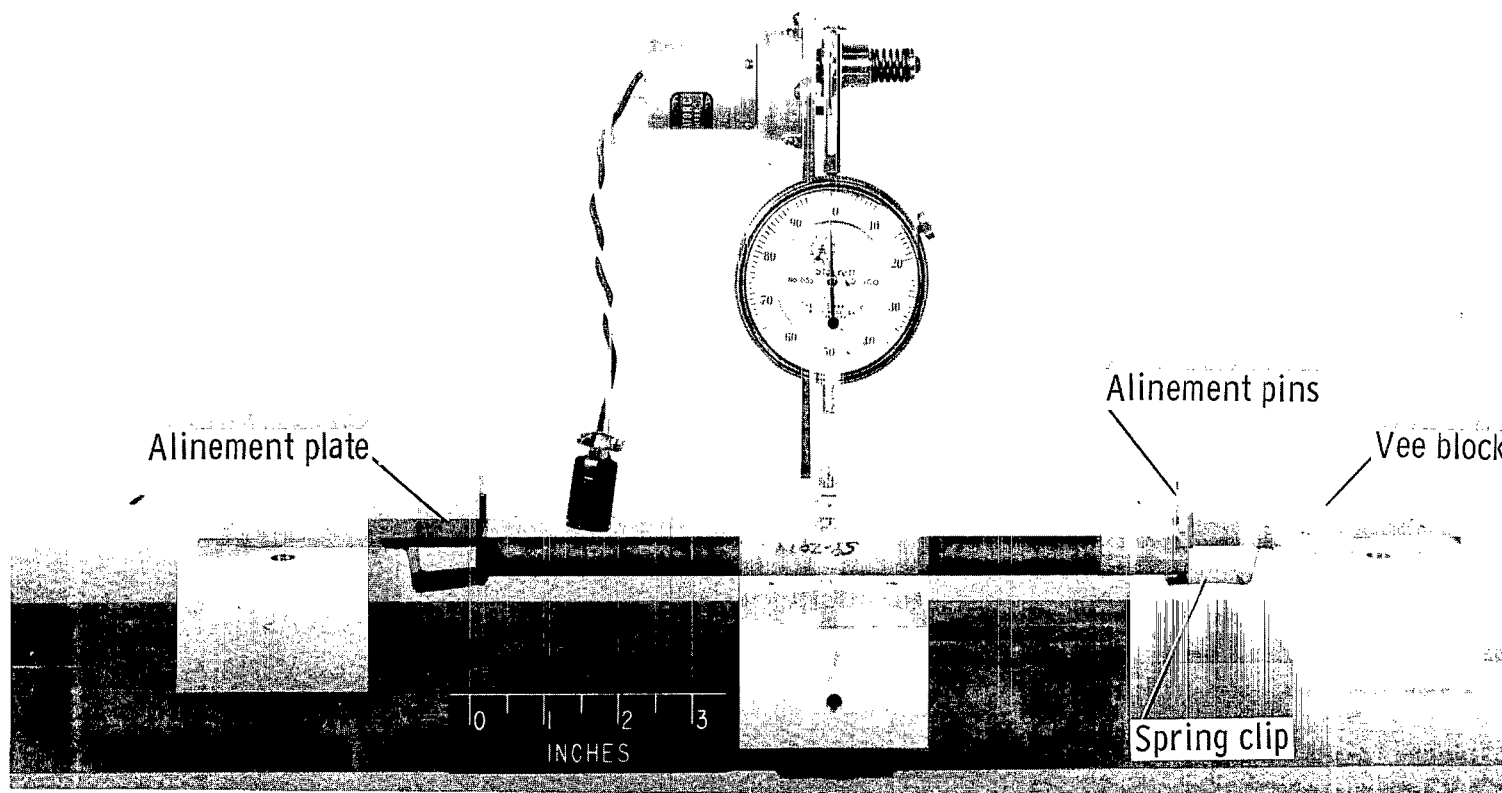


Figure 24.- Apparatus for straightness measurements.

L-65-2827.1

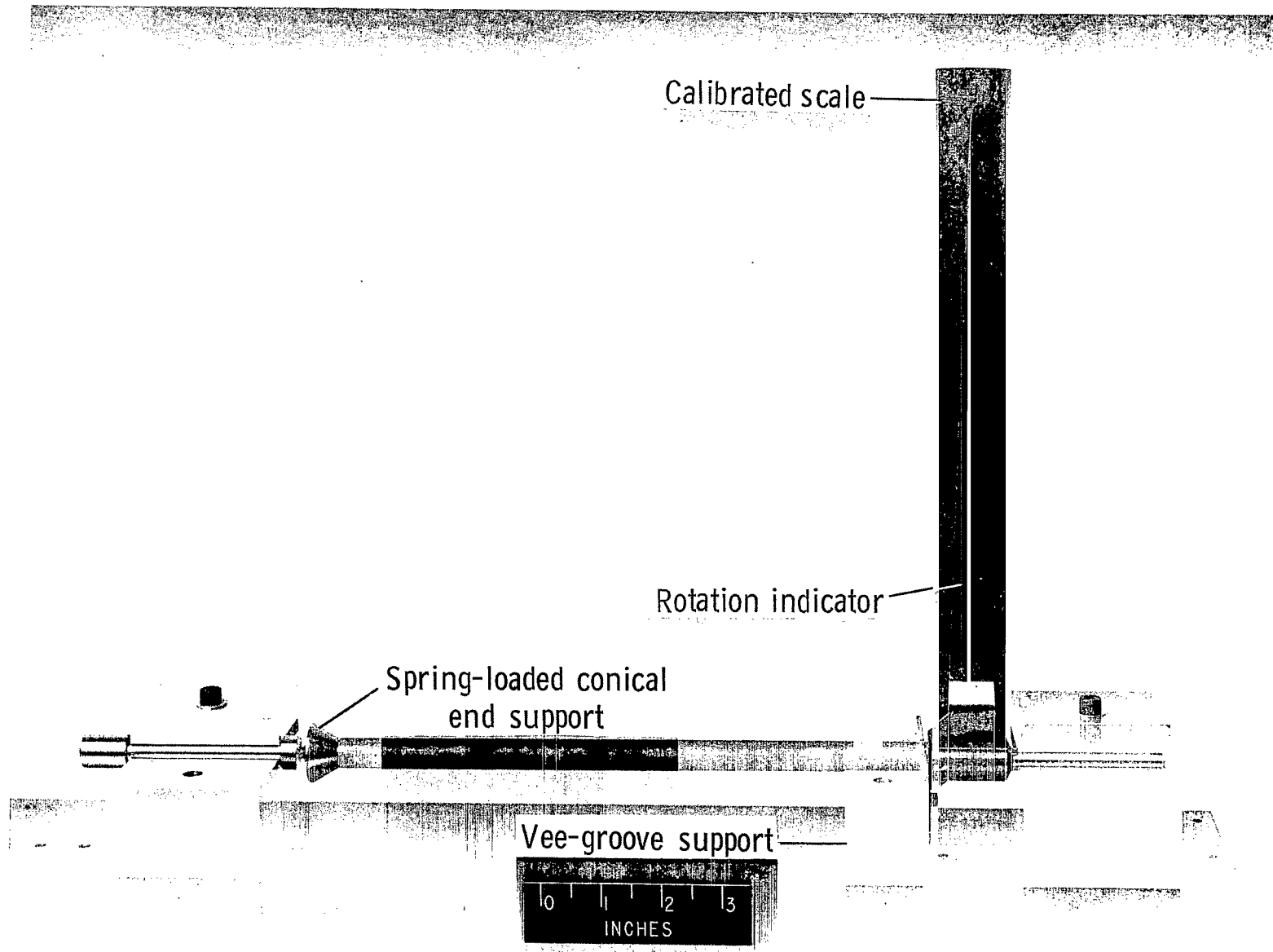


Figure 25.- Apparatus for measurement of angularity of tubing ends.

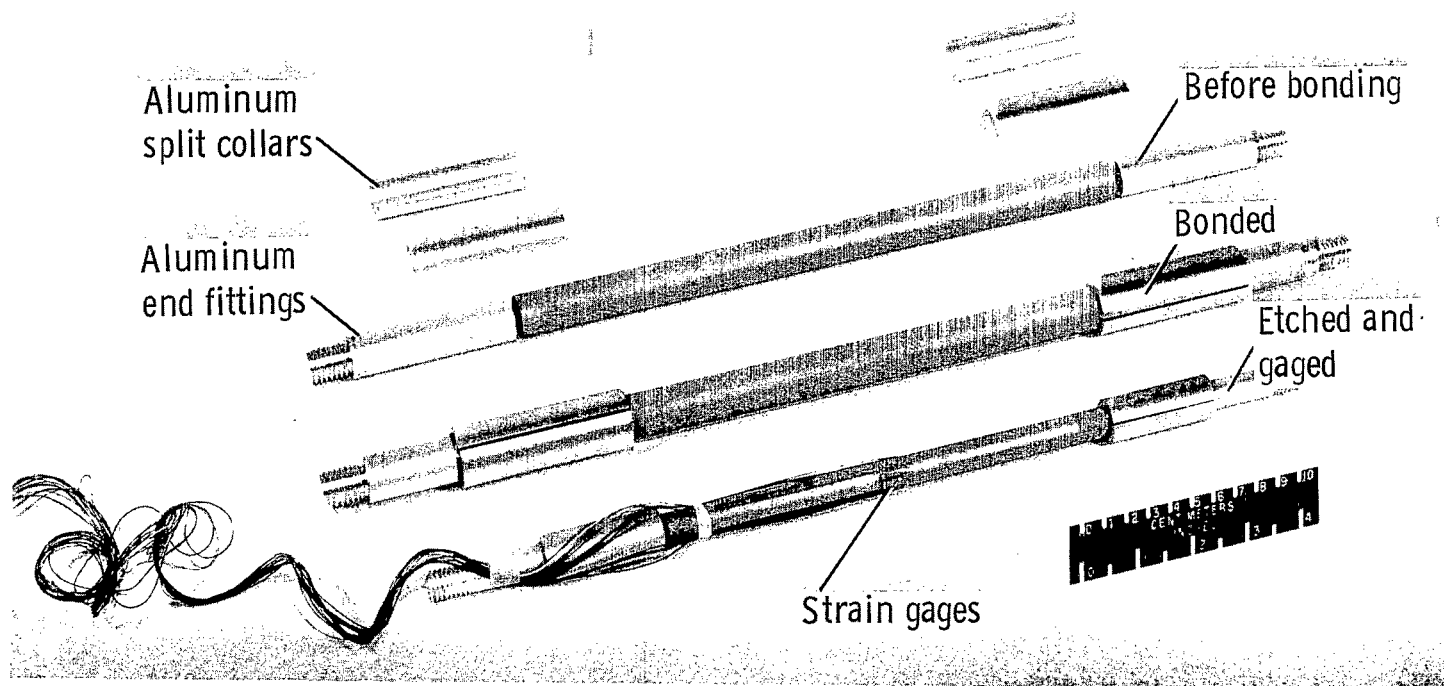


Figure 26.- Sequence of preparation of tubular beryllium tensile specimens.

L-67-1294.1

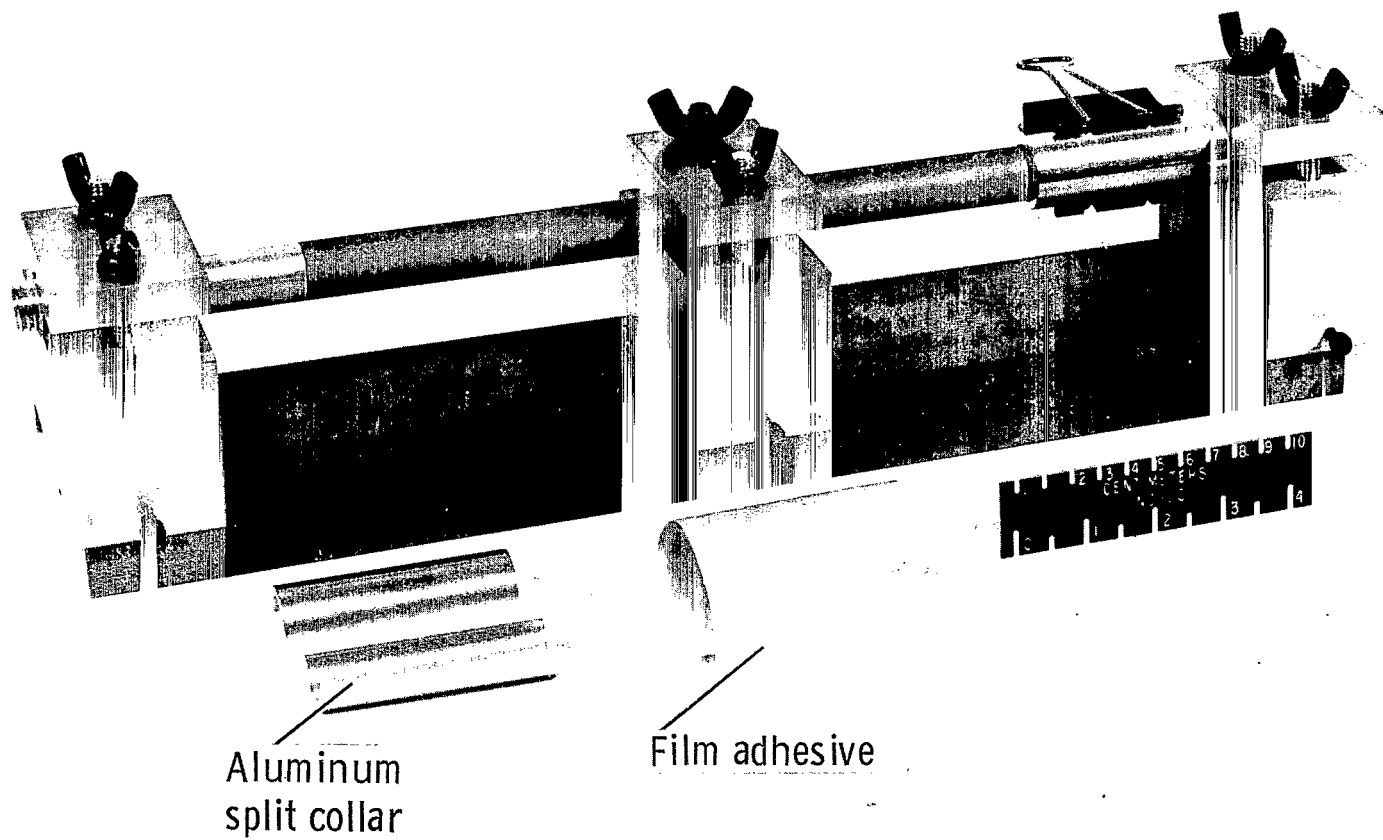
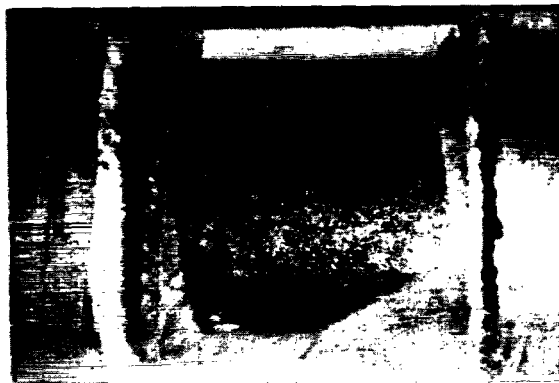


Figure 27.- Bonding fixtures for tensile specimen end fittings.

L-67-1292.1





(a) Etched section; X20.

Etchant  
surface →



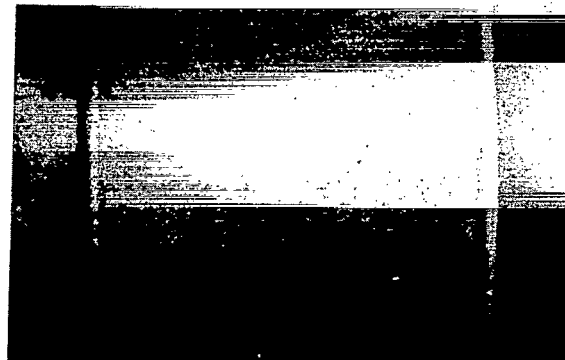
(b) Etched intersection; X20.



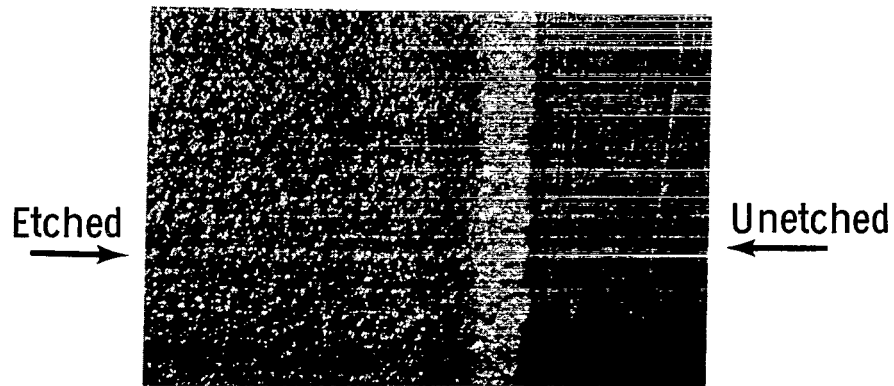
(c) Upper intersection radius; X20.

Figure 28.- Surface features produced with  $\text{Cr}_2\text{O}_3\text{-H}_2\text{SO}_4\text{-H}_3\text{PO}_4$  etchant on a type B tube.

L-68-5656



(a) Etched section; X2.



(b) Etched intersection; X20.



(c) Upper intersection radius; X20.

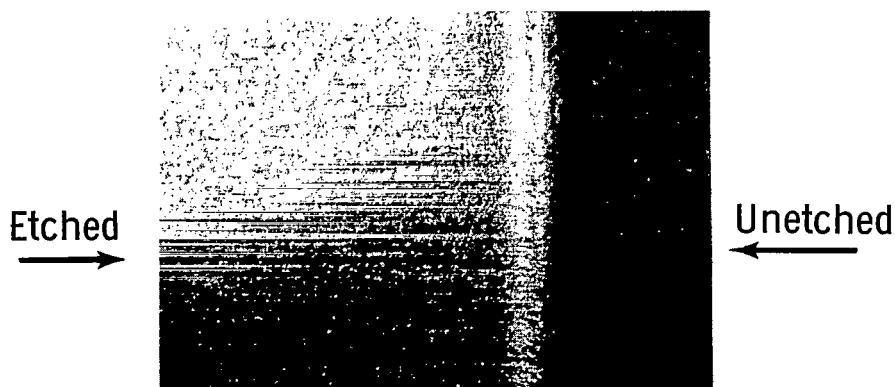
Figure 29.- Surface features produced with  $\text{HNO}_3\text{-H}_2\text{SO}_4\text{-H}_2\text{O}$  etchant on a type B tube.

L-68-5657

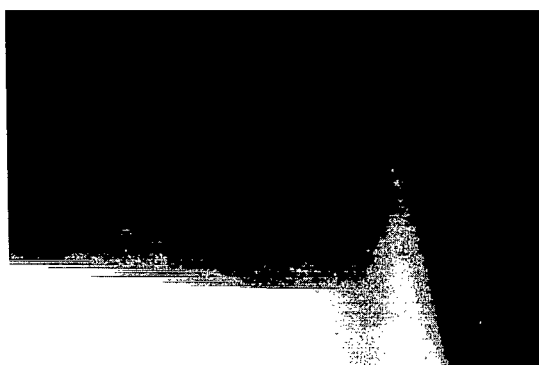


→  
Etchant  
surface

(a) Etched section; X2.



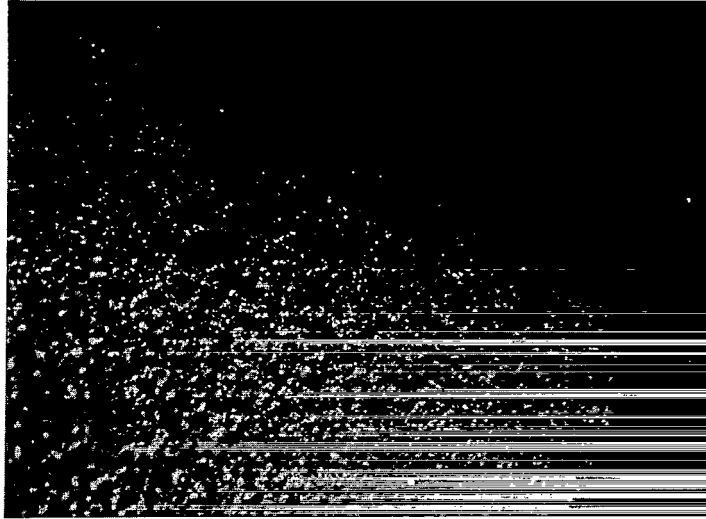
(b) Etched intersection; X20.



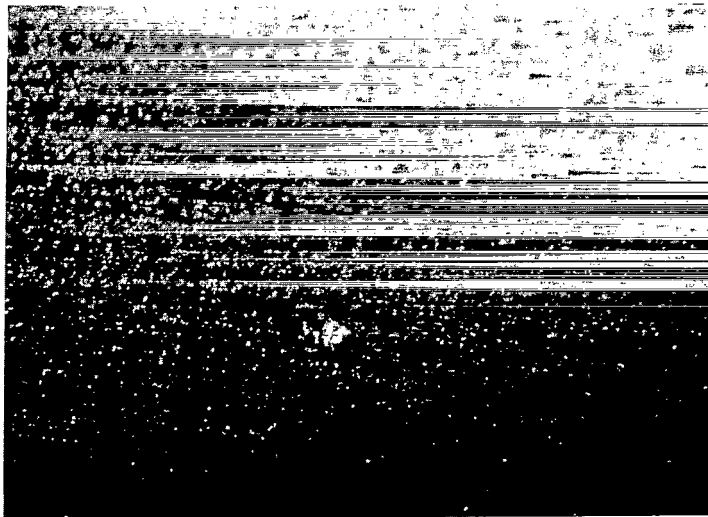
(c) Upper intersection radius; X20.

Figure 30.- Surface features produced with  $\text{HNO}_3\text{-HF-H}_2\text{O}$  etchant on a type B tube.

L-68-5658



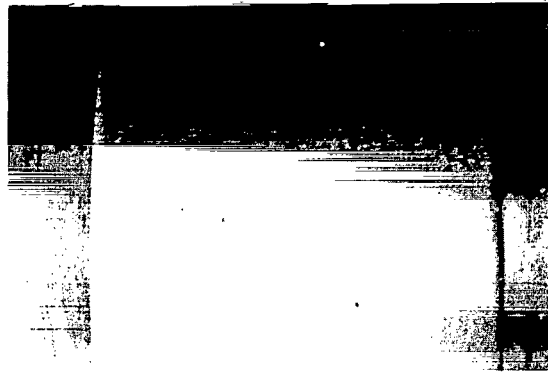
(a) After light etch; X20.



(b) After further etching; X20.

Figure 31.- Development of large pit during etching with  $\text{HNO}_3\text{-H}_2\text{SO}_4\text{-H}_2\text{O}$  etchant on a type B tube.

L-68-5659



→  
Etchant  
surface

(a) Etched section; X2.



(b) Etched intersection; X20.



(c) Upper intersection radius; X20.

Figure 32.- Surface features produced with  $\text{Cr}_2\text{O}_3\text{-HF-H}_2\text{O}$  etchant on a type B tube.

L-68-5660

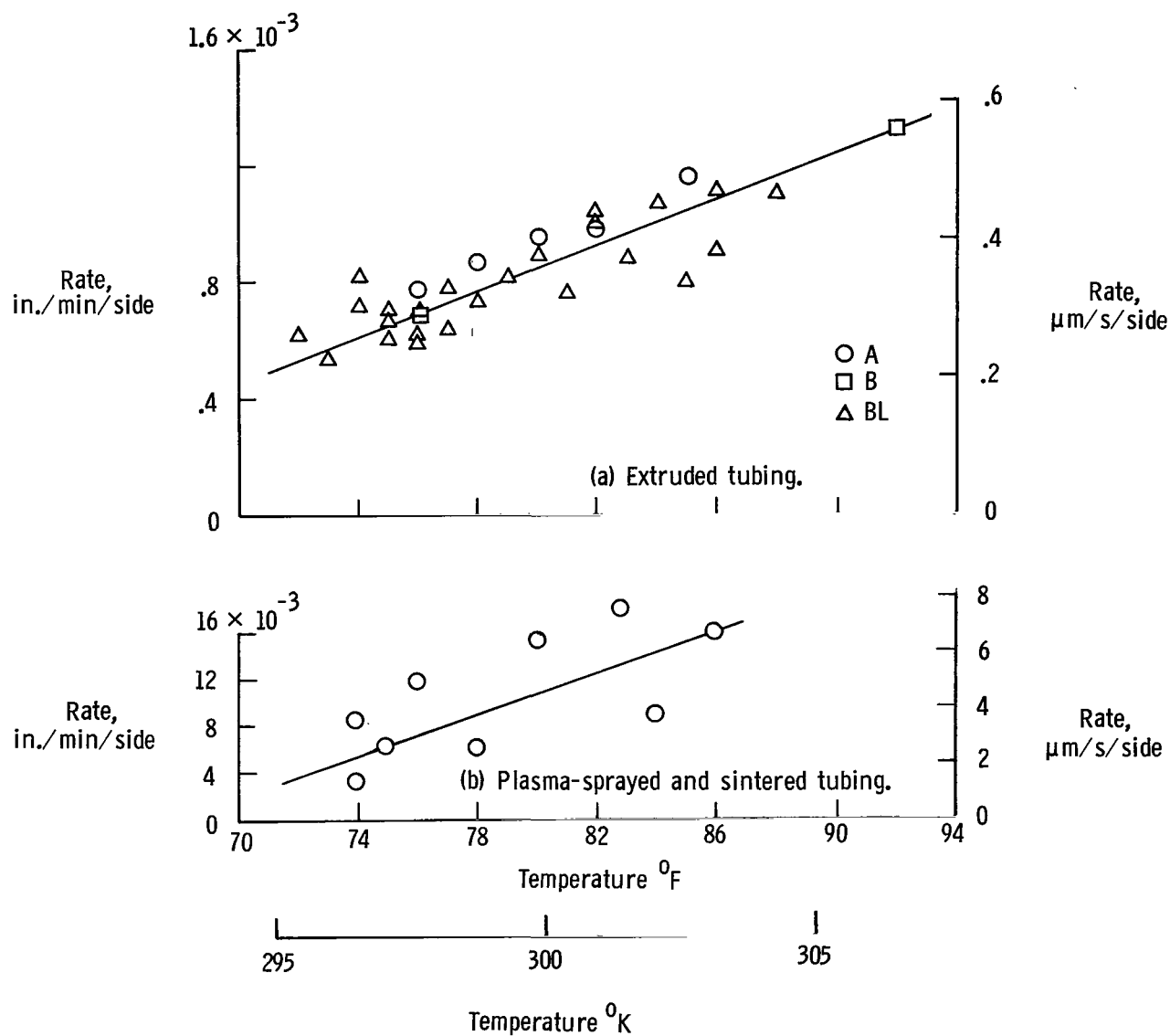


Figure 33.- Temperature dependence of etching rate for  $\text{Cr}_2\text{O}_3\text{-HF-H}_2\text{O}$  etchant on beryllium tubes.

R: If Undeliverable (Section 158  
Postal Manual) Do Not Return

*"The aeronautical and space activities of the United States shall be conducted so as to contribute . . . to the expansion of human knowledge of phenomena in the atmosphere and space. The Administration shall provide for the widest practicable and appropriate dissemination of information concerning its activities and the results thereof."*

— NATIONAL AERONAUTICS AND SPACE ACT OF 1958

## NASA SCIENTIFIC AND TECHNICAL PUBLICATIONS

**TECHNICAL REPORTS:** Scientific and technical information considered important, complete, and a lasting contribution to existing knowledge.

**TECHNICAL NOTES:** Information less broad in scope but nevertheless of importance as a contribution to existing knowledge.

**TECHNICAL MEMORANDUMS:** Information receiving limited distribution because of preliminary data, security classification, or other reasons.

**CONTRACTOR REPORTS:** Scientific and technical information generated under a NASA contract or grant and considered an important contribution to existing knowledge.

**TECHNICAL TRANSLATIONS:** Information published in a foreign language considered to merit NASA distribution in English.

**SPECIAL PUBLICATIONS:** Information derived from or of value to NASA activities. Publications include conference proceedings, monographs, data compilations, handbooks, sourcebooks, and special bibliographies.

**TECHNOLOGY UTILIZATION PUBLICATIONS:** Information on technology used by NASA that may be of particular interest in commercial and other non-aerospace applications. Publications include Tech Briefs, Technology Utilization Reports and Notes, and Technology Surveys.

*Details on the availability of these publications may be obtained from:*

SCIENTIFIC AND TECHNICAL INFORMATION DIVISION  
NATIONAL AERONAUTICS AND SPACE ADMINISTRATION  
Washington, D.C. 20546